(1) Comments from the Referees

Comment from Referee 1:
GENERAL COMMENTS

The authors provide a validation study of reactive gases modelled by the MACC system using a variety of data sources. In particular they validate O3 using GAW and EMEP data, CO using GAW station data and MOPITT retrievals, and NO2 using SCIAMACHY and GOME-2 retrievals. Given the extensive current and expected future use of MACC/CAMS products, this is a highly welcome and important contribution. With MACC soon becoming operational as CAMS this is a very much needed study at this point and it fits reasonably well within the scope of ACP although GMD probably would be more appropriate. The manuscript in general is structured consistently and well written, although some comprehensive editing by a native English speaker would be beneficial.

My main concern stems from the validation of modelled NO2 columns using satellite data. Satellite data of NO2 are extremely useful for comparing overall spatial patterns and providing an approximate qualitative assessment of the data. When using longterm averages they can even be used in a somewhat quantitative fashion to some extent. However, the uncertainty in the NO2 retrievals (both in terms of systematic biases and random errors!) themselves is too high to allow a full quantitative validation of model results. You are essentially comparing two similarly uncertain parameters with each other! Furthermore, NO2 is primarily relevant close to the surface and within the PBL (and the NO2 output from MACC/CAMS will be primarily used for such applications), whereas satellite-based validation of NO2 can only be carried out for tropospheric columns (and in addition the satellite instruments tend to be least sensitive near the surface!). It is thus impossible to draw robust quantitative conclusions from this, particularly for hourly/daily sampling and at the individual grid cell level (and this is very important for a full validation of the model results). A comprehensive validation of modelled NO2 with satellite data alone is not sufficient to draw accurate conclusions about the model performance. This is particularly relevant for validating the results from such a highly visible, high-profile, and heavily funded project as MACC/CAMS, whose model output will be used operationally for a wide variety of applications worldwide in future. As such, the validation methodology should be as robust as possible. Therefore, in addition to the comparison against satellite data provided in the current manuscript, the authors really need to perform a solid quantitative validation of modelled surface NO2 against reliable station observations (and possibly a validation of modelled NO2 columns against ground-based MAX-DOAS data) before this manuscript can be published.

Me second concern is related to the extensive use of the MNMB in this study. This is a highly non-standard statistical metric and is not readily understandable by a general audience. It is entirely unclear why the MNMB is arbitrarily multiplied by a factor of 2, for example, and how the percentage values of a bounded index should be interpreted.

Personally I think it would be preferable to stick to commonly used metrics such as for example the classic combination of mean bias and the standard deviation of the differences (representing systematic and random error, respectively) with RMSE as a measure of total error, possibly MAE, etc. I do realise that MNMB seems to have been adopted by the MACC validation team and is being used throughout several MACC related papers in order to make statistics between species comparable. However, the vast majority of readers of MACC-related papers will not be familiar with this metric and will not know about its properties. If the authors insist on using this metric as intensively as in the given manuscript, I think they need to much better justify the use of such a non-standard validation metric and further should provide a detailed background regarding its statistical properties as compared to standard metrics.

SPECIFIC COMMENTS

P6279 L1: What about MACC-III? Wouldn’t it be more sensible to call it something along the lines of a "series of MACC projects" or similar?

P6280-6281: This reads more like a textbook section on atmospheric chemistry than an introduction to a validation paper. Please be concise and focus on what is relevant for this study. It would also be useful here to discuss why we actually care about these gases and why we model them, i.e. what are some potential health effects or other impacts of these gases. See the submitted MACC validation paper by Eskes et al. (2015) in GMDD for an example on this.

P6281-6282 etc: Sometimes you talk about MACC/MACC-II, sometimes about MACCII and sometimes about MACC. Please be consistent. I recommend introducing the series of MACC projects (including MACC-III) once in the beginning and then referring to it simply as MACC in the remainder of the manuscript. Again, take a look at the submitted MACC validation paper by Eskes et al. (2015) in GMDD for finding out how to do this in a better way.

P6281 L19-20: This is worded a bit strangely. It is not the series of MACC projects that form the basis of CAMS, but rather the work that has been carried as part of MACC represents the preparatory activities that in the end are supposed to result in the operational CAMS.

P6281 L26: Are there more recent references on how data assimilation is being carried out within MACC/CAMS? If yes, cite them here. Maybe Inness et al. 2013 or similar?

P6282 L17-21: It is not clear how the availability of independent observations limits the period of this study to 2009-2012. For sure all the satellite datasets (MOPITT, SCIAMACHY, GOME-2) were available many years before 2009 and with exception of SCIAMACHY also continued after 2012. Surely GAW and EMEP data were available outside this period as well? Be precise about what is the limiting factor here.

P6282 L25: are -> is

P6282 L28: "encloses"? Better write something like "provides" or "contains"

P6283 L19: "MACC_osuite". Can you provide an explanation for this rather odd technical acronym?

P6283 L24: Be specific about the spatial resolution of the model. Is it 100 km x 100 km or irregular (and/or give it in degrees lat/lon)?

P6284 L9: What do you mean by "go back"? Do you mean the emissions are taken from or based on the RETRO-REAS inventory? Also, how exactly were the emissions merged?

P6284: Give more information about the spatial resolution of the various emission Inventories

P6284 L26: "lists up" -> "lists"

P6285 L20: Has this been studied (if yes, provide results) or is this just an assumption?

P6286 L5: WMO 2010 is not included in the list of references

P6286 L6: Why specify "tropospheric" here? These are surface observations, right?

P6286 L24: Why didn’t you use vertical interpolation between the two closest model levels. Discuss why the resulting error is negligible (or why not).

P6289 L1: The labels "Fires-Alaska" and "Fires-Siberia" look awkward compared to the other regions. Clarify why these specifically refer to fires and that they are only used for CO validation with MOPITT. Also in some of the Figures these labels are not used consistently. Please fix.
P6289 L11: "UV-VIS". Also I would recommend either writing "UV-VIS and NIR" or "ultraviolet-visible and near-infrared" and not mixed.
P6289: This section requires a discussion about the expected uncertainty of the satellite-based NO2 retrievals. Also, what is a reasonable minimum threshold of detection for the tropospheric NO2 column derived from SCIAMACHY and GOME-2?
P6290 L7: "linearly in time"
P6291 L8: Why does the MNMB used here range from -2 to 2 rather than -1 to 1? Why is this metric multiplied by 2? When using this metric in percent, as the authors do in this study you get a bounded range of -200% to 200%. How should this be interpreted? Please provide additional detail about the statistical properties of this non-standard evaluation metric.
P6291 L20: Keep the section headers consistent. Either spell out the species or not, but do not mix.
P6291 L23: It shows not one but two maps
P6291 L23: Figure 11? Figures 2-10 have not even been discussed yet. This also applies throughout the rest of the paper. Renumber Figures and Tables based on when they are introduced in the manuscript
P6292 L4: "far north" -> Better write "high latitudes in the northern hemisphere" or something similar to be specific
P6293 L6: better write "norther hemisphere winter months"
P6293 L24: This is not clear from Figure 14. It seems to show negative values of around -30% for Dec 2010?
P6293 L25-27: Can you provide an explanation for why Dec 2012 behaves so differently?
P6293 L27: "diurnal O3 cycle". This is misleading - Figure 15 does not really analyse the diurnal cycle but rather simply differentiates the result by day and night. Consider rewording this.
P6294 L21-23: Why do you need to refer to RMSEs and correlation coefficients in this sentence, when you are just talking about MNMBs? Please revise.
P6294 L24 "northern hemisphere"
P6295 L1: These correlation coefficients are indeed extremely low. A Pearson correlation coefficient of what is on average about 0.3 (Fig 2) translates to an R^2 of 0.09! And this is even for monthly averages and not hourly/daily observations - so the random error should already be reduced to a large extent. If a model can explain less than 10% of the variability in monthly averages, I think quite a bit of explanation about possible reasons for the poor performance is necessary. Please add a discussion on this here.
P6295 L3: How was the subset of stations in Figure 3 selected? Were only those stations selected at which the model performed well, or was some other selection process used? Please add information about this in the text.
P6295 L25 to P6296 L10: This section discusses solely differences between MOPITT and IASI but not the relevance of these differences with respect to the model. Please revise to better indicate how these differences affect the model performances? Is it due to assimilation of IASI CO products in the model?
P6296 L24: Be careful about interpreting too much into satellite-based NO2 columns

over the open oceans. The NO2 levels there tend to be below the detection limits of the instruments and the patterns observed there often represent no true geophysical signal.
P6298: Please clearly distinguish here between CO and NO2 here. These are intermixed
in the discussion making it difficult to follow.
P6299: This section also requires a brief discussion of the potential uncertainties introduced by transitioning from SCIAMACHY to GOME-2 in 2012 and how it affects the validation of NO2.
P6300 L5: Again, you are not really studying/validating the diurnal cycle. Please reword.
P6316: The combined label/region field is a bit confusing. Do only the GAW stations have a label whereas the EMEP stations have a region acronym? For clarity please highlight this in the caption and list the region acronyms.
P6319: This table has unrealistically high number of significant digits. Please modify.
P6322: The panels in this plot are missing labels as a) b) c), yet the caption refers to them. Also, why does the caption only refer to a) and b) instead of all three. Please be consistent. Also the panels are very small, such that the legend is not readable.
P6324: The legend here does not list the region names as "Fires-Alaska" and "Fires-Siberia", as they were introduced previously. Please decide on a label for these regions and then stick to it consistently in text and Figures.
P6325: Same in this Figure.
P6326: It would be helpful to use different symbols/colours for SCIAMACHY and GOME-2 in this Figure.
P6328: Same in this Figure.
P6329: The caption says "daily" but the Figure shows monthly averages. Please correct.
P6331: This Figure has an unclear colour scale, making the interpretation of MNMBs close to zero challenging. Plots with divergent colour scale such as this should ideally have only one colour gradient for positive and negative values, respectively, with a neutral colour (white or grey) in between. I recommend shades of red for positive values and shades of blue for negative values with white or grey symmetrically around zero.
P6332: These plots are extremely busy and the legend is unreadable. Please consider ways of reducing the overplotting to increase the visual impact of the Figure. Also, once again, please consistently format and label the panels. Why does subplot a) consist of two panels and subplot b) of one panel. Why not have 3 separate subplots?
P6333: Describe either in the caption or in the text how this seemingly random subset of stations was selected.

Comment from Referee 2:
GENERAL COMMENTS
In this paper an evaluation of the MACC operational forecast system is given with comparisons of the model with surface and satellite data of O3, NO2 and CO. The comparisons show deficiencies in the model or the model input that are pointed out. The paper gives the impression of hastily being put together leaving a lot of work to the reader. This should really be tidied up before publication. For example the number and choice of GAW stations shown should be motivated, or should be similar for the different comparisons (O3, CO and NO2). For NO2 ground based data is missing, FTIR or UV-VIS data could be used here. Figures and tables numbering need to be

tidied up. Figures with the lots of lines are illegible. Please try to be consistent with the analysis of the 3 different data sets.
page 6280:
line 4: Avoid one sentence paragraphs
line 19: better: "in their respective summer months" instead of just "in the summer months"
page 6282:
line 16: It is no the ’paper that investigates’, more something like this "In this paper we
describe the investigation of..."
page 6284:
line 24: "Table 2 lists the assimilated data products." instead of "...lists up..."
O_3
page 6291
line 23: The figure order needs to be checked. This should be Figure 2 and not Figure 11, the Figure order has to be changed.
Fig.1
Fig.11 should be 2
Fig.13 should be 3
Fig.12 should be 4
Fig.14 should be 5
Fig.15 should be 6
Fig.2-10 should be 7-15
page 6292:
line 8: Figure 13 (which should be plot 3) shows very large variability in the model data,
compared to the observations. The agreement does not seem very good for the high latitude stations but there seems to be indeed an amelioration after Jul 2012.
line 15: O_3 in tropical regions (30_S to 30_N) seem to have min 20% differences up to
40%
line 19: could you show the correlation coefficients on the plots?
Table 6 should be Table 4. Please change Table order.
Figure 12: Legends are not legible, there are too many lines. The plots should be numbered a, b, c. There are curves that stop, eg the pink line in plot a. in Dec 2011. Why? Or one starts in Jun 2010 (black?) Maybe the plots should be stacked on top of each other.
page 6293:
line 8: The correlation does not show a distinct seasonal behaviour in Fig 12, but the MNMBs or the RMSEs not either on this plot! How do you know this?
line 15: There also seems to be a phase shift at KOS, KOV and CVO. TSU seems to have random observations, but the black points are not really visible behind the red line.
line 27: Figure 15 should have the panels stacked and numbered a, b, c.
CO
page 6294:
line 6: MNMBs have already been described. These descriptions (also for RMSEs) could move to the O_3 section.
line 20: Reference to Table 4 should come earlier (line 7).
line 24: Figure 2 could have the 3 plots stacked again.

page 6395:
line 3: Fig 3: Why do you use different stations for O3 and CO?
page 6296:
line 1: Why do you use the IASI product, when you know that it is not as good as the MOPiTT product for higher latitudes?
NO2
page 6296:
line 27: There is a stray ’to’
Discussion
page 6298:
lines 7-9: ’realistically reproduces’: Isn’t this a bit of an exaggeration with up to 110% underestimations for NO2? Incidentally the values are all negative overall an range from 5% to 70% underestimation. The values for CO seem to be 15% to -23%, whereas
the overall values of -50% to 28% do not really agree well...
line 9: It would be good to have a Table with the satellite results for CO, too.
page 6299:
lines 27 to end of Discussion: O3 section should probably come first in the discussion.
Conclusion
page 6301:
line 8: ’however with a negative offset’ should probably be ’however, with a large negative offset’
line 18: Wasn’t the impact of the fire emmisson error rather large!!
Tables:
Check order of tables with first occurance in the text being first.
Figures:
General: Be consistent, sometimes it is Fig. in the text other times it is Figure.
Check order of figures with first occurance in the text being first.
Better use a, b, c, d, e, f, etc for the sub-figures.
Figure 9 Caption, the latitudina an longitudinal boundaries are defined in Figure 1 not in the text!

(2) Author’s response to the general comments:

Thank you very much for the comprehensive review of our paper!
We have tidied up the numbering of the figures and tables; we have changed the introduction and re-structured the discussion and conclusion and we included the requested changes.

Concerning the use of NO_2 surface observations for the validation:
We absolutely agree with the referee that surface measurements of NO_2 would indeed be very useful in addition to the satellite observations. However, for the global model validation this has not been implemented in MACC so far. For the validation of the global model, it was important for us to compare especially the spatial patterns of NO_2 which can hardly be captured globally by the sparse amount of GAW station observations. In MACC-III, the validation with MAX-DOAS is tested, however, with regional models with higher spatial resolution.

Concerning the use of the MNMB:

We use the MNMB in the MACC and future CAMS evaluations because verifying chemical species concentration values significantly differs from verifying standard meteorological fields. For example, spatial or temporal variations can be much greater and the differences between model and observed values ("model errors") are frequently much larger in magnitude. Most importantly, typical concentrations can vary quite widely between different pollutant types (e.g. O_3 and CO) and region (e.g. Europe vs. Antarctica), a given bias or error value can have a quite different significance. It is useful therefore to consider bias and error metrics which are normalized with respect to observed concentrations and hence can provide a consistent scale regardless of pollutant type (see e.g. Elguindi et al., 2010 or Savage et al., 2013). Moreover, the MNMB is robust to outliers, converges to the normal bias for biases approaching zero, while taking into account the representativeness issue when comparing coarse resolved global models versus site specific station observations. Though GAW stations prove regional representative in general, the experience is that local effects cannot always be ruled out reliably in long worldwide data sets, because transport, chemical processes and parameterizations are not selective for the super- to sub-grid-scale threshold. Referencing to the model/observation mean again constitutes a pragmatic workaround to avoid misleading bias tendencies, particularly in sensitive regions with sparse data coverage. Within MACC, the MNMB is used as an important standard score. It is used in the MACC quarterly evaluation reports and it appears in a lot of recent publications, e.g. Cuevas et al. (2015), Eskes et al. (2015), Sheel et al. (2014). As our paper is dedicated to the MACC special issue, we assume that most of the readers will be familiar with this metric and thus we would like to stick to the MNMB in our validations. In our paper, the MNMB is complemented with the commonly used standard metrics RMSE and R.

The specific comments of the referees have been addressed point-by-point in what follows:

Author's response point-by-point:

Referee 1:

Specific comments:

P6279 L1: What about MACC-III? Wouldn't it be more sensible to call it something along the lines of a "series of MACC projects" or similar?

-done

P6280-6281: This reads more like a textbook section on atmospheric chemistry than an introduction to a validation paper. Please be concise and focus on what is relevant for this study. It would also be useful here to discuss why we actually care about these gases and why we model them, i.e. what are some potential health effects or other impacts of these gases. See the submitted MACC validation paper by Eskes et al. (2015) in GMDD for an example on this.

-the introduction has been re-written to:

The impact of reactive gases on climate, human health and environment has gained increasing public and scientific interest in the last decade (Bell et al., 2006, Cape 2008, Mohnen et al., 2013, Seinfeld and Pandis 2006, Selin et al., 2009). As air pollutants, carbon monoxide (CO), nitrogen oxides (NO_x) and ozone (O_3) are known to have acute and chronic effects on human health, ranging from minor upper respiratory irritation to chronic respiratory and heart disease, lung cancer, acute respiratory infections in children and chronic bronchitis in adults (Bell et al., 2006, Kampa and Castanas 2006). Tropospheric ozone, even in small concentrations, is also known to cause plant damage in reducing plant primary productivity and crop yields (e.g. Ashmore 2005). It is also contributing to global warming by direct and indirect radiative forcing (Forster et al., 2007, Sitch et al., 2007). Pollution events can be caused by local sources and processes but are also influenced by continental and intercontinental transport of air masses. Global models can provide the transport patterns of air masses and deliver the boundary conditions for regional models, facilitating the forecast and investigation of air pollutants.

The EU-funded research project MACC - Monitoring Atmospheric Composition and Climate, (consisting of a series of European projects, MACC to MACC-III), provides the preparatory work that will form the basis of the Copernicus Atmosphere Monitoring Service (CAMS). This service is established by the EU to provide a range of products of societal and environmental value with the aim to help European governments respond to climate change and air quality problems. MACC provides reanalysis, monitoring products of atmospheric key constituents (e.g. Inness et al., 2013), as well as operational daily forecasting of greenhouse gases, aerosols and reactive gases (Benedetti et al., 2011, Stein et al., 2012) on a global and on European-scale level, and derived products such as solar radiation. An important aim of the MACC system is to describe the occurrence, magnitude and transport pathways of disruptive events, e.g., volcanoes (Flemming and Inness, 2013), major fires (Huijnen et al., 2012, Kaiser et al., 2012) and dust storms (Cuevas et al., 2015). The product catalogue can be found on the MACC website, http://copernicus-atmosphere.eu. For the generation of atmospheric products, state-of-the-art atmospheric modelling is combined with assimilated satellite data (Hollingsworth et al., 2008, Inness et al., 2013, 2015, more general information about data assimilation can be found in e.g. Ballabrera-Poy et al., 2009 or Kalnay 2003). Within the MACC project there is a dedicated validation activity to provide up-to-date information on the quality of the reanalysis, daily analyses and forecasts. Validation reports are updated regularly and are available on the MACC websites.

The MACC global near-real-time (NRT) production model for reactive gases and aerosol has operated with data assimilation from September 2009 onwards, providing boundary conditions for the MACC regional air quality products (RAQ), and other downstream users. The model simulations also provide input for the stratospheric ozone analyses delivered in near-real-time by the MACC stratospheric ozone system (Lefever et al., 2014).

In this paper we describe the investigation of the potential and challenges of near-real-time modelling with the MACC analysis system between 2009 and 2012. We concentrate on this period because of the availability of validated independent observations (namely surface observations from the Global Atmosphere Watch Programme GAW, the European Monitoring and Evaluation Programme EMEP, as well as total column satellite data from the MOPITT, SCIAMACHY and GOME-2 sensors) that are used for comparison. In particular, we study the model's ability to reproduce the seasonality and absolute values of CO and NO_2 in the troposphere as well as O_3 and CO at the surface. The impact of changes in model version, data assimilation and emission inventories on the model performance is examined and discussed. The paper is structured in the following way: Section 2 contains a description of the model and the validation data sets as well as the applied validation metrics. Section 3 presents the validation results for CO, NO_2 and O_3. Section 4 provides the discussion and section 5 the conclusions of the paper.

P6281-6282 etc: Sometimes you talk about MACC/MACC-II, sometimes about MACCII and sometimes about MACC. Please be consistent. I recommend introducing the series of MACC projects (including MACC-III) once in the beginning and then referring to it simply as MACC in the remainder of the manuscript. Again, take a look

at the submitted MACC validation paper by Eskes et al. (2015) in GMDD for finding out how to do this in a better way.
-done

P6281 L19-20: This is worded a bit strangely. It is not the series of MACC projects that form the basis of CAMS, but rather the work that has been carried as part of MACC represents the preparatory activities that in the end are supposed to result in the operational CAMS.
-done

P6281 L26: Are there more recent references on how data assimilation is being carried out within MACC/CAMS? If yes, cite them here. Maybe Inness et al. 2013 or similar?
-done

P6282 L17-21: It is not clear how the availability of independent observations limits the period of this study to 2009-2012. For sure all the satellite datasets (MOPITT, SCIAMACHY, GOME-2) were available many years before 2009 and with exception of SCIAMACHY also continued after 2012. Surely GAW and EMEP data were available outside this period as well? Be precise about what is the limiting factor here.
-The data availability is only limiting the end of the validation period. We chose 2009 as the beginning because the MACC_osuite model run with data assimilation was introduced in 09/2009.

P6282 L25: are -> is
-done

P6282 L28: "encloses"? Better write something like "provides" or "contains"
-done

P6283 L19: "MACC_osuite". Can you provide an explanation for this rather odd technical acronym?
-done
P6283 L24: Be specific about the spatial resolution of the model. Is it 100 km x 100 km or irregular (and/or give it in degrees lat/lon)?
-done
P6284 L9: What do you mean by "go back"? Do you mean the emissions are taken from or based on the RETRO-REAS inventory? Also, how exactly were the emissions merged?
-done
P6284: Give more information about the spatial resolution of the various emission Inventories
-done
P6284 L26: "lists up" -> "lists"
-done
P6285 L20: Has this been studied (if yes, provide results) or is this just an assumption?
-This is the experience (unpublished, however) of our validation work within MACC.
P6286 L5: WMO 2010 is not included in the list of references

-done

P6286 L6: Why specify "tropospheric" here? These are surface observations, right?

-done

P6286 L24: Why didn't you use vertical interpolation between the two closest model levels. Discuss why the resulting error is negligible (or why not).

The selection of the vertical model level is indeed a challenge. Within MACC, we initially did extensive sensitivity tests for level selection, but had to conclude that there is no clear optimal approach for all stations, terrains and species.

At the lowest levels, the narrow spacing of the model levels is often not significantly resolved by model processes and parameterizations, at large model/real surface differences the missing surface influence (e.g. deposition) could introduce more problematic inconsistencies (e.g. in diurnal cycle) than a precisely chosen model altitude, be it w.r.t. altitude, pressure or temperature (which all has been applied in published studies but each has clear pros and cons).

P6289 L1: The labels "Fires-Alaska" and "Fires-Siberia" look awkward compared to the other regions. Clarify why these specifically refer to fires and that they are only used for CO validation with MOPITT. Also in some of the Figures these labels are not used consistently. Please fix.

-done

P6289 L11: "UV-VIS". Also I would recommend either writing "UV-VIS and NIR" or "ultraviolet-visible and near-infrared" and not mixed.

-done

P6289: This section requires a discussion about the expected uncertainty of the satellite-based NO2 retrievals. Also, what is a reasonable minimum threshold of detection for the tropospheric NO2 column derived from SCIAMACHY and GOME-2?

We agree that a short section on uncertainties is needed and have added the following paragraph:

Satellite observations of tropospheric NO_2 columns have relatively large uncertainties, mainly linked to incomplete stratospheric correction (important over clean regions and at high latitudes in winter and spring) and to uncertainties in air mass factors (mainly over polluted regions) (e.g. Boersma et al., 2004 and Richter et al., 2005). The uncertainty varies with geolocation and time but in first approximation can be separated into an absolute error of 5x1014 molec cm-2 and a relative error of about 30%, whichever is larger. As some of the contributions to this uncertainty are systematic, averaging over longer time periods does not reduce the errors as much as one would expect for random errors. Over polluted regions, the uncertainty from random noise in the spectra is small in comparison to other error sources, in particular for monthly averages.

The question of a detection limit for satellite NO_2 observations is an interesting one. Averaging of large amounts of data will lower the random noise in the data significantly as has been demonstrated for many trace gases in studies looking at multi-annual averages. While the number of available measurements is limited in real world observations, it is not clear to us whether or not a detection limit in the sense of an absolute threshold exists for this type of absorption spectroscopy measurements.

We therefore preferred not to give a "detection limit" but rather an absolute uncertainty which for practical applications has the same meaning.

P6290 L7: "linearly in time"
-done

P6291 L8: Why does the MNMB used here range from -2 to 2 rather than -1 to 1? Why is this metric multiplied by 2? When using this metric in percent, as the authors do in this study you get a bounded range of -200% to 200%. How should this be interpreted? Please provide additional detail about the statistical properties of this non-standard evaluation metric.
The MNMB is a normalization based on the mean of the observed and forecast value. It is used as a standard score within MACC and been adopted in order to avoid asymmetry, which occurs in bias assessment when the mean observation is used as a reference, see also Elguindi et al. (2010). A detailed discussion on this has been added in the general part of the author's answers above.

P6291 L20: Keep the section headers consistent. Either spell out the species or not, but do not mix.
-done

P6291 L23: It shows not one but two maps
-done
P6291 L23: Figure 11? Figures 2-10 have not even been discussed yet. This also applies throughout the rest of the paper. Renumber Figures and Tables based on when they are introduced in the manuscript
-done

P6292 L4: "far north" -> Better write "high latitudes in the northern hemisphere" or something similar to be specific
-done

P6293 L6: better write "norther hemisphere winter months"
-done

P6293 L24: This is not clear from Figure 14. It seems to show negative values of around -30% for Dec 2010?
-done, mistake, is supposed to mean Dec 2012

P6293 L25-27: Can you provide an explanation for why Dec 2012 behaves so differently?
-We suppose because of the limited data availability towards the end of the validation period.

P6293 L27: "diurnal O3 cycle". This is misleading - Figure 15 does not really analyse the diurnal cycle but rather simply differentiates the result by day and night. Consider rewording this.
-done

P6294 L21-23: Why do you need to refer to RMSEs and correlation coefficients in this sentence, when you are just talking about MNMBs? Please revise.
-done

P6294 L24 "northern hemisphere"
-done

P6295 L1: These correlation coefficients are indeed extremely low. A Pearson correlation coefficient of what is on average about 0.3 (Fig 2) translates to an R^2 of 0.09! And this is even for monthly averages and not hourly/daily observations - so the random error should already be reduced to a large extent. If a model can explain less than 10% of the variability in monthly averages, I think quite a bit of explanation about possible reasons for the poor performance is necessary. Please add a discussion on this here.
-the low values of 0.1 during the period January 2011 to October 2011 result from the reading error in the fire emissions. The generally only moderate correlation coefficient is related to mismatches in the strong short-term variability seen in both the model and the measurements. Data assimilation also presumably impacts this.

P6295 L3: How was the subset of stations in Figure 3 selected? Were only those stations selected at which the model performed well, or was some other selection process used? Please add information about this in the text.
- done in the text, we chose representative examples for every region to underline the results in the text but certainly not only stations were the model performed well, as can be seen by the deviations between model and observations in the plots.

P6295 L25 to P6296 L10: This section discusses solely differences between MOPITT and IASI but not the relevance of these differences with respect to the model. Please revise to better indicate how these differences affect the model performances? Is it due to assimilation of IASI CO products in the model?
-done in the text

P6296 L24: Be careful about interpreting too much into satellite-based NO2 columns over the open oceans. The NO2 levels there tend to be below the detection limits of the instruments and the patterns observed there often represent no true geophysical signal.
We agree that NO_2 columns, which are close to the uncertainty, should be interpreted with care. We do not think that this is limited to columns over the open oceans although there might be small problems with the spectral signature of vibrational Raman scattering and possibly also liquid water absorption.
The patterns seen in the satellite data, which are referred to in the text are clearly linked to outflow from the continents and we do not think they are artefacts. The enhanced values in the Southern Ocean close to Antarctica are a well-known artefact from incomplete removal of stratospheric variability.
In response to the comment by the reviewer we have changed the corresponding paragraph as follows:
In the northern hemisphere, background values of NO2 VCD over the ocean are lower in the simulations than in the satellite data. The same is true for the South Atlantic Ocean to the west of Africa (see Fig.15). This might suggest a model underestimation of NO2 export from continental sources or too rapid conversion of NO2 into its reservoirs. However, as the NO2 columns over the oceans are close to the uncertainties in the satellite data, care needs to be taken when interpreting these differences.

P6298: Please clearly distinguish here between CO and NO2 here. These are intermixed in the discussion making it difficult to follow.
-done

P6299: This section also requires a brief discussion of the potential uncertainties introduced by transitioning from SCIAMACHY to GOME-2 in 2012 and how it affects the validation of NO2.
-we have repeated the validation with GOME-2 data and the conclusions are the same as for the combined SCIAMACHY and GOME-2 validation. For the region plots, the daily mean values of SCIAMACHY show a stronger temporal variability compared to the daily mean values of GOME-2. This is due to the differences in the data sampling (GOME-2 has a better spatial coverage). Figures are attached below.

P6300 L5: Again, you are not really studying/validating the diurnal cycle. Please reword.
-done

P6316: The combined label/region field is a bit confusing. Do only the GAW stations have a label whereas the EMEP stations have a region acronym? For clarity please highlight this in the caption and list the region acronyms.
-done

P6319: This table has unrealistically high number of significant digits. Please modify.
-done

P6322: The panels in this plot are missing labels as a) b) c), yet the caption refers to them. Also, why does the caption only refer to a) and b) instead of all three. Please be consistent. Also the panels are very small, such that the legend is not readable.
-done

P6324: The legend here does not list the region names as "Fires-Alaska" and "Fires-Siberia", as they were introduced previously. Please decide on a label for these regions and then stick to it consistently in text and Figures.
-done

P6325: Same in this Figure.
-done

P6326: It would be helpful to use different symbols/colours for SCIAMACHY and GOME-2 in this Figure.
For the daily values, different symbols are not an option due to the dense plotting in the long time series. We could use different colours; however, this would not be in accordance to the other Figures, then. We could, if this helps, introduce a vertical dashed line in the x-axis.

P6328: Same in this Figure.
-see above

P6329: The caption says "daily" but the Figure shows monthly averages. Please correct.

-done

P6331: This Figure has an unclear colour scale, making the interpretation of MNMBs close to zero challenging. Plots with divergent colour scale such as this should ideally have only one colour gradient for positive and negative values, respectively, with a neutral colour (white or grey) in between. I recommend shades of red for positive values and shades of blue for negative values with white or grey symmetrically around zero.
This is the colour bar used in the MACC validation exercises. We would like to keep it, for in this case we wanted to especially highlight large biases.

P6332: These plots are extremely busy and the legend is unreadable. Please consider ways of reducing the overplotting to increase the visual impact of the Figure. Also, once again, please consistently format and label the panels. Why does subplot a) consist of two panels and subplot b) of one panel. Why not have 3 separate subplots?
-done

P6333: Describe either in the caption or in the text how this seemingly random subset of stations was selected.
-done, we wanted to give some examples for every region to underline the findings in the text.

Referee 2:
Specific comments:

page 6280:
line 4: Avoid one sentence paragraphs
-done

line 19: better: "in their respective summer months" instead of just "in the summer months"
-done

page 6282:
line 16: It is no the 'paper that investigates', more something like this "In this paper we describe the investigation of..."
-done

page 6284:
line 24: "Table 2 lists the assimilated data products." instead of "...lists up..."
-done

page 6291
line 23: The figure order needs to be checked. This should be Figure 2 and not Figure 11, the Figure order has to be changed.
-done

page 6292:

line 8: Figure 13 (which should be plot 3) shows very large variability in the model data, compared to the observations. The agreement does not seem very good for the high latitude stations but there seems to be indeed an amelioration after Jul 2012.
-Yes, as described in the text

line 15: O3 in tropical regions (30_S to 30_N) seem to have min 20% differences up to 40%
-yes, but the average of all stations is 20%

line 19: could you show the correlation coefficients on the plots?
- We initially had MNMBs and correlation coefficients in the plots, which turned out somewhat busy and unreadable. So we decided to list them in the tables (Table 4 and 5).
Table 6 should be Table 4. Please change Table order.
- done

Figure 12: Legends are not legible, there are too many lines. The plots should be numbered a, b, c. There are curves that stop, eg the pink line in plot a. in Dec 2011. Why? Or one starts in Jun 2010 (black?) Maybe the plots should be stacked on top of each other.
-Because the observational data is not available for all stations during the whole time period

page 6293:
line 8: The correlation does not show a distinct seasonal behaviour in Fig 12, but the MNMBs or the RMSEs not either on this plot! How do you know this?
-MNMBs and RMSE show higher (positive MNMBs) values during the summer months and lower values (negative MNMBs) during the winter months.

line 15: There also seems to be a phase shift at KOS, KOV and CVO. TSU seems to have random observations, but the black points are not really visible behind the red line.
-done

line 27: Figure 15 should have the panels stacked and numbered a, b, c.
-done

page 6294:
line 6: MNMBs have already been described. These descriptions (also for RMSEs) could move to the O3 section.
- done

line 20: Reference to Table 4 should come earlier (line 7).
-done

line 24: Figure 2 could have the 3 plots stacked again.
-done

page 6395:line 3: Fig 3: Why do you use different stations for O3 and CO?
-the observational validation data sets are different for CO and O_3. Some stations provide measurements only for either CO or O_3.

page 6296:
line 1: Why do you use the IASI product, when you know that it is not as good as the MOPiTT product for higher latitudes?
-In the course of the validation work, it has become clear that these differences exist between the two data sets. Now, both data sets are assimilated in the MACC operational suite.

page 6296:
line 27: There is a stray 'to'
-done

page 6298:
lines 7-9: 'realistically reproduces': Isn't this a bit of an exaggeration with up to 110%underestimations for NO2? Incidentally the values are all negative overall and range from 5% to 70% underestimation. The values for CO seem to be 15% to -23%, whereas the overall values of -50% to 28% do not really agree well...
-done

line 9: It would be good to have a Table with the satellite results for CO, too.
-done

page 6299:
lines 27 to end of Discussion: O3 section should probably come first in the discussion.
-done

page 6301:
line 8: 'however with a negative offset' should probably be 'however, with a large negative offset'
-done

line 18: Wasn't the impact of the fire emisson error rather large!!
-done

General: Be consistent, sometimes it is Fig. in the text other times it is Figure.
-It was recommended by a referee to use "Figure", when starting a sentence, apart from that we use "Fig".

Figure 9 Caption, the latitudinal and longitudinal boundaries are defined in Figure 1 not in the text!
-done

Boersma, K.F., Eskes, H.J., Brinksma, E.J.: Error analysis for tropospheric NO_2 retrieval from space. J. Geophys. Res., 109, D4, doi:10.1029/2003JD003962, 2004.

Cuevas, E., Camino, C., Benedetti, A., Basart, S., Terradellas, E., Baldasano, J.M., Morcrette, J.-J., Marticorena, B., Goloub, P., Mortier, A., Berjón, A., Hernández, Y., Gil-Ojeda, M., Schulz, M.: The MACC-II 2007-2008 Reanalysis: Atmospheric Dust Evaluation and Characterization over Northern Africa and Middle East, Atmos. Chem. Phys. 15, 3991–4024, doi:10.5194/acp-15-3991-2015, 2015.

Elguindi, N., Clark, H., Ordóñez, C., Thouret, V., Flemming, J., Stein, O., Huijnen, V., Moinat, P., Inness, A., Peuch, V.-H., Stohl, A., Turquety, S., Athier, G., Cammas, J.-P., and Schultz, M.: Current status of the ability of the GEMS/MACC models to reproduce the tropospheric CO vertical distribution as measured by MOZAIC, Geosci. Model Dev., 3, 501-518, doi:10.5194/gmd-3-501-2010, 2010.

Eskes, H., Huijnen, V., Arola, A., Benedictow, A., Blechschmidt, A.-M.,
Botek, E., Boucher, O., Bouarar, I., Chabrillat, S., Cuevas, E., Engelen, R., Flentje, H., Gaudel, A., Griesfeller, J., Jones, L., Kapsomenakis, J.,Katragkou, E., Kinne, S., Langerock, B., Razinger, M., Richter, A., Schultz, M., Schulz, M., Sudarchikova, N., Thouret, V., Vrekoussis, M., Wagner, A., and Zerefos, C.: Validation of reactive gases and aerosols in the MACC global analysis and forecast system. Geosci. Model Dev. Discuss., 8, 1117-1169, doi:10.5194/gmdd-8-1117-2015, 2015.

Richter, A., Burrows, J. P., Nüß, H., Granier, C, Niemeier, U.: Increase in tropospheric nitrogen dioxide over China observed from space, Nature, 437-132,doi:10.1038/nature04092, 2005.

Savage, N. H., Agnew, P., Davis, L. S., Ordonez, C., Thorpe, R., Johnson, C. E., O'Connor, F. M., and Dalvi, M.: Air quality modelling using the Met Office Unified Model (AQUM OS24-26): model description and initial evaluation, Geosci. Model Dev., 6, 353–372, 2013, doi:10.5194/gmd-6-353-2013, 2013.

Sheel, V., Sahu, L.K., Kajinu, M., Deushi, M., Stein, O., Nedelec, P.: Seasonal and interannual variability of carbon monoxide based on MOZAIC observations, MACC reanalysis, and model simulations over an urban site in India. J. Geophys. Res., 119, 14, 9123–9141, 2014.

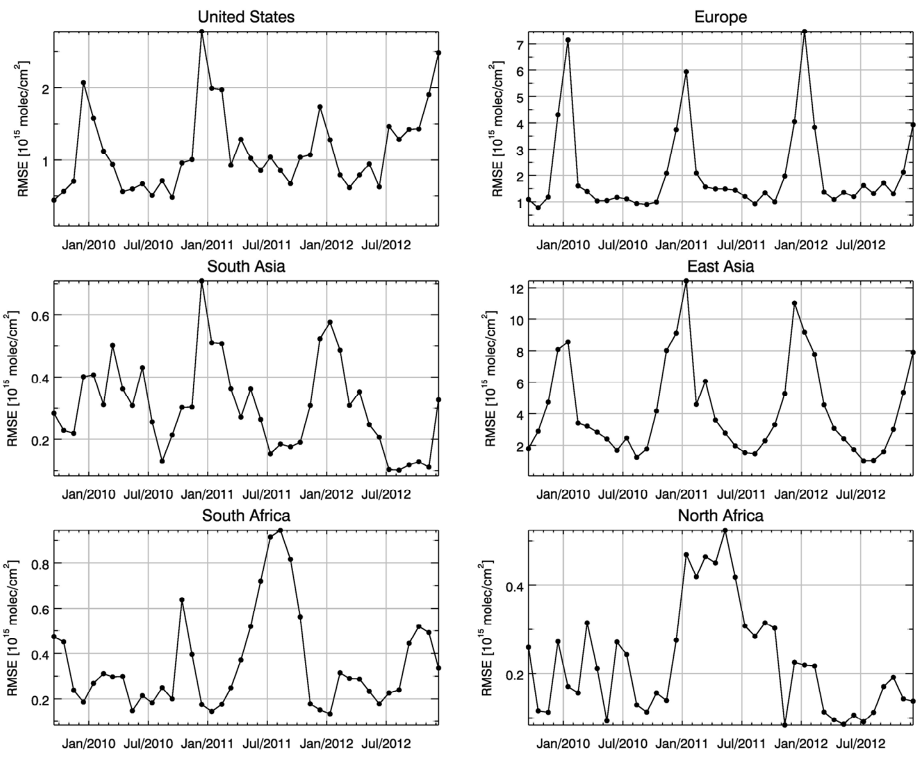

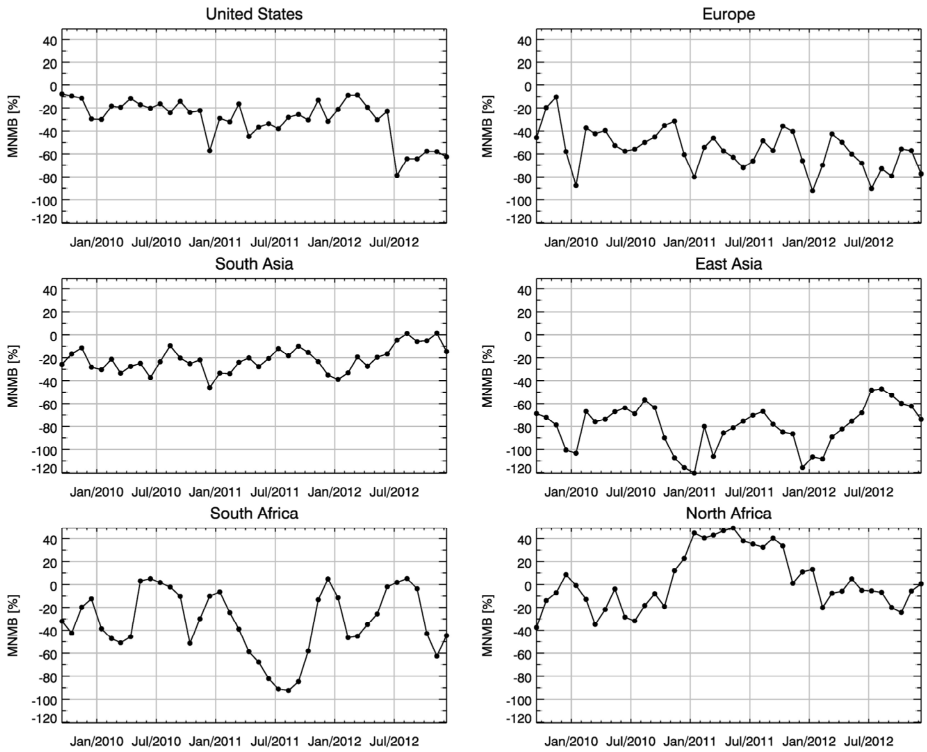
United States
Europe
South Asia
East Asia
South Africa
North Africa
MNMB [%]
40
20
0
-20
-40
-60
-80
-100
-120
Jan/2010
Jul/2010
Jan/2011
Jul/2011
Jan/2012
Jul/2012

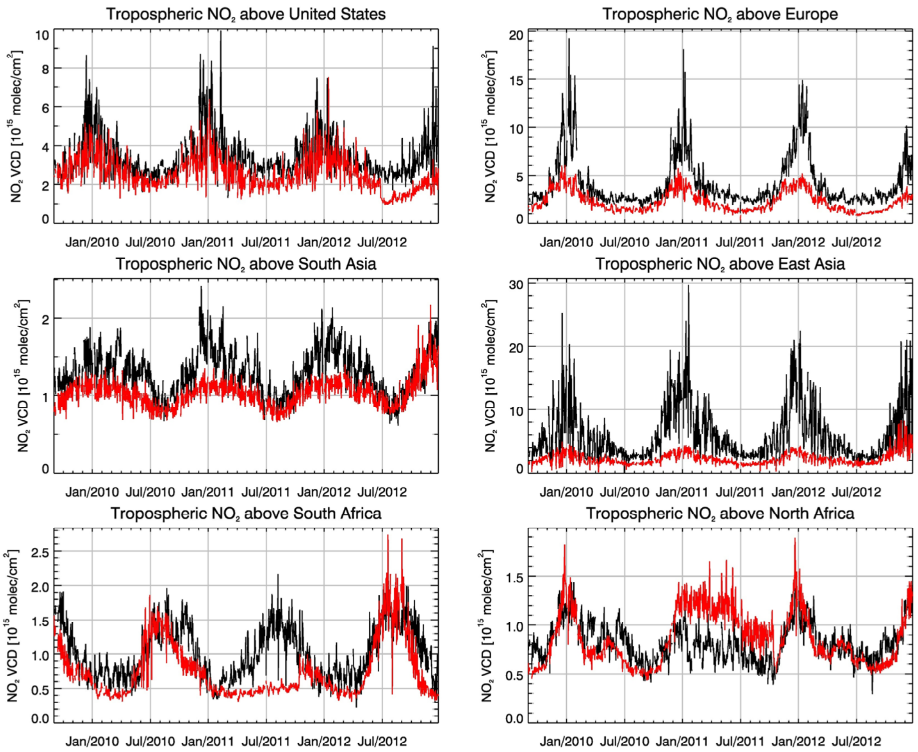
Tropospheric NO₂ above United States
Tropospheric NO₂ above Europe
Tropospheric NO₂ above South Asia
Tropospheric NO₂ above East Asia
Tropospheric NO₂ above South Africa
Tropospheric NO₂ above North Africa
NO₂ VCD [10¹⁵ molec/cm²]
Jan/2010
Jul/2010
Jan/2011
Jul/2011
Jan/2012
Jul/2012

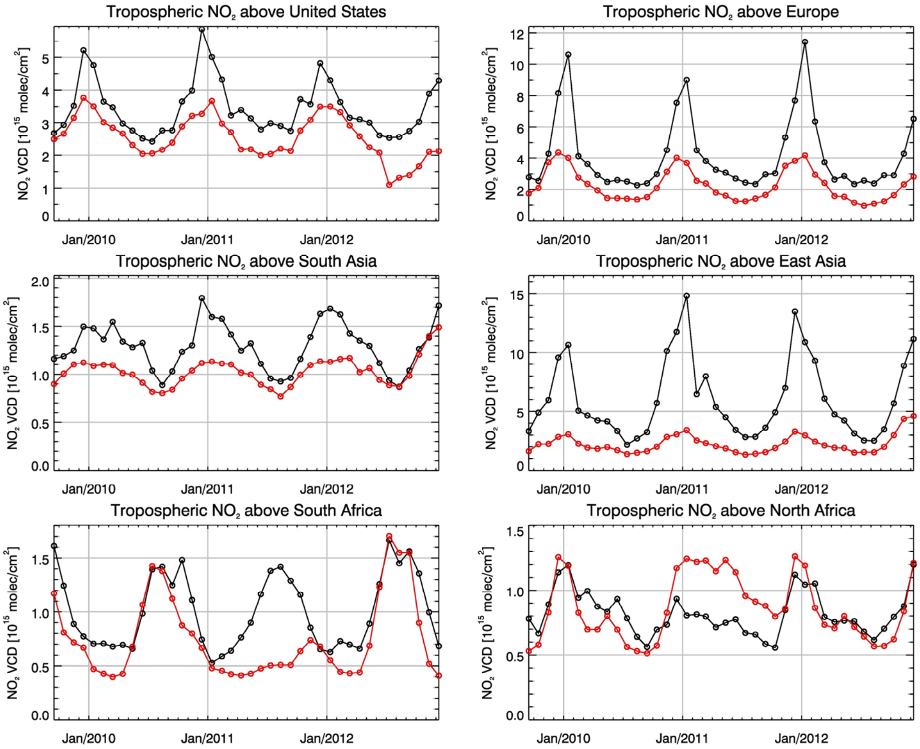
Tropospheric NO2 above United States
Tropospheric NO2 above Europe
Tropospheric NO2 above South Asia
Tropospheric NO2 above East Asia
Tropospheric NO2 above South Africa
Tropospheric NO2 above North Africa
NO2 VCD [10^15 molec/cm^2]
Jan/2010
Jan/2011
Jan/2012

(3) Marked-up manuscript version:

Evaluation of the MACC operational forecast system-potential and challenges of global near-real-time modelling with respect to reactive gases in the troposphere

A. Wagner1, A.–M. Blechschmidt2, I. Bouarar3[*], E.-G. Brunke4, C. Clerbaux3, M. Cupeiro5, P. Cristofanelli6, H. Eskes7, J. Flemming8, H. Flentje1, M. George3, S. Gilge1, A. Hilboll2, A. Inness8, J. Kapsomenakis9, A. Richter2, L. Ries10, W. Spangl11, O. Stein12, R. Weller13, C. Zerefos9

Gelöscht:

[1]{Deutscher Wetterdienst, Meteorologisches Observatorium Hohenpeissenberg, Germany}

[2]{Institute of Environmental Physics, University of Bremen, Germany}

[3]{Sorbonne Universités, UPMC Univ. Paris 06; Université Versailles St-Quentin; CNRS/INSU, LATMOS-IPSL, Paris, France}

[4]{South African Weather Service, Stellenbosch, South Africa}

[5]{National Meteorological Service, Ushuaia, Tierra del Fuego, Argentina}

[6]{National Research Council of Italy, ISAC, Bologna, Italy}

[7]{Royal Netherlands Meteorological Institute, De Bilt, The Netherlands}

[8]{European Centre for Medium-range Weather Forecasts, Reading, UK}

[9]{Academy of Athens, Research Centre for Atmospheric Physics and Climatology, Athens, Greece}

[10]{Federal Environment Agency, GAW Global Station Zugspitze/Hohenpeissenberg, Zugspitze 5, D-82475 Zugspitze}

[11]{Umweltbundesamt GmbH, Air Pollution Control & Climate Change Mitigation, Vienna, Austria}

[12]{Forschungszentrum Jülich, IEK-8 (Troposphere), Jülich, Germany}

[13]{Alfred Wegener Institute, Bremerhaven, Germany}

[*]{now at: Max-Planck-Institut for Meteorology, Hamburg, Germany}
Correspondence to: A. Wagner (Annette.wagner@dwd.de)

Abstract

Monitoring Atmospheric Composition and Climate (MACC) currently represents the European Union's Copernicus Atmosphere Monitoring Service (CAMS) (http://www.copernicus.eu/), which will become fully operational in the course of 2015. The global near-real-time MACC model production run for aerosol and reactive gases provides daily analyses and 5-day forecasts of atmospheric composition fields. It is the only assimilation system world-wide that is operational to produce global analyses and forecasts of reactive gases and aerosol fields. We have investigated the ability of the MACC analysis system to simulate tropospheric concentrations of reactive gases (CO, O_3, and NO_2) covering the period between 2009 and 2012. A validation was performed based on CO and O_3 surface observations from the Global Atmosphere Watch (GAW) network, O_3 surface observations from the European Monitoring and Evaluation Programme (EMEP) and furthermore, NO_2 tropospheric columns derived from the satellite sensors SCIAMACHY and GOME-2, and CO total columns derived from the satellite sensor MOPITT. The MACC system proved capable of reproducing reactive gas concentrations in consistent quality, however, with a seasonally dependent bias compared to surface and satellite observations: For northern hemisphere surface O_3 mixing ratios, positive biases appear during the warm seasons and negative biases during the cold parts of the years, with monthly Modified Normalised Mean Biases (MNMBs) ranging between -30% and 30% at the surface. Model biases are likely to result from difficulties in the simulation of vertical mixing at night and deficiencies in the model's dry deposition parameterization. Observed tropospheric columns of NO_2 and CO could be reproduced correctly during the warm seasons, but are mostly underestimated by the model during the cold seasons, when anthropogenic emissions are at a highest, especially over the US, Europe and Asia. Monthly MNMBs of the satellite data evaluation range between -110% and 40% for NO_2 and at most -20% for CO, over the investigated regions. The underestimation is likely to result from a combination of errors concerning the dry deposition

Gelöscht: /MACCII

Gelöscht: hemispheric

parameterization and certain limitations in the current emission inventories, together with an insufficiently established seasonality in the emissions.

1. Introduction

The impact of reactive gases on climate, human health and environment has gained increasing public and scientific interest in the last decade (Bell et al., 2006, Cape 2008, Mohnen et al., 2013, Seinfeld and Pandis 2006, Selin et al., 2009). As air pollutants, carbon monoxide (CO), nitrogen oxides (NO_x) and ozone (O_3) are known to have acute and chronic effects on human health, ranging from minor upper respiratory irritation to chronic respiratory and heart disease, lung cancer, acute respiratory infections in children and chronic bronchitis in adults (Bell et al., 2006, Kampa and Castanas 2006). Tropospheric ozone, even in small concentrations, is also known to cause plant damage in reducing plant primary productivity and crop yields (e.g. Ashmore 2005). It is also contributing to global warming by direct and indirect radiative forcing (Forster et al., 2007, Sitch et al., 2007). Pollution events can be caused by local sources and processes but are also influenced by continental and intercontinental transport of air masses. Global models can provide the transport patterns of air masses and deliver the boundary conditions for regional models, facilitating the forecast and investigation of air pollutants.

The EU-funded research project MACC - Monitoring Atmospheric Composition and Climate, (consisting of a series of European projects, MACC to MACC-III), provides the preparatory work that will form the basis of the Copernicus Atmosphere Monitoring Service (CAMS). This service is established by the EU to provide a range of products of societal and environmental value with the aim to help European governments respond to climate change and air quality problems. MACC provides reanalysis, monitoring products of atmospheric key constituents (e.g. Inness et al., 2013), as well as operational daily forecasting of greenhouse gases, aerosols and reactive gases (Benedetti et al., 2011, Stein et al., 2012) on a global and on European-scale level, and derived products such as solar radiation. An important aim of the MACC system is to describe the occurrence, magnitude and transport pathways of disruptive events, e.g., volcanoes (Flemming and Inness, 2013), major fires (Huijnen et al., 2012, Kaiser et al., 2012) and dust storms (Cuevas et al., 2015). The product catalogue can be found on the MACC website, http://copernicus-atmosphere.eu. For the generation of atmospheric products, state-of-the-art atmospheric modelling is combined with assimilated satellite data (Hollingsworth et al., 2008, Inness et al., 2013, 2015, more general information about data assimilation can be found in e.g. Ballabrera-Poy et al., 2009 or Kalnay 2003). Within the MACC project there is a dedicated validation activity to provide up-to-date information on the quality of the reanalysis, daily analyses and forecasts. Validation reports are updated regularly and are available on the MACC websites.

The MACC global near-real-time (NRT) production model for reactive gases and aerosol has operated with data assimilation from September 2009 onwards, providing boundary conditions for the MACC regional air quality products (RAQ), and other downstream users. The model simulations also provide input for the stratospheric ozone analyses delivered in near-real-time by the MACC stratospheric ozone system (Lefever et al., 2014).

In this paper we describe the investigation of the potential and challenges of near-real-time modelling with the MACC analysis system between 2009 and 2012. We concentrate on this period because of the availability of validated independent observations (namely surface observations from the Global Atmosphere Watch Programme GAW, the European Monitoring and Evaluation Programme EMEP, as well as total column satellite data from the MOPITT, SCIAMACHY and GOME-2 sensors) that are used for comparison. In particular, we study the model's ability to reproduce the seasonality and absolute values of CO and NO_2 in the troposphere as well as O_3 and CO at the surface. The impact of changes in model version, data assimilation and emission inventories on the model performance is examined and discussed. The paper is structured in the following way: Section 2 contains a description of the model and the validation data sets as well as the applied validation metrics. Section 3 presents the validation results for CO, NO_2 and O_3. Section 4 provides the discussion and section 5 the conclusions of the paper.

2. Data and Methods

2.1 The MACC model system in the 2009-2012 period

The MACC global products for reactive gases consist of a reanalysis performed for the years 2003-2012 (Inness et al., 2013) and the near-real-time analysis and forecast, largely based on the same assimilation and forecasting system, but targeting different user groups. The MOZART chemical transport model (CTM) is coupled to the

Formatiert: Nummerierung und Aufzählungszeichen

Gelöscht: Reactive gases play an important role in tropospheric chemistry. ¶
<#>Carbon monoxide (CO) is part of a photo-chemically driven reaction sequence that links methane (CH4), formaldehyde (HCHO), ozone (O3), and the hydroxyl radical (OH). It also is a precursor of tropospheric ozone. Carbon monoxide has natural and anthropogenic sources (Seinfeld and Pandis, 2006). Its main sources are incomplete fossil fuel and biomass burning, but also the oxidation of anthropogenic and biogenic volatile organic compounds (VOCs). ¶
<#>High CO concentrations in the troposphere are found especially over the industrial regions of Europe, Asia and North America as well as over biomass burning regions in Africa. In the northern hemisphere the surface CO concentration peak appears around March with typical mixing ratios of around 150 parts per billion (ppb) measured at background stations (e.g., Stein et al., 2014). The northern hemisphere winter CO maximum results largely from a build-up of anthropogenic emissions, while in the southern hemisphere, biomass burning is the dominant contributor of CO in the boreal summer (July-October). In both hemispheres, reaction with OH leads to a minimum of CO in their respective summer months. In areas with large biogenic emissions (e.g., tropical rain forests), the oxidation of biogenic VOCs contributes strongly to the production of CO (Griffin et al., 2007). ¶
<#>Ozone in the troposphere is highly relevant for the Earth's climate, ecosystems, and human health (e.g., Cape 2008, Mohnen et al., 2013, Selin et al., 2009). Due to its relatively short lifetime in the atmosphere when compared to carbon dioxide, ozone is often referred to as "short-lived climate forcer". It is the third largest contributor of anthropogenic greenhouse gas radiative forcing after carbon dioxide and methane (Forster et al., 2007) and it plays a crucial role in tropospheric chemistry as the main precursor of the OH radical which determines the oxidation capacity of the troposphere (e.g., Seinfeld and Pandis, 2006, Cooper et al., 2014). As a toxic air pollutant, higher concentrations of O3 can also affect human health (... [1]

Integrated Forecast System (IFS) of the European Centre for Medium-Range Weather forecast (ECMWF), which together represent the MOZART-IFS model system (Flemming et al., 2009 and Stein et al. 2012). An alternative analysis system has been set up based on the global CTM TM5 (Huijnen et al., 2010). Details of the MOZART version used in the MACC global products can be found in Kinnison et al., 2007 and Stein et al. (2011, 2012). In the simulation, the IFS and the MOZART model run in parallel and exchange several two- and three-dimensional fields every model hour using the OASIS4 coupling software (Valcke and Redler 2006), thereby producing three-dimensional IFS fields for O_3, CO, SO_2, NO_x, HCHO, sea salt aerosol, desert dust, black carbon, organic matter, and total aerosol. The IFS provides meteorological data to MOZART. Data assimilation and transport of the MACC species takes place in IFS, while the whole chemical reaction system is calculated in MOZART.

The MACC_osuite (operational suite) is the global near-real-time MACC model production run for aerosol and reactive gases. Here, we have investigated only the MACC analysis. In contrast to the reanalysis, the MACC_osuite is a near-real-time run, which implies that it is only run once in near-real-time and may thus contain inconsistencies in e.g. the assimilated data. The MACC_osuite was based on the IFS cycle CY36R1 with IFS model resolution of approximately 100 km by 100 km at 60 levels (T159L60) from September 2009 until July 2012. The gas-phase chemistry module in this cycle is based on MOZART-3 (Kinnison et al., 2007). The model has been upgraded, following updates of the ECMWF meteorological model and MACC-specific updates, i.e. in chemical data assimilation and with respect to the chemical model itself. Thus, from July 2012 onwards, the MACC_osuite has run with a change of the meteorological model to a new IFS cycle (version CY37R3), with an IFS model resolution of approximately 80 km at 60 levels (T255L60) and an upgrade of the MOZART version 3.5 (Kinnison et al., 2007; Emmons et al., 2011, Stein et al. 2013). This includes, amongst others, updated velocity fields for the dry deposition of O_3 over ice, as described in Stein et al. (2013). A detailed documentation of system changes can be found at:

http://www.copernicus-atmosphere.eu/oper_info/nrt_info_for_users/

2.1.1 Emission inventories and assimilated data sets

In the MACC_osuite, anthropogenic emissions are based on emissions out of the EU project RETRO merged with updated emissions for East Asia from the REAS

Gelöscht: ¶

Formatiert: Schriftart: 12 pt, Schriftartfarbe: Schwarz

Formatiert: Zeilenabstand: 1,5 Zeilen, Abstand zwischen asiatischem und westlichem Text anpassen

Gelöscht: go back to

Formatiert: Schriftart: 12 pt, Schriftartfarbe: Schwarz, Englisch (Großbritannien)

Formatiert: Schriftart: 12 pt, Schriftartfarbe: Schwarz inventory, (Schultz et al. 2007) in the following referred to as RETRO-REAS. The horizontal resolution is 0.5° in latitude and longitude and it contains a monthly temporal resolution. Biogenic emissions are taken from GEIA, fire emissions are based on a climatology derived from GFEDv2 (van der Werf et al., 2006) until April 2010, when fire emissions change to GFAS fire emissions (Kaiser et al., 2012). Between January 2011 and October 2011 there has been a fire emission reading error in the model, where, instead of adjusting emissions to the appropriate month, the same set of emissions have been read throughout this period.

Formatiert: Schriftart: 12 pt, Schriftartfarbe: Schwarz, Englisch (Großbritannien)

Formatiert: Schriftart: 12 pt, Schriftartfarbe: Schwarz, Englisch (Großbritannien)

Gelöscht:

Gelöscht: a merged RETRO-REAS inventory

Gelöscht: ; b

Gelöscht: both available in monthly resolution (Schultz et al., 2007). F

After the model upgrade to the new cycle version CY37R3, in July 2012, the emission inventories changed from the merged RETRO-REAS and GEIA inventories, used in the previous cycle, to the MACCity anthropogenic and biogenic emissions (Granier et al., 2011) and (climatological) MEGAN-v2 (Guenther et al., 2006) emission inventories. Wintertime anthropogenic CO emissions are scaled up over Europe and North America (see Stein et al., 2014). Near-real-time fire emissions are taken from GFASv1.0 (Kaiser et al. 2012), for both gas-phase and aerosol.

In the MACC_osuite, the initial conditions for some of the chemical species are provided by data assimilation of atmospheric composition observations from satellites (see Benedetti et al., 2009; Inness et al., 2009, 2013; Massart et al., 2014). Table 1 lists the assimilated data products. From September 2009 to June 2012, O_3 total columns of the MLS and SBUV-2 instruments are assimilated, as well as OMI and SCIAMACHY total columns (the latter only until March 2012, when the European Space Agency lost contact with the ENVIronmental SATellite ENVISAT). CO total columns are assimilated from the IASI sensor and aerosol total optical depth is assimilated from the MODIS instrument. After the model cycle update in July 2012, data assimilation also contains OMI tropospheric columns of NO_2 and SO_2, as well as CO MOPITT total columns. The CO total columns retrieved by MOPITT and IASI instruments have a relatively similar seasonality, but there is a systematic difference with MOPITT CO being higher over most regions in the northern hemisphere, especially during winter and spring. George et al. ("An examination of the long-term CO records from MOPITT and IASI and comparison of retrieval methodology", AMTD, 2015 submitted) investigated the differences between MOPITT and IASI, and showed the impact of a priori information on the retrieved measurements.

Gelöscht: 2

Gelöscht: up

Table 1 and 2 summarize the data assimilation and setup of the MACC_osuite.

Gelöscht: and data assimilation

2.2 Validation data and methodology

In this study, mainly the same evaluation data sets have been used as during the MACC near-real-time validation exercise. This implies some discontinuities in the evaluations, e.g. the substitution of SCIAMACHY data with GOME-2 data after the loss of the ENVISAT sensor or an exclusion of MOPITT satellite data after the start of its assimilation into the model. The continuous process of updating and complementation of data sets in databases requires the selection and definition of an evaluation data set at some point. The comparatively small inconsistencies between our data sets are considered to have a negligible impact on the overall evaluation results.

2.2.1 GAW Surface O_3 and CO Observations

The Global Atmosphere Watch (GAW) programme of the World Meteorological Organization (WMO) has been established to provide reliable long-term observations of the chemical composition and physical properties of the atmosphere, which are relevant for understanding atmospheric chemistry and climate change (WMO, 2013). GAW tropospheric O_3 measurements are performed in a way to be suitable for the detection of long-term regional and global changes. Furthermore, the GAW measurement programme focuses on observations, which are regionally representative and should be free from influence of significant local pollution sources and suited for the validation of global chemistry climate models (WMO 2007). Detailed information on GAW and GAW related O_3 and CO measurements can be found in WMO (2010, 2013).

Gelöscht: a

Gelöscht: 2007b,

Hourly O_3 and CO data have been downloaded from the WMO/GAW World Data Centre for Greenhouse Gases (WDCGG) for the period between 09/2009 and 12/2012 (status of download: 07/2013). Our evaluation includes 29 stations with surface observations for CO and 50 stations with surface observations for O_3. Table 3 lists the geographic coordinates and altitudes of the individual stations. Being a long-term data network, the data in the database is provided with a temporal delay of approximately 2 years. As the data in the database becomes sparse towards the end of the validation period, near-real-time observations, as used in the MACC-project for near-real-time validation, presented on the MACC website, have been included to complement the validation data sets. For the detection of long-term trends and year-to-year variability,

Gelöscht: Tropospheric h

Gelöscht: _new

the data quality objectives (DQOs) for CO in GAW measurements are set to a maximum uncertainty of ± 2 ppb and to ± 5 ppb for marine boundary layer sites and continental sites that are influenced by regional pollution and to ± 1 ppb for ozone (WMO, 2012, 2013).

For the evaluation with GAW station data, 6-hourly values (0, 6, 12, 18 UTC) of the analysis mode have been extracted from the model and are matched with hourly observational GAW station data. Model mixing ratios at the stations' location have been linearly interpolated from the model data in the horizontal. In the vertical, modelled gas mixing ratios have been extracted at the model level, which is closest to the GAW stations' altitude. Validation scores (see section 2.3) have been calculated for each station between the 6-hourly model analysis data and the corresponding observational data for the entire period (09/2009- 12/2012) and as monthly averages.

2.2.2 EMEP Surface O_3 Observations

The European Monitoring and Evaluation Programme (EMEP) is a scientifically based and policy driven programme under the Convention on Long-Range Transboundary Air Pollution (CLRTAP) for international co-operation to solve transboundary air pollution problems. Measurements of air quality in Europe have been carried out under the EMEP since 1977.

A detailed description of the EMEP measurement programme can be found in Tørseth et al. (2012). The surface hourly ozone data between 09/2009 and 12/2012 have been downloaded from the EMEP data web-page (http://www.nilu.no/projects/ccc/emepdata.html). For the validation, only stations meeting the 75% availability threshold per day and per month are taken into account. The precision is close to 1.5 ppb for a 10s measurement. More information about the ozone data quality, calibration and maintenance procedures can be found in Aas et al. (2000).

For comparison with EMEP data, 3-hourly model values (0, 3, 6, 12, 15, 18, 21 UTC) of the analysis mode have been chosen, in order to be able to evaluate day and night time performance of the model separately. Gas mixing ratios have been extracted from the model and are matched with hourly observational surface ozone data at 124 EMEP stations in the same way as for the GAW station data. The EMEP surface ozone values and the interpolated surface modeled values are compared on a monthly basis for the latitude bands of 30°N – 40°N (southern Europe), 40°N – 50°N (central Europe) and 50°N – 70°N (northern Europe). For the identification of differences in the MACC_osuite performance between day and night time, the MACC_osuite simulations and the EMEP observations for the three latitude bands have been additionally separated into day-time (12:00–15:00 Local Time LT) and night-time (00:00–03:00 LT) intervals.

2.2.3 MOPITT CO total column retrievals

The MOPITT (Measurement Of Pollution In The Troposphere) instrument is mounted on board the NASA EOS Terra satellite and provides CO distributions at the global scale (Deeter et al., 2004). MOPITT has a horizontal resolution of 22 km x 22 km and allows global coverage within 3 days. The data used in this study corresponds to CO total columns from version 5 (V5) of the MOPITT thermal infrared (TIR) product level 3. This product is available via the following web server: http://www2.acd.ucar.edu/mopitt/products. Validation of the MOPITT V5 product against in-situ CO observations showed a mean bias of 0.06×10^{18} molecules cm^{-2} (Deeter et al., 2013). Following the recommendation in the users' guide, (www.acd.ucar.edu/mopitt/v5_users_guide_beta.pdf), the MOPITT data were averaged by taking into account their relative errors provided by the Observation Quality Index (OQI).

Also, in order for better data quality we used only daytime CO data since retrieval sensitivity is greater for daytime rather than nighttime overpasses. A further description of the V5 data is presented in Deeter et al. (2013) and Worden et al. (2014).

For the validation, the model CO profiles (X) were transformed by applying the MOPITT averaging kernels (A) and the a priori CO profile (X_a) according to the following equation (Rodgers, 2000) to derive the smoothed profiles X* appropriate for comparison with MOPITT data:

$$X^* = X_a + A(X - X_a)$$

Details on the method of calculation are referred to in Deeter et al. (2004) and Rodgers (2000). The averaging kernels indicate the sensitivity of the MOPITT measurement and retrieval system to the true CO profile, with the remainder of the information set by the a priori profile and retrieval constraints (Emmons, 2009; Deeter et al., 2010). The model CO total columns used in the comparison with MOPITT observations, have been calculated using the averaging kernel smoothed profiles X* which have the same vertical resolution and a priori dependence as the MOPITT retrievals. For the evaluation, 8 regions are defined (see Fig. 1): Europe, Alaska, Siberia, North Africa, South Africa, South Asia, East Asia and the United States. The model update in July 2012 includes an integration of MOPITT CO total columns in the model's data assimilation system. With this, the MOPITT validation data has lost its independency for the rest of the validation period and MOPITT validation data has thus only been used until June 2012 for validation purposes.

Gelöscht: _new
Formatiert: Englisch (USA)
Gelöscht: Fires-
Formatiert: Englisch (USA)
Gelöscht: Fires-

2.2.4 SCIAMACHY and GOME-2 NO_2 Satellite Observations

The SCanning Imaging Absorption spectroMeter for Atmospheric CHartographY (SCIAMACHY; Bovensmann et al., 1999) onboard the ENVISAT and the Global Ozone Monitoring Experiment-2 (GOME-2; Callies et al., 2000) onboard the Meteorological Operational Satellite-A (MetOp-A) comprise UV-VIS and NIR sensors designed to provide global observations of atmospheric trace gases.

Gelöscht: UV-vis
Gelöscht: near-infrared

In this study, the tropospheric NO_2 column data set described in Hilboll et al. (2013a) has been used. In short, the measured radiances are analysed using Differential Optical Absorption Spectroscopy (DOAS), (Platt and Stutz, 2008) in the 425–450 nm wavelength window (Richter and Burrows, 2002). The influence of stratospheric NO_2 air masses has been accounted for using the algorithm detailed by Hilboll et al. (2013b), using stratospheric NO_2 fields from the B3dCTM model (Sinnhuber at al., 2003a; Sinnhuber et al., 2003b; Winkler et al., 2008). Tropospheric air mass factors have been calculated with the radiative transfer model SCIATRAN (Rozanov et al., 2005). Only measurements with FRESCO+ algorithm (Wang et al., 2008) cloud fractions of less than 20% are used.

Tropospheric NO_2 vertical column densitiy (VCD) from the MACC_osuite is compared to tropospheric NO_2 VCD from GOME-2 and SCIAMACHY. As the European Space Agency lost contact with ENVISAT in April 2012, GOME-2 data is used for model validation from 1 April 2012 onwards, while SCIAMACHY data is used for the remaining time period (September 2009 to March 2012). Satellite observations are gridded to the horizontal model resolution, i.e. 1.875° for IFS cycle CY36R1 (09/2009 -06/2012) and 1.125° for cycle CY37R3 (07/2012- 12/2012).

A few processing steps are applied to the MACC_osuite data to account for differences to the satellite data such as observation time. Firstly, model data are vertically integrated to tropospheric NO_2 VCDs by applying National Centers for Environmental Prediction (NCEP) reanalysis (Kalnay et al., 1996) climatological tropopause pressure shown in Fig.1 of Santer et al. (2003). Secondly, simulations are interpolated linearly in time to the SCIAMACHY equator crossing time (roughly 10:00 LT). This most likely leads to some minor overestimation of model NO_2 VCDs compared to GOME-2 data, as the equator crossing time for GOME-2 is about 9:30 LT. Moreover, only model data for which corresponding satellite observations exist are considered. For the evaluation, the same regions have been used as for MOPITT (Fig.1), except for Siberia and Alaska. In contrast to MOPITT data, no averaging kernel is applied.

Satellite observations of tropospheric NO_2 columns have relatively large uncertainties, mainly linked to incomplete stratospheric correction (important over clean regions and at high latitudes in winter and spring) and to uncertainties in air mass factors (mainly over polluted regions) (e.g. Boersma et al., 2004 and Richter et al., 2005). The uncertainty varies with geolocation and time but in first approximation can be separated into an absolute error of 5×10^{14} molec cm^{-2} and a relative error of about 30%, whichever is larger. As some of the contributions to this uncertainty are systematic, averaging over longer time periods does not reduce the errors as much as one would expect for random errors. Over polluted regions, the uncertainty from random noise in the spectra is small in comparison to other error sources, in particular for monthly averages.

Gelöscht: ure
Gelöscht:
Gelöscht: -new
Formatiert: Schriftart: Times New Roman, 12 pt, Muster: Transparent
Formatiert: Muster: Transparent
Gelöscht: ¶

2.3 Validation metrics

A comprehensive model evaluation requires the selection of validation metrics that provide complementary aspects of model performance. The following metrics have been used in the evaluation:

Modified Normalized Mean Bias MNMB

$$MNMB = \frac{2}{N}\sum_i \frac{f_i - o_i}{f_i + o_i} \qquad (1)$$

Root Mean Square Error RMSE

$$RMSE = \sqrt{\frac{1}{N}\sum_i (f_i - o_i)^2} \qquad (2)$$

Correlation Coefficient

$$R = \frac{\frac{1}{N}\sum_i \left(f_i - \bar{f}\right)\left(o_i - \bar{o}\right)}{\sigma_f \sigma_o} \qquad (3)$$

where: N is the number of observations, f are the modelled analysis and o the observed values, $\bar{f}$ and $\bar{o}$ are the mean values of the analysis and observed values and σ_f and σ_o are the corresponding standard deviations.

The validation metrics above have been chosen to provide complementary aspects of model performance. The modified normalized mean bias is a normalization based on the mean of the observed and forecast value (e.g. Elguindi et al. 2010). It ranges between

-2 and 2 and is very useful to check whether there is a negative or positive deviation between model and observations. When multiplied by 100%, it can be interpreted as a percentage bias. The advantage of the MNMB is that it varies symmetrically with respect to under- and overestimation and is robust with respect to outliers. However, when calculated over longer time periods, a balance in model error, with model over- and underestimation compensating each other, can lead to a small MNMB for the overall period. For this reason, it is important to additionally consider an absolute measure, such as the RMSE. However, it has to be noted that the RMSE is strongly influenced by larger values and outliers, due to squaring. The correlation coefficient R can vary between 1 (perfect correlation) and -1 (negative correlation) and is an important measure to check the linearity between model and observations.

3. Results

3.1 Evaluation of Ozone

The evaluation of the MACC_osuite run with O_3 from GAW surface observations (described in section 2.2.1) demonstrates good agreement in absolute values and seasonality for most regions. Figure 2 shows maps with Modified Normalized Mean Bias (MNMB, see section 2.3) evaluations for 50 GAW stations globally (top) and in Europe (below). Figure 3 presents selected time series plots representing the results for high latitudes, low latitudes and Europe. Large negative MNMBs over the whole period 09/2009 to 12/2012 (-30 to -82%) are observed for stations located in Antarctica (Neumayer-NEU, South Pole-SPO, Syowa-SYO and Concordia- CON) whereby O_3 surface mixing ratios are strongly underestimated by the model. For

Gelöscht:

Gelöscht:

Formatiert: Nummerierung und Aufzählungszeichen

Gelöscht: O_3

Gelöscht: mixing ratios

Gelöscht: 11

Gelöscht: _new

Gelöscht: a

Gelöscht: MNMB

Gelöscht:

stations located in high latitudes in the northern hemisphere (Barrow-BAR, Alaska and Summit-SUM, Denmark), the MACC_osuite exhibits similar underestimated values of up to -35% for the whole evaluation period. The time series plots for Arctic and Antarctic stations (e.g. Summit-SUM, Neumayer-NEU and South Pole-SPO) in Fig. 3 show that an underestimation visible in these regions has been remedied and model performance improved with an updated dry deposition parameterization over ice, which has been introduced with the new model cycle in July 2012 (see section 2.1).

Gelöscht: the far north

Gelöscht: 13

Gelöscht: _new

Large positive MNMBs (up to 50 to 70%, Fig. 2) are observed for stations that are located in or nearby cities and thus exposed to regional sources of contamination (Iskrba-ISK Slovenia, Tsukuba- TSU, Japan, Cairo-CAI, Egypt). In tropical and subtropical regions, O_3 surface mixing ratios are systematically overestimated (by about 20% on average) during the evaluation period. The time series plots for tropical and subtropical stations (e.g. for Ragged Point-RAG, Barbados and Cape Verde Observatory, Cape Verde –CVO, Fig. 3) reveal a slight systematic positive offset throughout the year, however with high correlation coefficients (0.6 on average).

Gelöscht: Fig. 11

Gelöscht: _new

Gelöscht: 13

Gelöscht: -new

For GAW stations in Europe, the evaluation of the MACC_osuite for the whole period shows MNMBs between -80 and 67%. Large biases appear only for 2 GAW stations located in Europe: Rigi- RIG, Switzerland (-80%), located near mountainous terrain and Iskrba- ISK, Slovenia (67%). For the rest of the stations MNMBs lie between 22 and -30%. Root Mean Square Errors (RMSEs, see section 2.3) range between 7 and 35 ppb (15 ppb on average). Again, results for Iskrba-ISK and Rigi-RIG show the largest errors. All other stations show RMSEs between 7 and 20 ppb. Correlation coefficients here range between 0.1 and 0.7 (with 0.5 on average). Table 4 summarizes the results for all stations individually.

Gelöscht: RMSEs

Gelöscht: 6

Gelöscht: _new

Monthly MNMBs (see Fig. 4) show a seasonally varying bias, with positive MNMBs occurring during the northern summer months (with global average ranging between 5 and 29% during the months June and October), and negative MNMBs during the northern winter months (between -2 and -33% during the months December to March). These deviations partly cancel each other out in MNMB for the whole evaluation period. For the RMSEs, (Fig. 5) maximum values also occur during the northern summer months with global average ranging between 11 and 16 ppb for June to September. The smallest errors appear during the northern hemisphere winter

Gelöscht: 12

Gelöscht: _new

Gelöscht: _new

months (global average falling between 8 and 10 ppb for December and January). The correlation does not show a distinct seasonal behaviour (see Fig. 6).

The time series plots in Fig. 3 show that the seasonal cycle of O_3 mixing ratios with maximum concentrations during the summer months and minimum values occurring during winter times for European stations (e.g. Monte Cimone-MCI, Italy, Kosetice-KOS, Czech Republic, and Kovk- KOV, Slovenia), could well be reproduced by the model, although there is some overestimation in summer resulting mostly from observed minimum concentrations that are not captured correctly by the MACC_osuite, (Kosetice-KOS, Czech Republic, and Kovk- KOV, Slovenia).

The validation with EMEP surface ozone observations (described in section 2.2.2) in three different regions in Europe for the period 09/2009 to 12/2012 likewise confirms the behaviour of the model to overestimate O_3 mixing ratios during the warm period and underestimate O_3 concentrations during the cold period of the year (see Fig. 7). The positive bias (May-November) is between -9 and 56% for northern Europe and Central Europe and between 8% and 48% for Southern Europe. Negative MNMBs appear, in accordance with GAW validation results, during the winter-spring period (December-April) ranging between -48 and -7% for EMEP stations in northern Europe (exception: December 2012 with 25%), between -1 and -39% in central Europe (exception: December 2012 with 31%), whereas in southern Europe, deviations are smaller and remain mostly positive (between -8 and 9%) in winter (exception: December 2012 with 37%). The different behaviour for December 2012 likely results from the limited availability of observations towards the end of the validation period. The separate evaluation of day and night-time O_3 mixing ratios (Fig. 8) shows that for northern Europe larger biases appear during night time. For central Europe and southern Europe night-time biases are larger during cold periods (December-April), whereas during warm periods (May–November) larger biases appear during day time.

3.2 Evaluation of Carbon Monoxide

The evaluation of the MACC_osuite with surface observations of 29 GAW stations (described in section 2.2.1) shows that over the whole period September 2009 to December 2012, CO mixing ratios could be reproduced with an average MNMB of -10%. The MNMBs for all stations range between -50 and +30%. Results are listed in

Gelöscht: winter
Gelöscht: 12
Gelöscht: _new
Gelöscht: 13
Gelöscht: _new
Gelöscht: 14
Gelöscht: _new
Gelöscht: 2010
Formatiert: Tiefgestellt
Gelöscht: the diurnal O_3 cycle
Gelöscht: 15
Gelöscht: _new
Gelöscht:
Gelöscht: 09/2009
Gelöscht: to 12/2012
Gelöscht: Modified Normalized Mean Bias (MNMB, see section 2.3)

Table 5, a selection of time series plots shows the results for stations in Europe, Asia and Canada in Fig. 9. MNMBs exceeding ± 30% appear for stations that are either located in or nearby cities and thus exposed to regional sources of contamination (Kosetice- KOS, Czech Republic) or are located in or near complex mountainous terrain (Rigi-RIG, Switzerland, BEO Moussala- BEO, Bulgaria) which is not resolved by the topography of the global model. RMSEs fall between 12 and 143 ppb (on average 48 ppb) for all stations during the validation period, but for only four stations (Rigi-RIG, Kosetice- KOS, Payerne-PAY, Switzerland and BEO Moussala-BEO, all located in Europe) do the RMSEs exceed 70 ppb. Correlation coefficients from the comparison with GAW station data calculated over the whole time period range between 0 and 0.8 (on average 0.4), with only four stations showing values smaller than 0.2 (Rigi-RIG, Moussala-BEO, East Trout Lake-ETL and Lac la Biche-LAC (the latter two located in Canada).

Considering the monthly MNMBs and RMSEs, it can be seen that during the northern hemisphere summer months, June to September, both are small (absolute differences less than 5%), see Fig. 10 and Fig. 11. Negative MNMBs (up to -35%) and larger RMSEs (up to 72 ppb) appear during the northern hemisphere winter months, November to March, when anthropogenic emissions are at a highest, especially for the US, northern latitudes and Europe. Monthly correlation coefficients are between 0.1 and 0.5 and do not show a distinct seasonal behaviour (see Fig. 12), the low values of 0.1 during the period January 2011 to October 2011 result from the reading error in the fire emissions (see section 2.1.1). The generally only moderate correlation coefficient is related to mismatches in the strong short-term variability seen in both the model and the measurements.

The time series plots for stations in Europe, Asia and Canada in Fig. 9 demonstrate that the annual CO cycle could to a large degree be reproduced correctly by the model with maximum values occurring during the winter period and minimum values appearing during the summer season. However, the model shows a negative offset during the winter period. Seasonal air mass transport patterns that lead to regular annual re-occurring CO variations could be reproduced for GAW stations in East Asia: The time series plots for Yonagunijima- YON and Minamitorishima- MNM station, Japan (Fig. 9) show that the drop of CO, associated with the air mass change from continental to cleaner marine air masses after the onset of the monsoon season during the early summer months, is captured by the MACC_osuite. Deterioration in

Gelöscht: _new
Gelöscht: Root Mean Square Errors (RMSEs, see section 2.3)
Gelöscht: All results are listed in Table 4.
Gelöscht: ,
Gelöscht: and correlation coefficients
Gelöscht: MNMBs
Gelöscht: 2a
Gelöscht: 9
Gelöscht: _new
Gelöscht: c
Gelöscht: 0
Gelöscht: _new
Gelöscht: Correlation coefficients are between 0.1 and 0.5 and do not show a distinct seasonal behaviour (see Fig 2).
Gelöscht: hemispheric
Gelöscht: 2b
Gelöscht: 1
Gelöscht: _new
Gelöscht: .
Gelöscht: of
Gelöscht:
Gelöscht: rather low
Gelöscht: 3
Gelöscht: 12
Gelöscht: _new
Gelöscht: 3
Gelöscht: 12
Gelöscht: _new

all scores is visible during December 2010 in the time series plots of several stations (e.g. Jungfraujoch-JFJ, and Sonnblick-SBL, Fig. 9). This is likely a result of changes in the processing of the L2 IASI data and a temporary blacklisting of IASI data (to avoid model failure) in the assimilation.

Gelöscht: 3
Gelöscht: 12
Gelöscht: _new

The comparison with MOPITT satellite CO total columns between October 2009 and June 2012 (described in section 2.2.3) shows a good qualitative agreement of spatial patterns and seasonality, see Table 6. The MNMBs for 8 regions are listed in Fig. 13 and range between 14% and -22%. The seasonality of the satellite observations is captured well by the MACC_osuite over Asia and Africa, with MNMBs between -6% and 9% (North Africa), -12% and 8% (South Africa), -11% and 12% (East Asia), and -3% and 14% (South Asia). The largest negative MNMBs appear during the winter periods, especially from December 2010 to May 2011 and from September 2011 to April 2012, for Alaska and Siberia and for the US and Europe (MNMBs up to -22%), which coincides with large differences between MOPITT and IASI satellite data (see Fig. 14). On the global scale the average difference between the IASI and MOPITT total columns is less than 10% (George et al., 2009), and there is a close agreement of MOPITT and IASI for S. Asia and Africa (see Fig. 14). However, larger differences between MOPITT and IASI data appear during the northern winter months over Alaska, Siberia, Europe and the US, which result in lower CO concentrations in the model, due to the assimilation of IASI CO data in the MACC_osuite. The differences between MOPITT and IASI data can be mainly explained by the use of different a priori assumptions in the IASI and MOPITT retrieval algorithms (George et al., 2015 submitted). Indeed, the Fast Optimal Retrievals on Layers for IASI (FORLI) software (IASI) is using a single a priori CO profile (with an associated variance-covariance matrix) whereas the MOPITT retrieval algorithm is using a variable a priori, depending on time and location. George et al., 2015 (submitted) show that differences above Europe and the US in January and December (for a 5 year study) decrease by a factor of 2 when comparing IASI with a modified MOPITT product using the IASI single a priori. Between January 2011 and October 2011 there has also been a reading error in the fire emissions that contributes to larger MNMBs during this period (see section 2.1.1).

Gelöscht: .
Gelöscht: 4
Gelöscht: _new
Gelöscht: 5
Gelöscht: 4
Gelöscht: _new
Gelöscht: . These

3.3 Evaluation of Tropospheric Nitrogen Dioxide

Figure 15 shows global maps of daily tropospheric NO_2 VCD averaged from September 2009 to March 2012. Overall, spatial distribution and magnitude of tropospheric NO_2 observed by SCIAMACHY are well reproduced by the model. This indicates that emission patterns and NO_x photochemistry are reasonably well represented by the model. However, the model underestimates tropospheric NO_2 VCDs over industrial areas in Europe, East China, Russia, and South East Africa compared to satellite data. This could imply that anthropogenic emissions from RETRO-REAS are underestimated in these regions, or that the lifetime in the model is too short. The model simulates larger NO_2 VCD maxima over Central Africa, which mainly originate from wild fires. It remains unclear if GFEDv2/GFAS fire emissions are too high here or if NO_2 fire plumes closer to the ground cannot be seen by the satellites due to light scattering by biomass burning aerosols (Leitao et al., 2010). In the northern hemisphere, background values of NO_2 VCD over the ocean are lower in the simulations than in the satellite data. The same is true for the South Atlantic Ocean to the west of Africa (see Fig.15). This might suggest a model underestimation of NO_2 export from continental sources or too rapid conversion of NO_2 into its reservoirs. However, as the NO_2 columns over the oceans are close to the uncertainties in the satellite data, care needs to be taken when interpreting these differences.

Time series of daily tropospheric NO_2 VCD averaged over different regions and corresponding monthly means are presented in Figs. 16 and 17, respectively. Time series of the MNMB and RMSE are shown in Figs. 18 and 19, respectively. Table 7 summarizes the statistical values derived over the whole time period. High anthropogenic emissions occur over the United States, Europe, South Asia and East Asia compared to other regions on the globe (e.g., Richter et al., 2005). In principle, the MACC_osuite catches the pattern of satellite NO_2 VCD over these regions. However, the model tends to underestimate NO_2 VCDs throughout the whole time period investigated here. The negative bias is most pronounced over East Asia with a modelled mean NO_2 VCD for September 2009 to December 2012 of about 3.8×10^{15} molec cm^{-2} lower than that derived from satellite measurements (see Table 7). Considering monthly values, the MACC_osuite strongly underestimates magnitude and seasonal variation of satellite NO_2 VCD over East Asia (MNMBs between about -

Gelöscht: _new. 6
Gelöscht: over six regions from
Gelöscht: December
Gelöscht: GOME-2 and
Formatiert: Schriftart: Times New Roman, 12 pt, Muster: Transparent
Formatiert: Schriftart: Times New Roman, 12 pt, Muster: Transparent
Formatiert: Schriftart: Times New Roman, 12 pt, Muster: Transparent
Formatiert: Muster: Transparent
Gelöscht: In the northern hemisphere, background values of NO_2 VCD over the ocean are lower in the simulations than in the satellite data. The same is true for the South Atlantic Ocean to the west of Africa (see Fig.
Gelöscht: 7
Gelöscht: 15-new). This might suggest complex processes involving NO_2 transport or chemistry, or point to inaccuracies in the bias correction applied in the satellite retrieval.¶
Gelöscht: Monthly means of
Gelöscht: 8
Gelöscht: _new
Gelöscht: A t
Gelöscht: is
Gelöscht: 9
Gelöscht: _new
Gelöscht: 10
Gelöscht: _new
Gelöscht: 5
Gelöscht: 6
Gelöscht: _new
Gelöscht: 3.74×10^{15}
Gelöscht: 5
Gelöscht: _new

40 % and _-110 % and RMSE between 1 x 10^{15} molec cm^{-2} and 14 x 10^{15} molec cm^{-2} throughout the whole time period). A change in the modelled NO_2 values is apparent in July 2012 when the emission inventories changed and the agreement with the satellite data improved for South and East Asia but deteriorated for the US and Europe. This results in a drop of MNMBs (Fig. 18) for Europe and the US with values approaching around -70% by the end of 2012. Nevertheless, correlations between daily satellite and model data derived for the whole time period (see Table 7) are high for East Asia (0.8), South Asia (0.8), Europe (0.8), and lower, but still rather high, for the US (0.6).

The North African and South African regions are strongly affected by biomass burning (Schreier et al., 2013). Magnitude and seasonality of daily and monthly tropospheric NO_2 VCDs (Figs. 16 and 17, respectively) are rather well represented by the model, apart from January 2011 to October 2011, due to difficulties in reading fire emissions for this time period (see section 2.1.1). The latter results in large absolute values of the MNMB (Fig. 18) and large RMSEs (Fig. 19) between January 2011 and October 2011 compared to the rest of the time period. As for other regions investigated in this section, mean values of simulated daily tropospheric NO_2 VCDs over North Africa and South Africa between September 2009 and December 2012 tend to be lower than the corresponding satellite mean values (see Table 7). The correlation between daily model and satellite data over the whole time period is about 0.6 for South Africa and 0.5 for North Africa. It should be investigated in future studies, if this difference in model performance for the African regions is due to meteorology, chemistry or emissions.

4. Discussion

The validation of global O_3 mixing ratios with GAW observations at the surface levels showed that the MACC_osuite could generally reproduce the observed annual cycle of ozone mixing ratios. Model validation with surface data shows global average monthly MNMBs between -30% and 30% (GAW) and for Europe between -50% and 60% (EMEP). The bias between measured O_3 surface mixing ratios and the MACC_osuite is seasonally dependent, with an underestimation of the observed O_3 mixing ratios during the northern winter season and an overestimation during the summer months.

Gelöscht: 9
Gelöscht: -60%
Gelöscht: 5
Gelöscht: _new
Gelöscht: East Asia (0.840), South Asia (0.744), Europe (0.781), and lower, but still rather high, for the US (0.567). ¶
Gelöscht: _new
Gelöscht: _new
Gelöscht: (Figs. 6 to 8)
Gelöscht: 9
Gelöscht: _new
Gelöscht: 10
Gelöscht: _new
Gelöscht: are
Gelöscht: 5
Gelöscht: -new
Gelöscht: 0
Gelöscht: 06
Gelöscht: South Africa but only 0.455 for North Africa, respectively.
Formatiert: Nummerierung und Aufzählungszeichen
Formatiert: Tiefgestellt
Formatiert: Tiefgestellt
Formatiert: Tiefgestellt

The validation of day-time versus night-time concentrations for Northern and Central Europe shows larger negative MNMBs in the winter months during night time than day time (Fig. 8), so that the negative bias in winter could be attributed to the simulation of vertical mixing at night, also described by Ordoñez (2010) and Schaap (2008), which remains a challenge in the model. The systematic underestimation of O_3 mixing ratios throughout the year for high latitude northern regions and Antarctica has its origin in an overestimation of the O_3 dry deposition velocities over ice. With the implementation of the new model cycle and MOZART model version, which includes updated velocity fields for the dry deposition of O_3, as described in Stein et al. (2013), the negative offset in the MACC_osuite model has been remedied for high latitude regions from July 2012 onwards (see the time series plots for the South Pole station- SPO and Neumayer- NEU in Fig. 3). The overestimation of O_3 mixing ratios for the northern hemisphere summer months is a well-known issue and has been described by various model validation studies (e.g., Brunner et al., 2003, Schaap et al., 2008, Ordoñez et al., 2010, Val Martin et al., 2014). Inadequate ozone precursor concentrations and aerosol induced radiative effects (photolysis) have been frequently identified as being the main factors. The time series plots in Fig. 3, however, demonstrate that the minimum concentrations in particular are not captured by the model during summer. Possible explanations include a general underestimation of NO titration which especially applies to stations with urban surroundings and strong sub-grid scale emissions (e.g. Tsukuba-TSU Fig. 3), including difficulties by the global model to resolve NO titration in urban plumes. It also seems likely that dry deposition at wet surfaces in combination with the large surface sink gradient due to nocturnal stability cannot be resolved with the model's vertical resolution. In regions such as Central and Southern Europe (Fig. 8) where day time biases exceed night time biases, the overestimation of O_3 might be related to an underestimation of day-time dry deposition velocities: Val Martin et al., (2014) describe a reduction of the summertime O_3 model bias for surface ozone after the implementation of adjustments in stomatal resistances in the MOZART model's dry deposition parameterization.

The MACC_osuite model realistically reproduces CO total columns over most of the evaluated regions with monthly MNMBs falling between 10% and -20% (Table 6). There is a close agreement of modelled CO total columns and satellite observations for Africa and South Asia throughout the evaluation period. However, there is a negative offset compared to the observational CO data over Europe and North

Gelöscht: the diurnal cycle

Gelöscht:

Gelöscht: 15

Formatiert: Tiefgestellt

Formatiert: Tiefgestellt

Formatiert: Tiefgestellt

Gelöscht: _new

Formatiert: Tiefgestellt

Gelöscht: _new

Gelöscht: _new

Gelöscht: _new

Formatiert: Tiefgestellt

Formatiert: Tiefgestellt

America. The largest deviations occur during the winter season when the observed CO concentrations are at a highest. The evaluation with GAW surface CO data accordingly shows a wintertime negative bias of up to -35% at the surface for stations in Europe and the US. A general underestimation of CO from global models in the northern hemisphere has been described by various authors (e.g., Shindell et al., 2006, Naik et al., 2013). According to Stein et al. (2014) this underestimation likely results from a combination of errors in the dry deposition parameterization and certain limitations in the current emission inventories. The latter include too low anthropogenic CO emissions from traffic or other combustion processes and missing anthropogenic VOC emissions in the inventories together with an insufficiently established seasonality in the emissions. An additional reason for the apparent underestimation of emissions in MACCity may be an exaggerated downward trend in the RCP8.5 (Representative Concentration Pathways) scenario in North America and Europe between 2000 and 2010, as this scenario was used to extrapolate the MACCity emissions from their bench mark year, i.e. 2000. For CO, uncertainties in the evaluation also include the retrieved amount of CO total columns between IASI and MOPITT. These vary with region, with IASI showing lower CO concentrations in several regions (Alaska, Siberia, Europe and the US) during the northern winter months, which possibly contribute to the deviations observed between the modelled data and MOPITT satellite data, as only IASI data has been assimilated in the model. The differences can primarily be explained by the use of different a priori assumptions in the IASI and MOPITT retrieval algorithms (George et al., 2015 submitted). On a global scale however, the average difference between the IASI and MOPITT total columns is less than 10% (George et al., 2009). From July 2012 onwards, MOPITT CO total columns are also assimilated in the MACC_osuite.

Gelöscht: emission

Gelöscht: se

Modelled NO_2 total columns agree well with satellite observations over the United States, South Asia and North Africa. However, there is also a negative offset for NO_2 over Europe and East Asia. Again, the largest deviations are occurring during the winter season. The quality of the emission inventory is even more crucial for short lived reactive species such as NO_2, where model results depend to a large extent on emission inventories incorporated in the simulations. This is highlighted by the deterioration of agreement between model results and satellite data for the US in July 2012 when anthropogenic emissions were changed from RETRO-REAS to MACCity.

Formatiert: Tiefgestellt

Gelöscht: with

This change led to an increasing negative bias in NO_2 over Europe and North America and to an improvement for South and East Asia (see Fig. 18). A deterioration in MNMBs associated with the fire emissions is visible between January 2011 and October 2011 over regions with heavy fire activity (Africa and East Asia), and goes back to a temporary error in the model regarding the reading of fire emissions (see Figs. 17 and 18). Particular challenges for an operational forecast system are regions with rapid changes in emissions such as China, where inventories need to be extrapolated to obtain reasonable trends. A large underestimation of NO_2 in China especially in winter has been reported for other CTMs in previous publications (He et al., 2007, Itahashi et al., 2014). The latter has been linked to an underestimation of NO_x and VOC emissions, unresolved seasonality in the emissions and expected non-linearity of NO_x chemistry. The change in validation data sets from SCIAMACHY to GOME-2 has shown to have negligible impact on the validation results and conclusions.

5. Conclusion

The MACC_osuite is the global near-real-time MACC model analysis run for aerosol and reactive gases. The model has been evaluated with surface observations and satellite data concerning its ability to simulate reactive gases in the troposphere. Results showed that the model proved capable of a realistic reproduction of the observed annual cycle for CO and O_3 mixing ratios at the surface, however, with seasonally dependent biases. For ozone, these seasonal biases likely result from difficulties in the simulation of vertical mixing at night and deficiencies in the model's dry deposition parameterization. For CO, a negative offset in the model during the winter season is attributed to limitations in the emission inventories together with an insufficiently established seasonality in the emissions.

CO and NO_2 total columns derived from satellite sensors could be reproduced over most of the evaluated regions, but showed a negative offset compared to the observational data over Europe and North America (CO) and over Europe and East Asia (NO_2). It has become clear, that that the emission inventories play a crucial role for the quality of model results and remain a challenge for near-real-time modeling, especially over regions with rapid changes in emissions. Inco nsistencies in the

Gelöscht: _new

Gelöscht: South Africa and

Gelöscht:

Gelöscht: 5

Gelöscht: -new

Gelöscht: 17_new

Gelöscht: The change in validation data sets from SCIAMACHY to GOME-2 has shown to have negligible impact on the validation results and conclusions. Due to the differences in the data sampling, the daily mean values of SCIAMACHY show a stronger temporal variability compared to the daily mean values of GOME-2 in the region plots. This is due to the differences in the data sampling (GOME-2 has a better spatial coverage).

Gelöscht: ¶

Formatiert: Englisch (USA)

Formatiert: Leerraum zwischen asiatischem und westlichem Text nicht anpassen, Leerraum zwischen asiatischem Text und Zahlen nicht anpassen

Gelöscht: The MACC_osuite model realistically reproduces CO and NO_2 total columns over most of the evaluated regions with monthly MNMBs falling between 10% and -20% (CO) and between 40% and -110% for NO_2. There is a close agreement of modelled CO total columns and satellite observations for Africa and South Asia throughout the evaluation period. NO_2 total columns agree well with satellite observations over the United States, South Asia an ... [2]

Formatiert: Nummerierung und Aufzählungszeichen

Gelöscht: The validation of the diurnal cycle for Northern ... [3]

Gelöscht: global

Formatiert: Tiefgestellt

Gelöscht: This model run proved capable of reproducing

Gelöscht: however with

Gelöscht: for CO

Gelöscht: for NO_2

Formatiert: Tiefgestellt

Gelöscht: shown

Gelöscht: for CO and NO_2,

Gelöscht: I

Gelöscht: for

Gelöscht: ¶
The validation of global O_3 m ... [4]

assimilated satellite data and fire emissions showed only a temporary impact on the quality of model results.

The MACC NRT system is constantly evolving. A promising step in model development is the on-line integration of modules for atmospheric chemistry in the IFS, currently being tested for implementation in the MACC_osuite. In contrast to the coupled model configuration as used in this paper, the on-line integration in the Composition IFS (C-IFS) provides major advantages; apart from an enhanced computational efficiency, C-IFS promises an optimization of the implementation of feedback processes between gas-phase/aerosol chemical processes and atmospheric composition and meteorology, which is expected to improve the modeling results for reactive gases. Additionally, C-IFS will be available in combination with different CTMs, (MOZART and TM5), which will help to explain whether deviations between model and observations go back to deficiencies in the chemistry scheme of a model.

Acknowledgements

This work has been carried out in the framework of the MACC projects, funded under the EU Seventh Research Framework Programme for research and technological development. The authors thank the MACC validation and reactive gas subproject teams for the fruitful discussions. Model simulations were carried out using the ECMWF supercomputer. We wish to acknowledge the provision of GAW hourly station data from the World Data Centre of Greenhouse Gases (WDCGG) and hourly EMEP station data from the NILU database. Specifically, we like to thank: the CSIRO Oceans and Atmosphere Flagship for making the data freely available and the Australian Bureau of Meteorology for continued operation and support of the Cape Grim station. We also like to thank Izaña Atmospheric Research Center (AEMET) for providing CO and O_3 data. Special thanks to the providers of NRT data to the MACC project, namely: Institute of Atmospheric Sciences and Climate (ISAC) of the Italian National Research Council (CNR), South African Weather Service, The University of York and National Centre for Atmospheric Science (NCAS (AMF)) (UK), and the Instituto Nacional de Meteorologia e Geofisica (INMG) (Cape Verde), National Air Pollution Monitoring Network (NABEL) (Federal Office for the Environment FOEN and Swiss Federal Laboratories for Materials Testing and Research EMPA), Japan Meteorological Agency (JMA), Alfred Wegener Institute, Umweltbundesamt (Austria), National Meteorological Service (Argentina), Umweltbundesamt (UBA,

Gelöscht: minor

Gelöscht: overall

Gelöscht: its

Gelöscht: l

Gelöscht: and MACC-II

Gelöscht:

Germany). We thank the National Center for Atmospheric Research (NCAR) MOPITT science team and the NASA Langley Research Center, Atmospheric Science Data Center (ASDC), for producing and archiving the MOPITT CO product. IASI has been developed and built under the responsibility of the Centre National D'Etudes Spatiales (CNES, France). We are grateful to Juliette Hadji-Lazaro and the UBL/ LATMOS IASI team for establishing the IASI-MACC near real time processing chain. We wish to acknowledge that SCIAMACHY lv1 (level 1) radiances were provided to the Institute of Environmental Physics, University of Bremen by ESA through DLR/DFD.

References

Aas, W., Hjellbrekke, A.-G., Schaug, J.: Data quality 1998, quality assurance and field comparisons. Kjeller, Norwegian Institute for Air Research (EMEP/CCC-Report 6/2000), 2000.

Ashmore, M. R.: Assessing the future global impacts of ozone on vegetation. Plant Cell Environ. 28, 949–964, 2005.

Ballabrera-Poy, J., Kalnay, E. and Yang, S.: Data assimilation in a system with two scales—combining two initialization techniques. Tellus (2009), 61A, 539–549, doi:10.1111/j.1600-0870.2009.00400.x, 2009.

Gelöscht: ¶

Gelöscht:

Bell M.L., R.D. Peng and F. Dominici: The exposure–response curve for O_3 and risk of mortality and the adequacy of current O_3 regulations. Environmental Health Perspectives,

114 (4), 2006.

Formatiert: Tiefgestellt

Benedetti, A., Morcrette, J.-J., Boucher, O., Dethof, A., Engelen, R. J., Fisher, M., Flentje, H., Huneeus, N., Jones, L., Kaiser, J. W., Kinne, S., Mangold, A., Razinger, M., Simmons, A. J., Suttie, M., and the GEMS-AER team: Aerosol analysis and forecast in the European Centre for Medium-Range Weather Forecasts Integrated Forecast System: Data Assimilation. J. Geophys. Res., D13205, 114, doi:10.1029/2008JD011115, 2008.

Formatiert: Englisch (USA)

Gelöscht:

Benedetti, A., Kaiser, J. W., and Morcrette J.-J:. [Global Climate] Aerosols [in "State of the Climate in 2010"]. B. Am.Meterol. Sci., 92(6):S65–S67, 2011.

Gelöscht: AMS,

Gelöscht: ¶

Boersma, K.F., Eskes, H.J., Brinksma, E.J.: Error analysis for tropospheric NO2 retrieval from space. J. Geophys. Res., 109, D4, doi:10.1029/2003JD003962, 2004.

Bovensmann, H., J. P. Burrows, M. Buchwitz, J. Frerick, S. Noël, V. V. Rozanov, K. V. Chance, A. P. H. Goede: SCIAMACHY: Mission Objectives and Measurement Modes. J. Atmos. Sci., 56, 127–150, 1999.

Brunner, D., Staehelin, J., Rogers, H. L., Köhler, M. O., Pyle, J. A., Hauglustaine, D., Jourdain, L., Berntsen T. K., Gauss, M., Isaksen, I. S. A., Meijer, E., van Velthoven, P., Pitari, G., Mancini, E., Grewe, V. and Sausen, R.: An evaluation of the performance of

chemistry transport models by comparison with research aircraft observations. Part 1: Concepts and overall model performance. Atmos. Chem. Phys.., 3, 1609–1631, doi:10.5194/acp-3-1609-2003, 2003.

Callies, J., Corpaccioli, E., Eisinger, M., Hahne, A., and Lefebvre, A.: GOME-2 Metop's Second-Generation Sensor for Operational Ozone Monitoring, ESA Bull., 102, 28–36, 2000.

Cammas, J.-P., A. Gilles, S. Chabrillat, F. Daerden, N. Elguindi, J. Flemming, H. Flentje, C.

Deshler, T., J.L. Mercer, H.G.J. Smit, R. Stubi, G. Levrat, B.J. Johnson, S.J. Oltmans, R. Kivi, A.M. Thompson, J. Witte, J. Davies, F.J. Schmidlin, G. Brothers, T. Sasaki Atmospheric comparison of electrochemical cell ozonesondes from different maufacturers, and with different cathode solution strengths: The Balloon Experiment on Standards for Ozonsondes. J. Geophys. Res.113, D04307, doi:10.1029/2007JD008975, 2008.

Cape, J.N.: Surface ozone concentrations and ecosystem health: Past trends and a guide to future projections. Science of the Total Environment Vol. 400, 257-269., doi:10.1016/j.scitotenv.2008.06.025, 2008.

Clarisse, L., R'Honi, Y., Coheur, P.-F., Hurtmans, D., and Clerbaux, C.: Thermal infrared nadir observations of 24 atmospheric gases, Geophys. Res. Lett., 38, L10802, doi:10.1029/2011GL047271, 2011.

Clerbaux, C., Boynard, A., Clarisse, L., George, M., Hadji-Lazaro, J., Herbin, H., Hurtmans, D., Pommier, M., Razavi, A., Turquety, S., Wespes, C., and Coheur, P.-F.:

Formatiert: Schriftart: 12 pt, Englisch (Großbritannien)

Formatiert: Schriftart: 12 pt, Englisch (Großbritannien)

Formatiert: Sprechblasentext

Formatiert: Schriftart: 12 pt, Englisch (Großbritannien), Nicht Hochgestellt/ Tiefgestellt

Gelöscht:

Gelöscht:

Gelöscht:

Monitoring of atmospheric composition using the thermal infrared IASI/MetOp sounder, Atmos. Chem. Phys., 9, 6041–6054, doi:10.5194/acp-9-6041-2009, 2009.

Cooper, O. R., Parrish, D. D., Ziemke, J., Balashov, N. V., Cupeiro, M., Galbally, I. E., Gilge, S., Horowitz, L., Jensen, N. R., Lamarque, J.-F., Naik, V., Oltmans, S. J., Schwab, J., Shindell, D. T., Thompson, A. M., Thouret, V., Wang, Y., Zbinden, R. M.: Global distribution and trends of tropospheric ozone: an observation-based review, Elem. Sci. Anth., 2,10 000029, doi:10.12952/journal.elementa.000029, 2014.

Cuevas, E., Camino, C., Benedetti, A., Basart, S., Terradellas, E., Baldasano, J.M., Morcrette, J.-J., Marticorena, B., Goloub, P., Mortier, A., Berjón, A., Hernández, Y., Gil-Ojeda, M., Schulz, M.: The MACC-II 2007-2008 Reanalysis: Atmospheric Dust Evaluation and Characterization over Northern Africa and Middle East, Atmos. Chem. Phys. 15, 3991–4024, doi:10.5194/acp-15-3991-2015, 2015.

Gelöscht: submitted to

Formatiert: Schriftart: 12 pt, Schriftartfarbe: Schwarz, Englisch (USA)

Gelöscht: MACC special issue on 27 June

Gelöscht: 4

Formatiert: Schriftart: 12 pt, Schriftartfarbe: Schwarz, Englisch (USA)

Deeter, M. N., Emmons, L. K., Edwards, D. P., Gille, J. C., and Drummond, J. R.: Vertical resolution and information content of CO profiles retrieved by MOPITT, Geophys. Res. Lett., 31, L15112, doi:10.1029/2004GL020235, 2004.

Deeter, M. N., et al.: The MOPITT version 4 CO product: Algorithm enhancements, validation, and long-term stability, J. Geophys. Res., 115, D07306, doi:10.1029/2009JD013005, 2010.

Deeter, M. N., H. M. Worden, D. P. Edwards, J. C. Gille, D. Mao, and J. R. Drummond: MOPITT multispectral CO retrievals: Ori-gins and effects of geophysical radiance errors, J. Geophys. Res., 116, doi:10.1029/2011JD015703, 2011.

Gelöscht:

Deeter, M. N., Worden, H. M., Edwards, D. P., Gille, J. C., Andrews, A. E.: evaluation of MOPITT retrievals of lower-tropospheric carbon monoxide over the United States, J. Geophys. Res., 117, D13306, doi:10.1029/2012JD017553, 2012.

Gelöscht:

Deeter, M. N., Martínez-Alonso, S., Edwards, D. P., Emmons, L. K., Gille, J. C., Worden, H. M., Pittman, J. V., Daube, B. C., Wofsy, S. C.: Validation of MOPITT Version 5 thermal-infrared, near-infrared, and multispectral carbon monoxide profile retrievals for 2000–2011, J. Geophys. Res. Atmos., 118, 6710–6725, doi:10.1002/jgrd.50272, 2013.

De Wachter, E., Barret, B., Le Flochmoën, E., Pavelin, E., Matricardi, M., Clerbaux, C., Hadji-Lazaro, J., George, M., Hurtmans, D., Coheur, P.-F., Nedelec, P., and Cammas, J. P.: Retrieval of MetOp-A/IASI CO profiles and validation with MOZAIC data, Atmos. Meas. Tech., 5, 2843-2857, doi:10.5194/amt-5-2843-2012, 2012.

Drummond, J. R. and Mand, G. S.: The Measurements of Pollution in the Troposphere (MOPITT) Instrument: Overall Performance and Calibration Requirements. J. Atmos. Oceanic Technol., 13, 314–320, 1996.

Elguindi, N., Clark, H., Ordóñez, C., Thouret, V., Flemming, J., Stein, O., Huijnen, V., Moinat, P., Inness, A., Peuch, V.-H., Stohl, A., Turquety, S., Athier, G., Cammas, J.-P., and Schultz, M.: Current status of the ability of the GEMS/MACC models to reproduce the tropospheric CO vertical distribution as measured by MOZAIC, Geosci. Model Dev., 3, 501-518, doi:10.5194/gmd-3-501-2010, 2010.

Emmons, L. K., Edwards, D. P., Deeter, M. N., Gille, J. C., Campos, T., Nédélec, P., Novelli, P. and G. Sachse: Measurements of Pollution In The Troposphere (MOPITT) validation through 2006, Atmos. Chem. Phys., 9(5), 1795–1803, doi:10.5194/acp-9-1795-2009, 2009.

Engelen R. J., Serrar, S., Chevallier, F.: Four-dimensional data assimilation of atmospheric CO_2 using AIRS observations, J. Geophys. Res., 114, D03303, doi:10.1029/2008JD010739, 2009.

Flemming, J., and Inness, A., Volcanic sulfur dioxide plume forecasts based on UV satellite retrievals for the 2011 Grímsvötn and the 2010 Eyjafjallajökull eruption, Journal of Geophysical Research: Atmospheres 118, 10172-10189, doi:10.1002/jgrd.50753, 2013.

Flemming, J., Inness, A., Flentje, H., Huijnen, V., Moinat, P., Schultz, M.G., Stein, O.: Coupling global chemistry transport models to ECMWF's integrated forecast system, Geosci. Model Dev., 2, 253-265, doi:10.5194/gmd-2-253-2009, 2009.

Forster, P., V. Ramaswamy, P. Artaxo, T. Berntsen, R. Betts, D.W. Fahey, J. Haywood, J. Lean, D.C. Lowe, G. Myhre, J. Nganga, R. Prinn, G. Raga, M. Schulz and R. Van Dorland: Changes in Atmospheric Constituents and in Radiative Forcing. In: Climate Change 2007: The Physical Science Basis. Contribution of Working Group I to the Fourth Assessment Report of the Intergovernmental Panel on Climate Change [S. Solomon, D. Qin, M. Manning, Z. Chen, M. Marquis, K.B. Averyt, M. Tignor and H.L. Miller (eds.)]. USA, 2007.

George, M., Clerbaux, C., Hurtmans, D., Turquety, S., Coheur, P.-F., Pommier, M., Hadji-Lazaro, J., Edwards, D. P., Worden, H., Luo, M., Rinsland, C., and McMillan,W.: Carbon monoxide distributions from the IASI/METOP mission:

Gelöscht:

Gelöscht:

evaluation with other space-borne remote sensors, Atmos. Chem. Phys., 9, 8317–8330, doi:10.5194/acp-9-8317-2009, 2009.

George, M., Clerbaux, C., Bouarar, I., Coheur, P.-F., Deeter, M. N., Edwards, D. P., Francis, G., Gille, C., Hadji-Lazaro, J., Hurtmans, D., Inness, A., Mao, D., Worden H. M.: An examination of the long-term CO records from MOPITT and IASI and comparison of retrieval methodology, Atmos. Meas. Tech. Discuss., submitted, 2015.

Gomez-Pelaez, A. J., Ramos, R., Gomez-Trueba, V., Novelli, P. C., and Campo-Hernandez, R.: A statistical approach to quantify uncertainty in carbon monoxide measurements at the Izaña global GAW station: 2008–2011, Atmos. Meas. Tech., 6, 787-799, doi:10.5194/amt-6-787-2013, 2013.

Granier, C., Huijnen, V., Inness, A., Jones, L., Katragkou E., Khokhar, F., Kins, L., Law, K., Lefever, K., Leitao, J., Melas, D., Moinat, P., Ordonez, C., Peuch, V.-H., Reich, G., Schultz, M., Stein, O., Thouret, V., Werner, T., Zerefos, C., GEMS GRG Comprehensive Validation Report. Available as project report at http://gems.ecmwf.int (last access: February 2015), 2009.

Granier, C., Bessagnet, B., Bond, T., D'Angiola, A., van der Gon, H. D., Frost, G. J., Heil, A., Kaiser, J. W., Kinne, S., Klimont, Z., Kloster, S., Lamarque, J.-F., Liousse, C., Masui, T., Meleux, F., Mieville, A., Ohara, T., Raut, J. C., Riahi, K., Schultz, M. G., Smith, S. J., Thompson, A., van Aardenne, J., van der Werf, G. R., and van Vuuren, D. P.: Evolution of anthropogenic and biomass burning emissions of air pollutants at global and regional scales during the 1980–2010 period, Climatic Change, 109, 163–190, doi:10.1007/s10584-011-0154-1, 2011.

Griffin, R.J., Chen, J., Carmody, K. and Vutukuru, S.: Contribution of gas phase oxidation of volatile organic compounds to atmospheric carbon monoxide levels in two areas of the united States. J. Geophys. Res., 11, D10S17, doi:10.1029/2006JD007602, 2007.

Guenther, A., Karl, T., Harley, P., Wiedinmyer, C., Palmer, P.I., and Geron, C.: Estimates of global terrestrial isoprene emissions using MEGAN (Model of Emissions of Gases and Aerosols from Nature), Atmos. Chem. Phys., 6, 3181-3210, doi:10.5194/acp-6-3181-2006, 2006.

Gelöscht:

Gelöscht:

Gelöscht: last visited Feb. 2015

Formatiert: Deutsch (Deutschland)

He, Y, Uno, I., Wang, Z., Ohara, T., Sugimoto, N., Shimizu, A., Richter, A., Burrows, J. P.: Variations of the increasing trend of tropospheric NO_2 over central east China during the past decade, Atmospheric Environment, 41, 4865–4876, 2007.

Hilboll, A., Richter, A., and Burrows, J.P.: Long-term changes of tropospheric NO_2 over megacities derived from multiple satellite instruments, Atmos. Chem. Phys., 13, 4145-4169, doi:10.5194/acp-13-4145-2013, 2013a.

Hilboll, A., Richter, A., Rozanov, A., Hodnebrog, Ø., Heckel, A., Solberg, S., Stordal, F., and Burrows, J.P.,: Improvements to the retrieval of tropospheric NO_2 from Satellite – stratospheric correction using SCIAMACHY limb/nadir matching and comparison to Oslo CTM2 simulations. Atmos. Meas. Tech., 6, 565–584. doi:10.5194/amt-6-565-2013, 2013, 2013b.

Hollingsworth, A., Engelen, R.J., Benedetti, A., Dethof, A., Flemming, J., Kaiser, J.W., Simmons, A.J.: Toward a monitoring and forecasting system for atmospheric composition: The GEMS project, B.Am. Meteoro. Soc., 89, 1147–1164, doi:10.1175/2008BAMS2355.1, 2008.

Hudman, R.C., Murray, L.T., Jacob, D.J., Millet, D.B., Turquety, S., Wu, S., Blake, D.R., Goldstein, A.H., Holloway, J., Sachse, G.W.: Biogenic versus anthropogenic sources of CO over the United States. Geophys. Res. Let., 35, L04801, doi:10.1175/2007GL032393, 2008.

Huijnen, V., Williams, J., vanWeele, M., van Noije, T., Krol, M., Dentener, F., Segers, A., Houweling, S., Peters, W., de Laat, J., Boersma, F., Bergamaschi, P., van Velthoven, P., Le Sager, P., Eskes, H., Alkemade, F., Scheele, R., Nédélec, P., and Pätz, H.-W.: The global chemistry transport model TM5: description and evaluation of the tropospheric chemistry version 3.0, Geosci. Model Dev., 3, 445–473, doi:10.5194/gmd-3-445-2010, 2010.

Huijnen, V., Flemming, J., Kaiser, J. W., Inness, A., Leitao, J., Heil, A., Eskes, H. J., Schultz, M. G., Benedetti, A., Dufour, G., and Eremenko, M., Hindcast experiments of tropospheric composition during the summer 2010 fires over Western Russia, Atmos. Chem. Phys. 12, 4341-4364, doi:10.5194/acp-12-4341-2012, 2012.

Hurtmans, D., Coheur, P.-F., Wespes, C., Clarisse, L., Scharf, O., Clerbaux, C., Hadji-Lazaro, J., George, M., and Turquety, S.: FORLI radiative transfer and retrieval

Gelöscht: Term
Gelöscht: Changes
Gelöscht: Tropospheric
Gelöscht: M
Gelöscht: D
Gelöscht:
Gelöscht: Multiple
Gelöscht: Satellite
Gelöscht: I
Gelöscht: .
Gelöscht: no. 8
Gelöscht: (2013a): 4145–4169.
Gelöscht: Retrieval
Gelöscht: Tropospheric
Formatiert: Tiefgestellt
Gelöscht: Stratospheric
Gelöscht: Correction
Gelöscht: Using
Gelöscht: Limb
Gelöscht: Matching
Gelöscht: Comparison
Gelöscht: Simulations
Gelöscht: pheric
Gelöscht: Measurement
Gelöscht: Techniques
Gelöscht: (2013b):
Gelöscht:
Gelöscht: ulletin of the
Gelöscht: erican
Gelöscht: Meteorological
Gelöscht: Society
Gelöscht:
Formatiert: Niederländisch (Niederlande)
Gelöscht:
Feldfunktion geändert
Formatiert: Niederländisch (Niederlande)
Formatiert: Niederländisch (Niederlande)
Gelöscht: Geophysical
Gelöscht: Research
Gelöscht: Letters
Gelöscht: Huijnen, V., Williams, J. E., van Weele, M., van Noije, T. P. C., Krol, M. C., Dentener, F., Segers, A., Houweling, S., Peters, W., de Laat, A. T. J., Boersma, K. F., Bergamaschi, P., van Vel ... [5]

code for IASI. J Quant Spectrosc Radiat Transfer, 113, 1391–1408, doi:10.1016/j.jqsrt.2012.02.036, 2012.

Inness, A., Flemming, J., Suttie, M. and Jones, L.: GEMS data assimilation system for chemically reactive gases. ECMWF RD Tech Memo 587. Available from http://www.ecmwf.int. (last access: February 2015), 2009.

Gelöscht: last visited Feb. 2015

Inness, A., F. Baier, F., 2, Benedetti, A., Bouarar, I., Chabrillat, S., Clark, H., Clerbaux, C., Coheur, P., Engelen, R. J., Errera, Q., Flemming, J., George, M., Granier, C., Hadji-Lazaro, J., Huijnen, V., Hurtmans, D., Jones, L., Kaiser, J. W., Kapsomenakis, J., Lefever, K., Leitão J., Razinger, M., Richter, A., Schultz, M. G., Simmons, A. J., Suttie,M., Stein O., Thépaut J.-N., Thouret,V., Vrekoussis, M., Zerefos, C, .al.: The MACC reanalysis: an 8 yr data set of atmospheric composition, Atmos. Chem. Phys, 13, 4073–4109, doi:10.5194/acp-13-4073-2013, 2013.

Gelöscht: Atmospheric
Gelöscht: Chemistry
Gelöscht: and
Gelöscht: ics

Inness, A., Blechschmidt, A.-M., Bouara, I., Chabrillat, S., Crepulja, M., Engelen, R. J., Eskes, H., Flemming, J., Gaudel, A., Hendrick, F., Huijnen, V., Jones, L., Kapsomenakis, J., Katragkou, E., Keppens, A., Langerock, B., de Mazière, M., Melas, D.,M. Parrington, V.H. Peuch, M. Razinger, A. Richter, M.G. Schultz, M. Suttie, V. Thouret, Vrekoussis, M., Wagner, A.,and Zerefos C.: Data assimilation of satellite retrieved ozone, carbon monoxide and nitrogen dioxide with ECMWF's Composition-IFS. Atmos. Chem. Phys., 15, 1–29, 2015.doi:10.5194/acp-15-1-2015.

Itahashi,S., Uno,I., Irie,H., Kurokawa,J.-I., and Ohara,T.: Regional modeling of tropospheric NO2 vertical column density over East Asia during the period 2000–2010: comparison with multisatellite observations, Atmos. Chem. Phys., 14, 3623-3635, doi:10.5194/acp-14-3623-2014, 2014.

Gelöscht: ¶
Gelöscht:
Gelöscht:
Gelöscht:
Gelöscht:
Gelöscht:

Kaiser, J. W., Heil, A., Andreae, M. O., Benedetti, A., Chubarova, N., Jones, L., Morcrette, J.-J., Razinger, M., Schultz, M. G., Suttie, M., and van der Werf, G. R.: Biomass burning emissions estimated with a global fire assimilation system based on observed fire radiative power. Biogeosciences, 9, 527–554, doi:10.5194/bg-9-527-2012, 2012.

Kalnay, E., M. Kanamitsu, R. Kistler, W. Collins, D. Deaven, L. Gandin, M. Iredell, S. Saha, G. White, J. Woollen, Y. Zhu, M. Chelliah, W. Ebisuzaki, W. Higgins, J. Janowiak, K. C. Mo, C. Ropelewski, J. Wang, A. Leetmaa, R. Reynolds, R. Jenne, and D. Joseph: The NCEP/NCAR 40-Year Reanalysis Project. Bull. Amer. Meteor.

Soc., 77, 437–471, doi:http://dx.doi.org/10.1175/1520-0477(1996)077<0437:TNYRP>2.0.CO;2, 1996.

Kalnay, E.: Atmospheric Modeling, Data Assimilation and Predictability. Cambridge University Press, 2003.

Kampa, M. and Castanas, E.: Human health effects of air pollution. Environmental PollutionVolume 151, Issue 2, 362–367, 2008.

Kerzenmacher, T., Dils, B., Kumps, N., Blumenstock, T., Clerbaux, C., Coheur, P.-F., Demoulin, P., García, O., George, M., Griffith, D. W. T., Hase, F., Hadji-Lazaro, J., Hurtmans, D., Jones, N., Mahieu, E., Notholt, J., Paton-Walsh, C., Raffalski, U., Ridder, T., Schneider, M., Servais, C., and De Mazi´ere, M.: Validation of IASI FORLI carbon monoxide retrievals using FTIR data from NDACC, Atmos. Meas. Tech., 5, 2751–2761, doi:10.5194/amt-5-2751-2012, 2012.

Kinnison, D. E., Brasseur, G. P., Walters, S., Gracia, R. R., Marsh, D. R., Sassi, F., Harvey, V. L., Randall, C.E., Emmons, L., Lamarque, J. F., Hess, P., Orlando, J. J., Tie, X. X., Randel, W., Pan, L. L., Gettelman, A., Granier, C., Diehl, T., Niemeier, U. and Simmons, A. J.: Sensitivity of chemical tracers to meteorological parameters in the MOZART-3 chemical transport model. J. Geophys. Res, 112, D20302, doi:10.1029/2006JD007879, 2007.

Lefever, K., van der A, R., Baier, F., Christophe, Y., Errera, Q., Eskes, H., Flemming, J., Inness, A., Jones, L., Lambert, J.-C., Langerock, B., Schultz, M. G., Stein, O., Wagner, A., and Chabrillat, S.: Copernicus atmospheric service for stratospheric ozone: validation and intercomparison of four near real-time analyses, 2009–2012, Atmos. Chem. Phys. Discuss., 14, 12461-12523, doi:10.5194/acpd-14-12461-2014, 2014.

Leitão, J., Richter, A., Vrekoussis, M., Kokhanovsky, A., Zhang, Q. J., Beekmann, M., and Burrows, J. P.: On the improvement of NO_2 satellite retrievals – aerosol impact on the airmass factors, Atmos. Meas. Tech., 3, 475-493, doi:10.5194/amt-3-475-2010, 2010.

Leue, C., Wenig, M., Wagner, T., Platt, U. & Jähne, B. Quantitative analysis of NOx emissions from GOME satellite image sequences. J. Geophys. Res, 106, 5493–5505, 2001.

Gelöscht:

Gelöscht:

Formatiert: Deutsch (Deutschland)

Gelöscht:

Gelöscht:

Gelöscht:

Gelöscht:

Gelöscht:

Gelöscht:

Gelöscht:

Gelöscht:

Massart, S., Agusti-Panareda, A., Aben, I., Butz, A., Chevallier, F., Crevosier, C., Engelen, R., Frankenberg, C., and Hasekamp, O.: Assimilation of atmospheric methane products into the MACC-II system: from SCIAMACHY to TANSO and IASI. Atmos. Chem. Phys., 14, 6139-6158, doi:10.5194/acp-14-6139-2014, 2014.

Mohnen, V.A., Goldstein, and Wang, W.-C.: Tropospheric Ozone and Climate Change, Air &
Waste, 43:10, 1332-1334, doi:10.1080/1073161X.1993.10467207, 1993.

Morcrette, J.-J., Boucher, O., Jones, L., Salmond, D., Bechthold, P., Beljaars, A., Benedetti, A., Bonet, A., Kaiser, J.W., Razinger, M., Schulz, M., Serrar, S., Simmons, A.J., Sofiev, M., Suttie, M., Tompkins, A.M., Untch, A.: Aerosol analysis and forecast in the European Centre for Medium- Range Weather Forecasts Integrated Forecast System: forward modeling, J. Geophys. Res., 114, D06206, doi:10.1029/2008JD011235, 2009.

Naik, V., Voulgarakis, A., Fiore, M., Horowitz, L.W., Lamarque, J.-F., Lin, M., Prather, M. J., Young, P. J., Bergmann, D., Cameron-Smith, P. J., Cionni I., Collins W. J., Dalsøren, S. B., Doherty, R., Eyring V., Faluvegi, G., Folberth, G. A., Josse, B., Lee, Y. H., MacKenzie, I. A., Nagashima,T., van Noije, T. P. C., Plummer, D. A., Righi, M., Rumbold, S. T., Skeie, R. D., Shindell, T., Stevenson, D. S., Strode, S., Sudo, K., Szopa, S., and Zeng, G. : Preindustrial to present-day changes in tropospheric hydroxyl radical and methane lifetime from the Atmospheric Chemistry and Climate Model Intercomparison Project (ACCMIP). Atmos. Chem. Phys., 13, 5277–5298, doi:10.5194/acp-13-5277-2013, 2013.

Novelli, P.C., Masarie, K.A. and Lang, P.M.: Distributions and recent changes of carbon monoxide in the lower troposphere, J. Geophys. Res., 103, 19015-19033, doi:10.1029/98JD01366, 1998.

Ordoñez, C., Elguindi, N., Huijnen, V., Flemming, J., inness, A., Flentje, H., Katragkou, E., Moinat, P., Peuch, V.-H., Segers, A., Thouret, V., Athier, G., van Weele, M., Zerefos, C.s., Cammas, J.-P., Schulz, M.G.: Global Model simulations of air pollution during the 2003 European heat wave. Atmos. Chem. Phys., 10, 789-815, doi:10.5194/acp-10-789-2010, 2010.

Gelöscht:

Gelöscht:

Park, R.J., Pickering, K.E., Allen, D. J : Global simulation of tropospheric ozone using the University of Maryland Chemical Transport Model (UMD-CTM): 1. model description and evaluation. J. Geophys. Res., 109, doi:101029/2003JD004266, 2004.

Penkett, S., Gilge, S., Plass-Duelmer, C. Galbally, I.: WMO/GAW Expert Workshop on Global Long-term Measurements of Nitrogen Oxides and Recommendations for GAW Nitrogen Oxides Network, WMO, Geneva, 2011.

Platt, U., and Stutz, J.: Differential Optical Absorption Spectroscopy. Physics of Earth and Space Environments. Berlin: Springer, http://www.springerlink.com/content/978-3-540-21193-8 (last access: February. 2015), 2008.

Richter, A., and Burrows, J.P.: "Tropospheric NO_2 from GOME Measurements." Advances in Space Research 29, no. 1, 1673–1683. doi:10.1016/S0273-1177(02)00100-X, 2002.

Richter, A., Burrows, J. P., Nüß, H., Granier, C, Niemeier, U.: Increase in tropospheric nitrogen dioxide over China observed from space, Nature, 437-132,doi:10.1038/nature04092, 2005.

Richter, A. Begoin, M., Hilboll, A., and Burrows, J. P.: An improved NO_2 retrieval for the GOME-2 satellite instrument, Atmos. Meas. Tech., 4, 1147-1159, doi:10.5194/amt-4-1147-2011, 2011.

Rodgers, C. D.: Inverse Methods for Atmospheric Sounding, Theory and Practice, World Scientific, Singapore, 2000.

Rozanov, A., Vladimir V., Rozanov, M., Buchwitz, A., Kokhanovsky, A. and Burrows, J.P.:. "SCIATRAN 2.0 - A New Radiative Transfer Model for Geophysical Applications in the 175-2400 Nm Spectral Region." Advances in Space Research 36, no. 5: 1015–1019. doi:10.1016/j.asr.2005.03.012, 2005.

Santer, B. D., Sausen, R., Wigley, T. M. L. , Boyle, J. S. , AchutaRao, K., Doutriaux, C., Hansen, J. E, Meehl, G. A. , Roeckner, E., Ruedy, R., Schmidt, G., Taylor, K. E.: Behavior of tropopause height and atmospheric temperature in models, reanalyses, and observations: Decadal changes, J. Geophys. Res., 108(D1), 4002, doi:10.1029/2002JD002258, 2003.

Schaap, M., Renske, M. A., Timmermans, M. R., Boersen, G. A. C., Builtjes, P. J. H.: The LOTOS–EUROS model: description, validation and latest developments, Int. J. Environ. Pollut., 32, No. 2, 270-290, 2008.

Gelöscht: visited
Gelöscht: ,
Gelöscht: ,
Gelöscht: ,
Gelöscht: ,
Gelöscht: ,
Gelöscht: ,
Gelöscht: ,
Gelöscht:
Gelöscht: ,
Gelöscht:
Gelöscht: R.
Gelöscht: T. M. L.
Gelöscht: J. S.
Gelöscht: K.
Gelöscht: C.
Gelöscht: J. E
Gelöscht: G. A.
Gelöscht: E.
Gelöscht: R.
Gelöscht: G.
Gelöscht: and
Gelöscht: K. E.
Gelöscht:

Schreier, S. F., Richter, A., Kaiser, J. W., and Burrows, J. P.: The empirical relationship between satellite-derived tropospheric NO2 and fire radiative power and possible implications for fire emission rates of NOx, Atmos. Chem. Phys., 14, 2447–2466, doi:10.5194/acp-14- 2447-2014, 2014.

Schultz, M.G., Backman, L., Balkanski, Y., Bjoerndalsaeter, S., Brand, R., Burrows, J.P., Dalsoeren, S., de Vasconcelos, M., Grodtmann, B., Hauglustaine, D.A., Heil, A., Hoelzemann, J.J., Isaksen, I.S.A., Kaurola, J., Knorr, W., Ladstaetter-Weißenmayer, B., Mota, A., Oom, D., Pacyna, J., Panasiuk, D., Pereira, J.M.C., Pulles, T., Pyle, J., Rast, S., Richter, A., Savage, N., Schnadt, C., Schulz, M., Spessa, A., Staehelin, J., Sundet, J.K., Szopa, S., Thonicke, K., van het, Bolscher M., van Noije, T. , van Velthoven, P., Vik, A.F., Wittrock, F. (2007): REanalysis of the TROpospheric chemical composition over the past 40 years (RETRO) — A long-term global modeling study of tropospheric chemistry, Final Report Jülich/ Hamburg, Germany, published as report no. 48/2007 in the series „Reports on Earth System Science“ of the Max Planck Institute for Meteorology, Hamburg, ISSN 1614-1199, 2007.

Seinfeld, J. H., and Pandis, S. N.: Atmospheric Chemistry and Physics: From Air Pollution to Climate Change, John Wiley, Hoboken, N. J., 2006.

Selin, N.E., Wu, S., Reilly, J. M., Paltsev, S., Prinn, R.G. and Webster, M.D.: Global health and economic impacts of future ozone pollution. Environ. Res. Lett. 4, doi:10.1088/1748-9326/4/4/044014, 2009.

Shindell, D. T., et al.: Multimodel simulations of carbon monoxide: Comparison with observations and projected near-future changes, J. Geophys. Res., 111, D19306, doi:10.1029/2006JD007100, 2006.

Sinnhuber, B.M., Weber, M., Amankwah, A. and Burrows, J.P.: “Total Ozone during the Unusual Antarctic Winter of 2002.” Geophysical Research Letters 30, no. 11, 1580–1584. doi:10.1029/2002GL016798, 2003.

Sinnhuber, M., Burrows, J.P., Chipperfield, M., P., Jackman, C. H., Kallenrode, M.-B., Künzi, K.F., and Quack, M.: A Model Study of the Impact of Magnetic Field Structure on Atmospheric Composition during Solar Proton Events., Geophys., Res. Lett., 30, 1818–1821, doi:10.1029/2003GL017265, 2003.

Gelöscht: ¶

Gelöscht:

Gelöscht: Seinfeld, J. H., and Pandis, S. N.: Atmospheric Chemistry and Physics: From Air Pollution to Climate Change, John Wiley, Hoboken, N. J., 2006.¶

Gelöscht: iriam

Gelöscht: John P.

Gelöscht: , Martyn P.

Gelöscht: Charles H.

Gelöscht: May-Britt

Gelöscht: Klaus F.

Gelöscht: Manuel

Gelöscht: .

Gelöscht: “

Gelöscht: ”

Gelöscht: ical

Gelöscht: Research

Gelöscht: Letters

Gelöscht: no. 15,

Gelöscht: .

S. Sitch, S., Cox, P. M., Collins, W. J., Huntingford, C.: Indirect radiative forcing of climate change through ozone effects on the land-carbon sink. Nature 448, 791-794, doi:10.1038/nature06059, 2007.

Stein, O., Schultz, M. G., Flemming, J., Inness, A., Kaiser, J., Jones, L., Benedetti, A., Morcrette, J.-J.: MACC Global air quality services – Technical Documentation. MACC project deliverable D_G-RG_3.8, available at: www.gmes-atmosphere.eu/documents/deliverables/g-rg/ (last access: February 2015), 2011.

Stein, O., Flemming, J., Inness, A., Kaiser, J. W., and Schultz, M. G.: Global reactive gases and reanalysis in the 5 MACC project, J. Integr. Environ. Sci., doi:10.1080/1943815X.2012.696545, 2012.

Stein, O., Huijnen, V., Flemming, J.: Model description of the IFS-MOZART and IFS-TM5 coupled systems. MACC-II project deliverable D_55.4, available at: https://www.gmes-atmosphere.eu/documents/maccii/deliverables/grg/ (last access: February 2015), 2013.

Stein, O., Schultz, M. G., Bouarar, I., Clark, H., Huijnen, V., Gaudel, A., George, M., and Clerbaux, C.: On the wintertime low bias of Northern Hemisphere carbon monoxide found in 10 global model simulations, Atmos. Chem. Phys., 14, 9295–9316, doi:10.5194/acp-14-9295- 2014, 2014.

Tørseth, K., Aas, W., Breivik, K., Fjæraa, A. M., Fiebig, M., Hjellbrekke, A. G., Lund Myhre, C., Solberg, S., and Yttri, K. E.: Introduction to the European Monitoring and Evaluation Programme (EMEP) and observed atmospheric composition change during 1972–2009, Atmos. Chem. Phys., 12, 5447-5481, doi:10.5194/acp-12-5447-2012, 2012.

Valcke, S., Redler, R.: OASIS4 User Guide (OASIS4_0_2). PRISM–Support Initiative, Technical Report No 4, available at: http://www.prism.enes.org/Publications/Reports/OASIS4_User_Guide_T4.pdf (last access: February 2015), 2006.

Val Martin, M., Heald, C.L., Arnold, S.R.: Coupling dry deposition to vegetation phenology in the Community Earth System Model: Implications for the simulation of surface O_3. Geophys Res. Lett., 41, 2988-2996, doi:10.1002/2014GL059651, 2014.

Gelöscht: ¶

Gelöscht: visited

Gelöscht: .

Gelöscht:

Gelöscht: last visited Feb. 2015

Gelöscht: last visited Feb. 2015

Gelöscht:

Van der Werf, G. R., Randerson, J. T., Giglio, L., Collatz, G. J., and Kasibhatla, P. S.: Interannual variability in global biomass burning emissions from 1997 to 2004. Atmos. Chem. Phys., 6(11):3423–3441, doi:10.5194/acp-6-3423-2006, 2006.

Velders, G. J. M., Granier, C., Portmann, R. W., Pfeilsticker, K., Wenig, M., Wagner, T., Platt, U., Richter, A., and Burrows, J. P.: Global tropospheric NO_2 column distributions: Comparing 3-D model calculations with GOME measurements, J. Geophys. Res., 106, 12643– 12660, 2001.

Wang, P., Stammes, P., van der A, R., Pinardi, G., and van Roozendael, M.: FRESCO+: An improved O_2 A-band cloud retrieval algorithm for tropospheric trace gas retrievals, Atmos. Chem. Phys., 8, 6565-6576, doi:10.5194/acp-8-6565-2008, 2008.

Winkler, H., Sinnhuber, M., Notholt, J., Kallenrode, M.B., Steinhilber, F., Vogt, J., Zieger, B., Glassmeier, K.H. and Stadelmann, A.: Modeling impacts of geomagnetic field variations on middle atmospheric ozone responses to solar proton events on long timescales, J. Geophys. Res. 113, D02302, doi:10.1029/2007JD008574, 2008.

WMO: WMO Global Atmosphere Watch (GAW) Strategic Plan: 2008 – 2015. World Meteorological Organization, Geneva, Switzerland, 2007.

WMO: Guidelines for the Measurement of Atmospheric Carbon Monoxide, GAW Report No. 192, World Meteorological Organization, Geneva, Switzerland, 2010.

WMO: 16th WMO/IAEA Meeting on Carbon Dioxide, Other greenhouse Gases and Related Measurement Techniques (GGMT-2011), Geneva, 2012.

WMO: Guidelines for the Continuous Measurements of Ozone in the Troposphere, GAW Report No. 209, World Meteorological Organization, Geneva, Switzerland, 2013.

Worden, H. M., Deeter, M. N., Edwards, D. P., Gille, J. C., Drummond, J. R. and Nedelec, P. P.: Observations of near-surface carbon monoxide from space using MOPITT multispectral retrievals, J. Geophys. Res., 115, doi:10.1029/2010JD014242, 2010.

Worden, H. M., Deeter, M. N., Edwards, D. P., Gille, J., Drummond, J., Emmons, L. K., Francis, G., Martínez-Alonso, S.: 13 years of MOPITT operations: lessons from MOPITT retrieval algorithm development, Ann. Geophys., 56, doi:10.4401/ag-6330, 2014.

Gelöscht: , 6
Gelöscht: ,
Gelöscht: “
Gelöscht: Impacts
Gelöscht: Geomagnetic
Gelöscht: Field
Gelöscht: Variations
Gelöscht: Middle
Gelöscht: Atmospheric
Gelöscht: Ozone
Gelöscht: Responses
Gelöscht: Solar
Gelöscht: Proton
Gelöscht: Events
Gelöscht: Long
Gelöscht: Timescales
Gelöscht: .”
Gelöscht: ournal of
Gelöscht: Geophysical
Gelöscht: Research
Gelöscht: :
Gelöscht: .
Gelöscht: (2007),
Gelöscht: ¶
Gelöscht: (2010),
Gelöscht: 2007
Gelöscht: (2012),
Gelöscht: (2013),
Gelöscht: (0)

Table 1: List of assimilated data in the MACC_osuite

Instrument	Satellite	Provider	Version	Type	Status
MLS	AURA	NASA	V02	O_3 Profiles	20090901 - 20121231
OMI	AURA	NASA	V883	O_3 Total column	20090901 - 20121231
SBUV-2	NOAA	NOAA	V8	O_3 6 layer profiles	20090901 - 20121231
SCIAMACHY	Envisat	KNMI		O_3 total column	20090916 - 20120408
IASI	MetOp-A	LATMOS/ULB		CO Total column	20090901 - 20121231
MOPITT	TERRA	NCAR	V4	CO Total column	20120705 - 20121231
OMI	AURA	KNMI	DOMINO V2.0	NO_2 Tropospheric column	20120705 - 20121231
OMI	AURA	NASA	v003	SO_2 Tropospheric column	20120705 - 20121231
MODIS	AQUA / TERRA	NASA	Col. 5	Aerosol total optical depth	20090901 - 20121231

Gelöscht: ¶

Gelöscht: ---Seitenumbruch--- ¶

Gelöscht: 2

Gelöscht: ¶
Table 1: Description of the set-up of the MACC_osuite between 9/2009 and 12/2012. Details on the assimilated data are provided in Table 2. A description of the emissions is given in section 2.1.1 in the text. ¶
Model Cycle ... [6]

Table 2: Description of the set-up of the MACC_osuite between 9/2009 and 12/2012. Details on the assimilated data are provided in Table 1. A description of the emissions is given in section 2.1.1 in the text.

Gelöscht: _new

Model Cycle	**CTM**	**Assimilated Data**	**Emissions**
CY36R1	MOZART v3.0	O_3 (MLS, OMI, SBUV-2 SCIAMACHY), CO (IASI)	RETRO / REAS / GEIA / GFEDv2/GFAS
CY37R3	MOZART v3.5	O_3 (MLS, OMI, SBUV-2), CO (IASI, MOPITT), NO_2 (OMI), SO_2 (OMI)	MACCity / MEGAN / GFASv1.0 daily

Table 3: List of GAW and EMEP stations used in the evaluation (GAW listed by label, EMEP listed by region: Northern Europe NE, Central Europe CE and Southern Europe SE).

Gelöscht: _new

Gelöscht:

Station	Label/Region	Programme	Lat	Lon	Alt [m a.s.l.]	Station	Label/Region	Programme	Lat	Lon	Alt [m a.s.
Ähtäri II	**NE**	EMEP	62.58	24.18	180	Masenberg	**CE**	EMEP	47.35	15.88	11
Alert	ALT	GAW	82.45	-62.52	210	Mauna Loa	MAU	GAW	19.54	-155.58	33
Arrival Heights	ARH	GAW	-77.80	166.67	184	Minamitorishima	MNM	GAW	24.29	153.98	
Aspvreten	**NE**	EMEP	58.80	17.38	20	Montandon	**CE**	EMEP	47.30	6.83	8
Assekrem	ASS	GAW	23.27	5.63	2710	Monte Cimone	MCI	GAW	44.18	10.70	21
Aston Hill	**NE**	EMEP	52.50	-3.03	370	Monte Velho	**SE**	EMEP	38.08	-8.80	
Auchencorth	**NE**	EMEP	55.79	-3.24	260	Montelibretti	**CE**	EMEP	42.10	12.63	
Ayia Marina	**SE**	EMEP	35.04	33.06	532	Montfranc	**CE**	EMEP	45.80	2.07	8
Barcarrola	**SE**	EMEP	38.47	-6.92	393	Morvan	**CE**	EMEP	47.27	4.08	6
Baring Head	BAH	GAW	-41.41	174.87	85	Narberth	**NE**	EMEP	51.23	-4.70	1
Barrow	BAR	GAW	71.32	-156.60	11	Neuglobsow	NGW/**NE**	GAW/EMEP	53.17	13.03	
BEO Moussala	BEO	GAW	42.18	23.59	2925	Neumayer	NEU	GAW	-70.65	-8.25	
Birkenes	**NE**	EMEP	58.38	8.25	190	Niembro	**CE**	EMEP	43.44	-4.85	1
Bredkälen	**NE**	EMEP	63.85	15.33	404	Norra-Kvill	**NE**	EMEP	57.81	15.56	2
Bush	**NE**	EMEP	55.86	-3.21	180	O Saviñao	**CE**	EMEP	43.23	-7.70	5
Cabauw	**NE**	EMEP	51.97	4.92	60	Offagne	**CE**	EMEP	49.88	5.20	4
Cabo de Creus	**CE**	EMEP	42.32	3.32	23	Oulanka	**NE**	EMEP	66.32	29.40	3
Cairo	CAI	GAW	30.08	31.28	35	Pallas	**NE**	EMEP	68.00	24.15	3
Campisabalos	**CE**	EMEP	41.28	-3.14	1360	Payerne	PAY/**CE**	GAW/EMEP	46.81	6.94	5
Cape Grim	CAG	GAW	-40.68	144.68	94	Penausende	**CE**	EMEP	41.28	-5.86	9
Cape Point	CAP	GAW	-34.35	18.48	230	Peyrusse Vieille	**CE**	EMEP	43.62	0.18	2
Cape Verde	CVO	GAW	16.85	-24.87	10	Pic du Midi	PIC/**CE**	GAW/EMEP	42.94	0.14	28
Charlton Mackrell	**NE**	EMEP	51.06	-2.68	54	Pillersdor	**CE**	EMEP	48.72	15.94	3
Chaumont	**CE**	EMEP	47.05	6.98	1130	Preila	**NE**	EMEP	55.35	21.07	
Chibougamau	CHI	GAW	49.68	-74.34	393	Prestebakke	**NE**	EMEP	59.00	11.53	1
Chopok	**CE**	EMEP	48.93	19.58	2008	Puy de Dôme	PUY/**CE**	GAW/EMEP	45.77	2.95	14
Concordia	CON	GAW	-75.10	123.33	3233	Ragged Point	RAG	GAW	13.17	-59.43	
De Zilk	**NE**	EMEP	52.30	4.50	4	Rao	**NE**	EMEP	57.39	11.91	
Diabla Gora	**NE**	EMEP	54.15	22.07	157	Revin	**CE**	EMEP	49.90	4.63	3
Dobele	DOB	GAW	56.37	23.19	42	Rigi	RIG/**CE**	GAW/EMEP	47.07	8.46	10
Doñana	**SE**	EMEP	37.03	-6.33	5	Rojen Peak	**CE**	EMEP	41.70	24.74	17
Donon	**CE**	EMEP	48.50	7.13	775	Rucava	RUC/**NE**	GAW/EMEP	56.10	21.10	
Dunkelsteinerwald	**CE**	EMEP	48.37	15.55	320	Ryori	RYO	GAW	39.03	141.82	2
East Trout Lake	ETL	GAW	54.35	-104.98	492	Sable Island	SAB	GAW	43.93	-60.02	
Egbert	EGB	GAW	44.23	-79.78	253	San Pablo de los Montes	**SE**	EMEP	39.55	-4.35	9
Eibergen	**NE**	EMEP	52.08	6.57	20	Sandve	**NE**	EMEP	59.20	5.20	
Els Torms	**CE**	EMEP	41.40	0.72	470	Schauinsland	SCH/**CE**	GAW/EMEP	47.92	7.92	12
Eskdalemuir	**NE**	EMEP	55.31	-3.20	243	Schmücke	**NE**	EMEP	50.65	10.77	9
Esrange	**NE**	EMEP	67.88	21.07	475	Sibton	**NE**	EMEP	52.29	1.46	
Estevan Point	ESP	GAW	49.38	-126.55	39	Śnieżka	**NE**	EMEP	50.73	15.73	16

Eupen	NE	EMEP	51.46	6.00	295	Sonnblick	SBL/CE	GAW/EMEP	47.05	12.96	31
Everest - Pyramid	EVP	GAW	27.96	86.82	5079	South Pole	SPO	GAW	-89.98	-24.80	28
Finokalia	SE	EMEP	35.32	25.67	250	Spitsbergen	NE	EMEP	78.90	11.88	4
Forsthof	CE	EMEP	48.10	15.91	581	St. Osyth	NE	EMEP	51.78	1.08	
Fraserdale	FRA	GAW	49.88	-81.57	210	Stará Lesná	CE	EMEP	49.15	20.28	8
Gänserndorf	CE	EMEP	48.33	16.73	161	Starina	CE	EMEP	49.05	22.27	3
Gerlitzen	CE	EMEP	46.69	13.92	1895	Stixneusiedl	CE	EMEP	48.05	16.68	2
Graz Platte	CE	EMEP	47.11	15.47	651	Strath Vaich Dam	NE	EMEP	57.73	-4.77	2
Great Dun Fell	NE	EMEP	54.68	-2.45	847	Summit	SUM	GAW	72.58	-38.48	32
Grebenzen	CE	EMEP	47.04	14.33	1648	Svratouch	CE	EMEP	49.73	16.05	7
Grimsoe	NE	EMEP	59.73	15.47	132	Syowa Station	SYO	GAW	-69.00	39.58	
Harwell	NE	EMEP	51.57	-1.32	137	Tänikon	CE	EMEP	47.48	8.90	5
Haunsberg	CE	EMEP	47.97	13.02	730	Topolniky	CE	EMEP	47.96	17.86	1
Heidenreichstein	CE	EMEP	48.88	15.05	570	Trinidad Head	TRI	GAW	41.05	-124.15	1
High Muffles	NE	EMEP	54.33	-0.80	267	Tsukuba	TSU	GAW	36.05	140.13	
Hurdal	NE	EMEP	60.37	11.08	300	Tudor Hill	TUD	GAW	32.27	-64.87	
Illmitz	CE	EMEP	47.77	16.77	117	Tustervatn	NE	EMEP	65.83	13.92	4
Iskrba	ISK/CE	GAW/EMEP	45.56	14.86	520	Tutuila	TUT	GAW	-14.24	-170.57	
Izaña (Tenerife)	IZO	GAW	28.30	-16.50	2367	Ushuaia	USH	GAW	-54.85	-68.32	
Jarczew	NE	EMEP	51.82	21.98	180	Utö	NE	EMEP	59.78	21.38	
Jungfraujoch	JFJ/CE	GAW/EMEP	46.55	7.99	3578	Vavihill	NE	EMEP	56.01	13.15	1
Karasjok	NE	EMEP	69.47	25.22	333	Vezin	NE	EMEP	50.50	4.99	1
Keldsnor	NE	EMEP	54.73	10.73	10	Vilsandi	NE	EMEP	58.38	21.82	
Kollumerwaard	KOW/NE	GAW/EMEP	53.33	6.28	1	Vindeln	VIN/NE	GAW/EMEP	64.25	19.77	2
Košetice	KOS/CE	GAW/EMEP	49.58	15.08	534	Virolahti II	NE	EMEP	60.53	27.69	
Kovk	KOV/CE	GAW/EMEP	46.12	15.11	600	Vorhegg	CE	EMEP	46.68	12.97	10
K-puszta	CE	EMEP	46.97	19.58	125	Vredepeel	NE	EMEP	51.54	5.85	
Krvavec	CE	EMEP	46.30	14.54	1740	Waldhof	WAL/NE	GAW/EMEP	52.80	10.77	
La Coulonche	CE	EMEP	48.63	-0.45	309	Westerland	WES/NE	GAW/EMEP	54.93	8.32	
La Tardière	CE	EMEP	46.65	-0.75	143	Weybourne	NE	EMEP	52.95	1.12	
Lac La Biche	LAC	GAW	54.95	-112.45	540	Wicken Fen	NE	EMEP	52.30	-0.29	
Ladybower Res.	NE	EMEP	53.40	-1.75	420	Yarner Wood	NE	EMEP	50.59	-3.71	1
Lahemaa	NE	EMEP	59.50	25.90	32	Yonagunijima	YON	GAW	24.47	123.02	
Lauder	LAU	GAW	-45.03	169.67	370	Zarodnje	CE	EMEP	46.42	15.00	7
Le Casset	CE	EMEP	45.00	6.47	750	Zarra	SE	EMEP	39.09	-1.10	8
Leba	NE	EMEP	54.75	17.53	2	Zavodnje	ZAV	GAW	46.43	15.00	7
Lerwick	NE	EMEP	60.13	-1.18	85	Zillertaler Alpen	CE	EMEP	47.14	11.87	19
Lille Valby	NE	EMEP	55.69	12.13	10	Zingst	ZIN/NE	GAW/EMEP	54.43	12.73	
Lough Navar	NE	EMEP	54.44	-7.87	126	Zoebelboden	CE	EMEP	47.83	14.44	8
Lullington Heath	NE	EMEP	50.79	0.17	120	Zoseni	ZOS/NE	GAW/EMEP	57.13	25.90	1
Mace Head	NE	EMEP	53.17	-9.50	15	Zugspitze	SFH	GAW	47.42	10.98	26
Market Harborough	NE	EMEP	52.55	-0.77	145						

Table 4: Modified normalized mean bias (MNMB) [%], correlation coefficient (R), and root mean square error (RMSE) [ppb] derived from the evaluation of the MACC_osuite with Global Atmosphere Watch (GAW) O_3 surface observations during the period 09/2009 to 12/2012.

Station	ARH	ASS	BAH	BAR	BEO	CAI	CAG	CAP	CVO	CON	DOB	EVP	ISK	IZO	JFJ	K[illegible]	[illegible]
MNMB	-39.8	-6.3	-8.6	-35.1	-21.4	70.1	-12.7	13.7	15.2	-81.6	6.3	18.4	67.2	10.4	1.9	5.8	-5.9
R	0.6	0.7	0.5	0.3	0.4	-0.1	0.4	0.6	0.6	0.3	0.3	0.7	0.1	0.5	0.7	0.6	0.6
RMSE	10.6	6.5	8.0	13.8	20.4	29.2	8.9	7.6	8.0	17.2	14.3	12.0	34.5	10.8	7.4	12.0	16.3

Station	KOV	KRV	LAU	MAU	MNM	MCI	NGW	NEU	PAY	PIC	PUY	RAG	RIG	RUC	RYO	SCH	SBL
MNMB	21.2	9.5	-5.5	13.7	38.6	2.3	-11.4	-45.2	-28.8	5.5	12.8	38.6	-80.3	-0.1	10.5	8.5	8.1
R	0.6	0.6	0.5	0.6	0.8	0.7	0.5	0.5	0.7	0.6	0.6	0.6	0.3	0.3	0.1	0.7	0.6
RMSE	19.5	11.1	9.0	11.5	13.0	8.2	14.3	11.4	15.6	7.7	10.6	10.6	28.4	15.0	14.4	12.2	9.3

Station	SFH	SPO	SUM	SYO	TRI	TSU	TUD	TUT	USH	VIN	WAL	WES	YON	ZAV	ZIN	ZOS
MNMB	10.1	-70.6	-24.4	-31.2	3.2	55.1	45.3	40.2	-7.0	4.6	-18.0	-12.3	22.0	19.7	-17.5	22.3
R	0.6	0.4	0.5	0.7	0.3	0.0	0.5	0.8	0.5	0.4	0.6	0.6	0.7	0.6	0.4	0.2
RMSE	9.3	16.3	11.7	8.9	13.3	27.6	18.2	8.0	7.6	11.2	13.6	11.6	13.6	18.6	13.9	17.0

Gelöscht: ¶

Gelöscht: _new

Formatiert: Englisch (USA)

Table 5: Modified normalized mean bias (MNMB) [%], correlation coefficient (R), and root mean square error (RMSE) [ppb] derived from the evaluation of the MACC_osuite with Global Atmospheric Watch (GAW) CO surface observations during the period 09/2009 to 12/2012.

Station	ALT	BEO	CAP	CHI	CVO	EGB	ESP	ETL	FRA	IZO	JFJ	KOS	KOW	KRV	LAC	MCI	MNM
MNMB	-6.9	-36.1	29.7	-7.3	-0.6	4.5	-1.7	-19.9	-12.0	-6.8	-15.1	-50.1	-5.9	-30.4	-24.2	-19.0	6.4
R	0.5	0.0	0.6	0.4	0.7	0.3	0.5	0.1	0.3	0.7	0.6	0.2	0.4	0.4	0.0	0.6	0.8
RMSE	23.4	90.3	20.4	31.1	14.2	60.1	25.7	53.9	35.9	15.3	25.8	131.1	70.1	49.1	58.5	32.0	22.0

Station	NGW	PAY	PIC	PUY	RIG	RYO	SAB	SBL	SCH	SFH	USH	YON
MNMB	-1.7	-7.3	-9.3	-10.4	28.2	-4.8	-8.1	-25.1	-15.8	-25.7	-9.1	-1.6
R	0.4	0.3	0.7	0.6	0.0	0.4	0.4	0.5	0.5	0.4	0.6	0.7
RMSE	61.6	99.2	18.4	30.6	143.5	44.5	31.6	36.8	39.8	45.0	12.3	62.3

Gelöscht: _new

Formatiert: Englisch (USA)

Table 6: Modified normalized mean bias (MNMB) [%] derived from CO satellite observations (MOPITT) and the MACC_osuite simulations of CO total columns from 10/2009 until 06/2012 averaged over different regions.

Gelöscht: _new

	Oct 09	Nov 09	Dec 09	Jan 10	Feb 10	Mar 10	Apr 10	May 10	Jun 10	Jul	
Europe	4.17	1.35	-7.02	-7.17	-7.84	-8.56	-5.20	-2.15	-2.96	0.75	-2.88
Alaska	0.31	-3.16	-6.71	-8.85	-6.39	-3.13	-4.49	-3.85	-8.69	-6.18	-3.94
Siberia	2.02	1.62	-1.44	-2.75	-1.36	-2.27	-3.58	-2.93	-5.30	4.21	-8.43
N. Africa	6.53	9.17	5.82	7.05	3.45	-2.96	-3.53	-1.75	-3.40	-1.21	-3.58
S. Africa	-12.45	-9.44	3.10	6.53	8.27	6.63	3.57	2.33	7.34	0.57	-2.75
S. Asia	9.20	13.73	6.95	6.41	6.69	1.12	3.18	1.26	-3.01	1.98	2.15
E. Asia	8.04	12.33	-5.86	-9.18	-6.64	-4.49	-5.12	-5.61	-7.72	-4.34	-2.80
US	9.73	6.71	-5.42	-7.75	-10.88	-6.26	-3.80	-2.04	1.58	2.54	2.98

Formatiert: Englisch (USA)

	Sep 10	Oct 10	Nov 10	Dec 10	Jan 11	Feb 11	Mar 11	Apr 11	May 11	Jun 11	Jul 11
Europe	-1.97	-0.92	-2.94	-7.78	-15.41	-17.22	-18.78	-17.34	-13.34	-6.62	-3.91
Alaska	-5.00	-1.89	-4.87	-7.51	-14.54	-9.90	-9.29	-12.54	-11.95	-10.04	-4.73
Siberia	-2.94	-1.93	-1.73	-3.02	-7.71	-7.78	-12.09	-21.99	-17.23	-11.59	-4.97
N. Africa	-1.22	3.33	5.98	7.03	-0.53	4.31	2.66	1.37	4.23	4.71	4.37
S. Africa	-5.13	2.84	7.39	4.37	1.41	3.39	3.80	0.99	5.71	3.45	-2.75
S. Asia	5.05	6.72	9.63	10.30	2.19	2.91	1.48	-1.76	1.68	1.62	2.90
E. Asia	6.13	6.93	2.44	3.23	-11.25	-9.18	-9.63	-8.58	-4.73	-1.62	5.00
US	0.08	-0.71	1.20	-8.06	-18.30	-16.98	-14.33	-13.52	-8.10	-4.72	-0.64

	Aug 11	Sep 11	Oct 11	Nov 11	Dec 11	Jan 12	Feb 12	Mar 12	Apr 12	May 12	Jun 12
Europe	-2.57	-7.28	-10.80	-11.85	-14.79	-13.50	-14.16	-15.30	-11.49	-7.00	-3.65
Alaska	-5.69	-11.86	-18.05	-14.33	-12.29	-11.50	-11.24	-11.92	-9.42	-8.71	-4.74
Siberia	-6.05	-15.16	-16.50	-10.32	-11.59	-10.15	-8.45	-13.14	-12.18	-11.08	-4.45
N. Africa	6.15	5.35	6.27	-0.93	3.37	2.04	1.11	-5.90	-3.40	-3.59	-0.95
S. Africa	-6.70	-4.43	-0.58	3.64	4.66	4.25	2.91	0.91	3.41	1.33	-1.23
S. Asia	3.80	2.27	4.24	4.76	7.00	3.24	1.72	-1.23	-0.90	0.49	-0.61
E. Asia	3.05	1.60	-2.60	-2.48	-5.15	-5.56	-4.63	-0.85	-0.36	-2.63	0.68
US	-1.17	-2.40	-4.23	-6.14	-10.84	-13.30	-14.87	-9.19	-6.94	-2.88	-2.55

Table 7: Statistics derived from satellite observations (SCIAMACHY from 09/2009 until 03/2012, GOME-2 from 04/2012 to 12/2012) and the MACC_osuite simulations of daily tropospheric NO_2 VCD [10^{15} molec cm^{-2}] averaged over different regions for September 2009 to December 2012.

Region	**United States**	**Europe**	**South Asia**	**East Asia**	**South Africa**	**North Africa**
Model mean NO_2 VCD [10^{15} molec cm^{2}]	2.6	2.1	1.0	2.4	0.8	0.9
Satellite mean NO_2 VCD [10^{15} molec cm^{2}]	3.1	3.6	1.2	6.2	1.1	0.9
Modified normalized mean bias (MNMB) [%]	-17.3	-49.0	-13.4	-70.7	-36.8	-0.4
Root mean square error (RMSE) [10^{15} molec cm^{2}]	1.2	2.0	0.3	6.0	0.5	0.3
Correlation coefficient (R) [dimensionless]	0.6	0.8	0.8	0.8	0.6	0.5

Gelöscht: _new

Gelöscht: 1

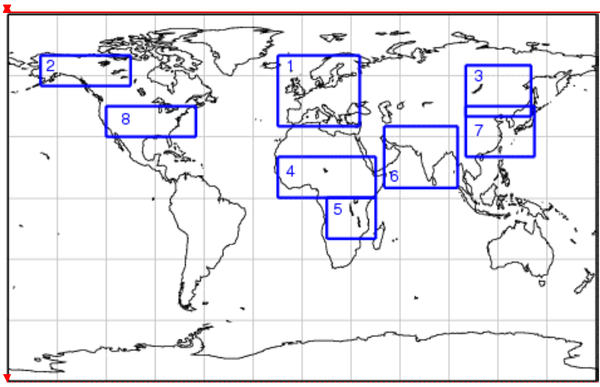

Figure 1: Regions used for regional data-stratification in the troposphere for the comparison with satellite data. The following regions are defined: **1** Europe (15W–35E, 35N–70N), **2** Alaska (150W–105W, 55N–70N), **3** Siberia (100E–140E, 40N–65N), **4** North Africa (15W–45E, 0N–20N), **5** South Africa (15E–45E, 20S–0S), **6** South Asia (50E–95E, 5N–35N), **7** East Asia (100E–142E, 20N–45N), **8** United States (120W–65W, 30N–45N).

Gelöscht: ¶
--------Seitenumbruch--------

Gelöscht: Table 3: List of GAW and EMEP stations used in the evaluation ¶
Station ... [7]

Gelöscht: ¶
--------Seitenumbruch--------

Gelöscht: Table 5: Statistics derived from satellite observations (SCIAMACHY from 09/2009 until 03/2012, GOME-2 from 04/2012 to 12/2012) and the MACC_osuite simulations of daily tropospheric NO_2 VCD [10^{15} molec cm^{-2}] averaged over different regions for September 2009 to December 2012¶
Region ... [8]

Gelöscht: ¶
--------Seitenumbruch--------
¶

Formatiert ... [9]

Gelöscht: Table 6: Modified normalized mean bias (MNMB) [%], correlation coefficient (R), and root mean square error (RMSE) [ppb] derived from the evaluation of the MACC_osuite with Global Atmosphere Watch (GAW) O_3 surface observations during the period 09/2009 to 12/2012 ¶
Station ... [10]

Gelöscht: ---Seitenumbruch---

Gelöscht: Fires-…Fires- ... [11]

Formatiert: Englisch (USA)

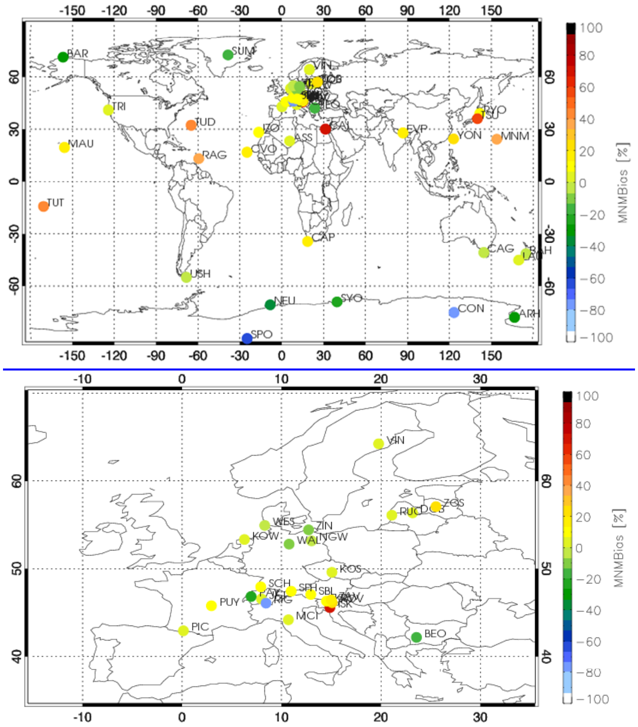

Figure 2: Modified normalized mean biases (MNMBs) [%] derived from the evaluation of the MACC_osuite with GAW O_3 surface observations during the period 09/2009 to 12/2012 globally (top), and for Europe (below). Blue colours represent large negative values; red/brown colours represent large positive values.

Formatiert: referentie, Block, Zeilenabstand: 1,5 Zeilen

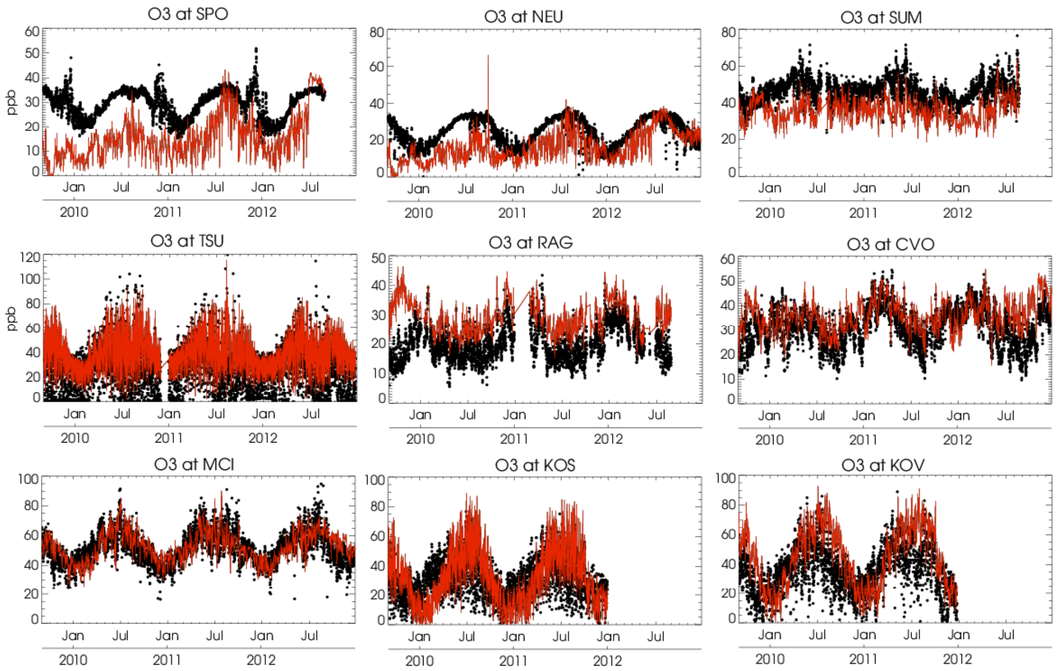

Figure 3: Time series plots of the MACC_osuite 6-hourly O_3 mixing ratios (red) and GAW surface observations (black) for South Pole-SPO (Antarctica), Neumayer-NEU (Antarctica), Summit-SUM (Denmark), Tsukuba-TSU (Japan), Ragged Point-RAG, (Barbados), Cape Verde Observatory-CVO (Cape Verde), Monte Cimone-MCI (Italy), Kosetice-KOS (Czech Republic), Kovk- KOV(Slovenia) during the period 09/2009 to 12/2012. Unit: ppb

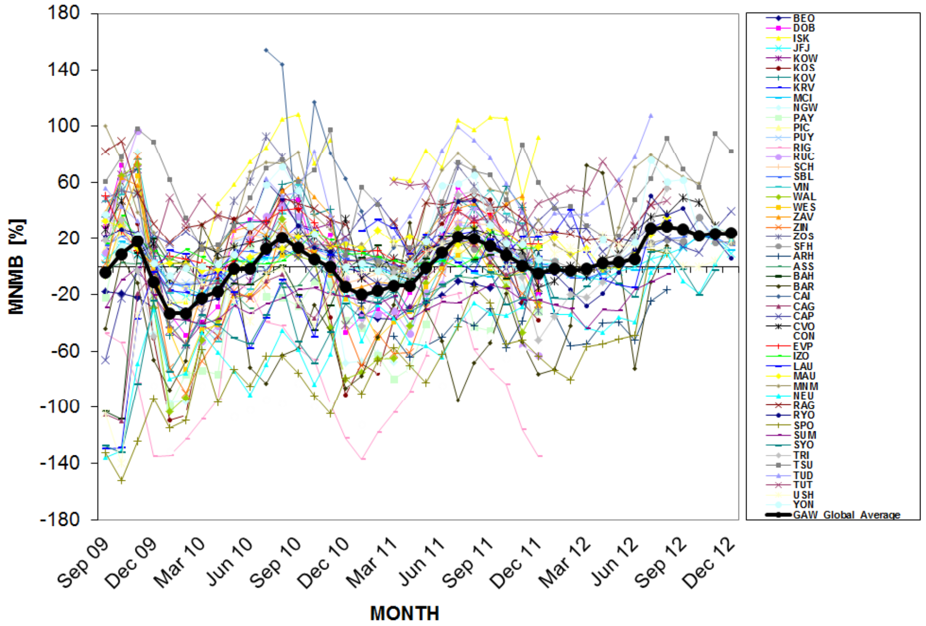

Figure 4: Modified normalized mean bias (MNMB) in % derived from the evaluation of the MACC_osuite with GAW O_3 surface observations during the period September 2009 to December 2012 (black line: global average of 50 GAW stations. Multi-coloured lines: individual station results, see legend to the right).

Gelöscht: _new

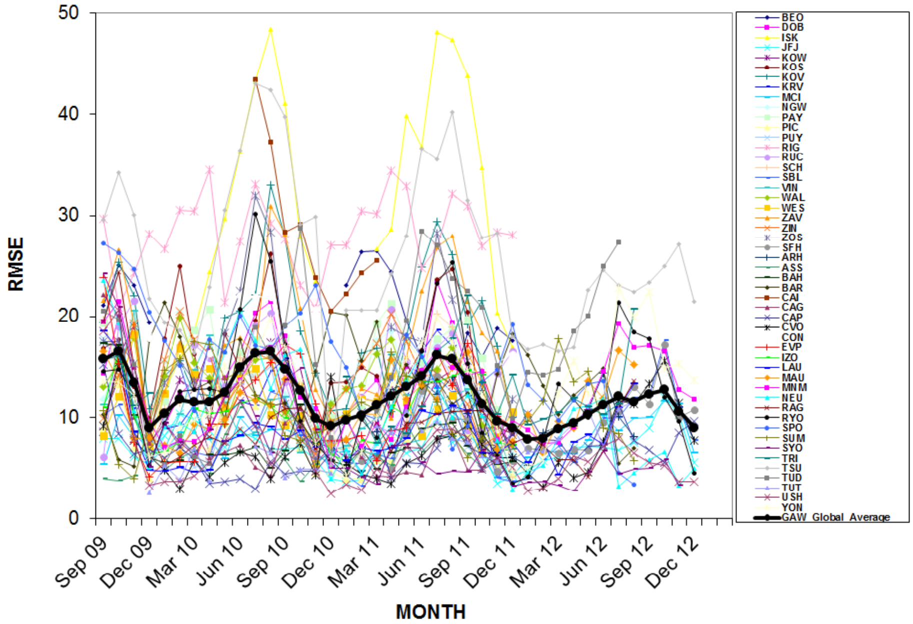

Figure 5: Root mean square error (RMSE) in ppb derived from the evaluation of the MACC_osuite with GAW O_3 surface observations during the period September 2009 to December 2012 (black line: global average of 50 GAW stations. Multi-coloured lines: individual station results, see legend to the right).

Gelöscht: _new

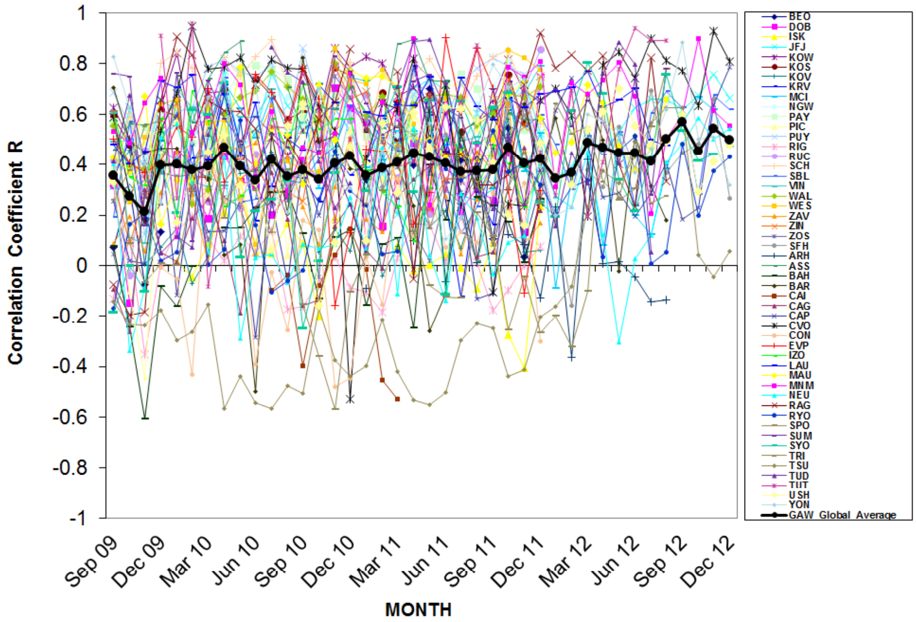

Figure 6: Correlation coefficient (R), derived from the evaluation of the MACC_osuite with GAW O_3 surface observations during the period September 2009 to December 2012 (black line: global average of 50 GAW stations. Multi-coloured lines: individual station results, see legend to the right).

Gelöscht: _new

Gelöscht: ¶

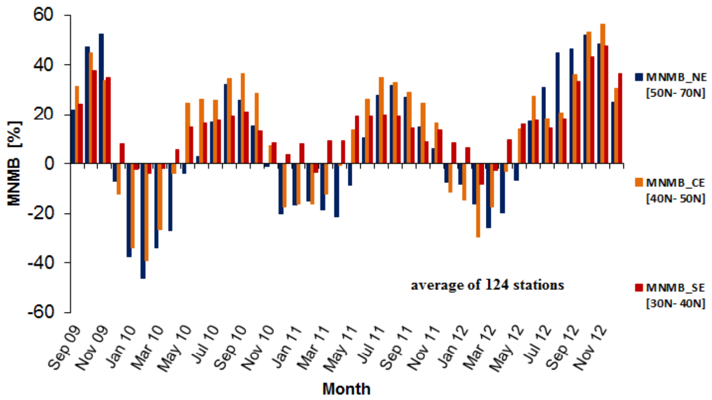

Figure 7: Modified normalized mean biases (MNMBs) derived from the evaluation of the MACC_osuite with EMEP O_3 surface observations in three different parts in Europe (blue: Northern Europe, orange: Central Europe, red: Southern Europe) during the period September 2009 to December 2012.

Gelöscht: _new

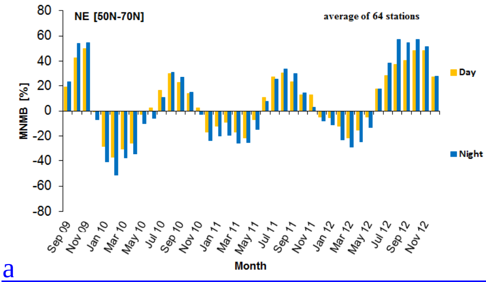

a

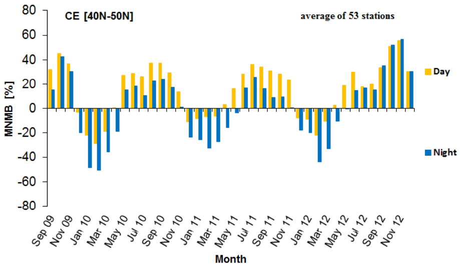

b

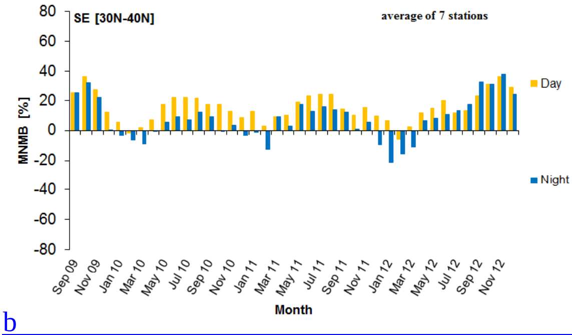

b

Figure 8: Modified normalized mean biases (MNMBs) derived from the evaluation of the MACC_osuite with EMEP O_3 surface observations during day-time (yellow color), and night-time (blue color) over northern Europe (a), central Europe (b) and southern Europe (c) during the period September 2009 to December 2012.

Gelöscht: _new

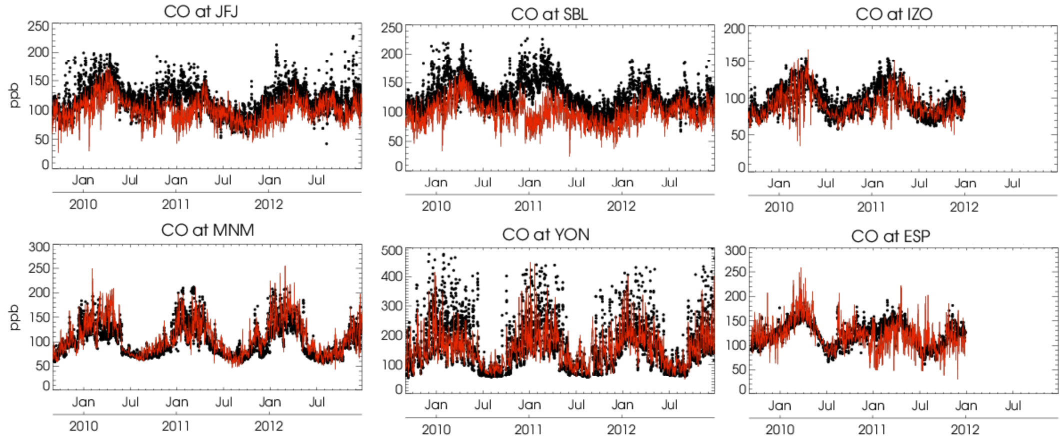

Figure 9: Time series plots of the MACC_osuite 6-hourly CO mixing ratios (red) and GAW surface observations (black) for Jungfraujoch- JFJ (Switzerland), Sonnblick- SBL (Austria), Izana Observatory- IZO (Tenerife), Minamitorishima- MNM (Japan), Yonagunijima- YON (Japan), Estevan Point- EVP (Canada) during the period 09/2009 to 12/2012. Unit: ppb.

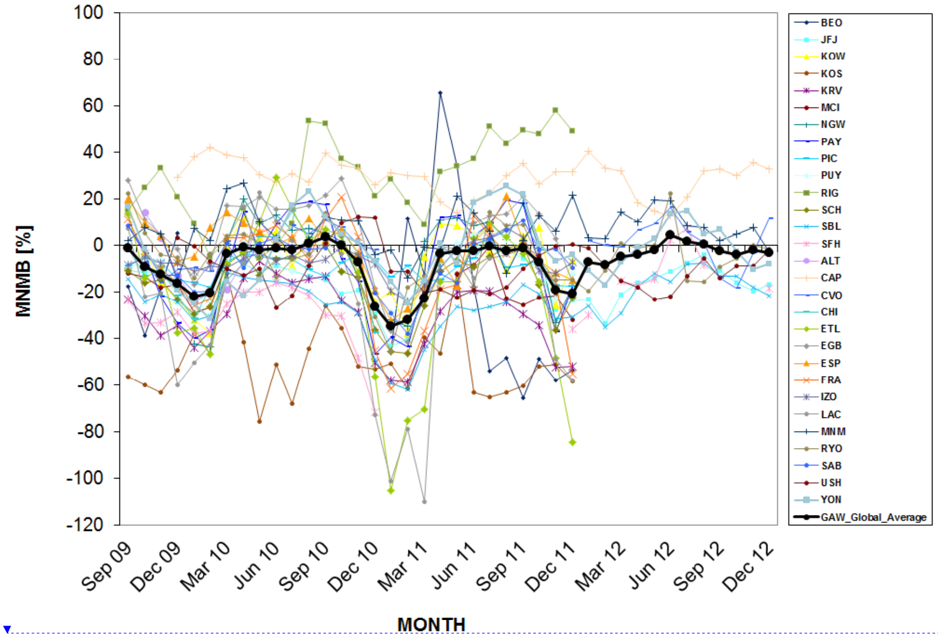

Figure 10: Modified normalized mean bias (MNMB) in % derived from the evaluation of the MACC_osuite with GAW CO surface observations over the period September 2009 to December 2012 (black line: global average of 29 GAW stations. Multi-coloured lines: individual station results, see legend to the right).

Gelöscht: ---Seitenumbruch---

Gelöscht: 2a

Gelöscht: 9

Gelöscht: _new

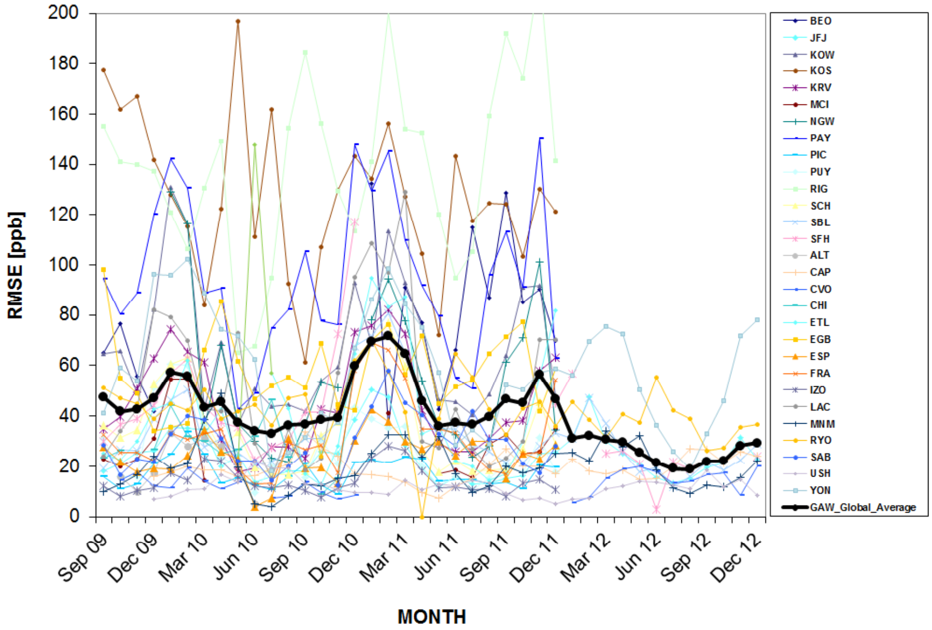

Figure 11: Root mean square error (RMSE) in ppb derived from the evaluation of the MACC_osuite with GAW CO surface observations over the period September 2009 to December 2012 (black line: global average of 29 GAW stations multi-coloured lines: individual station results, see legend to the right).

Gelöscht: 0

Gelöscht: _new

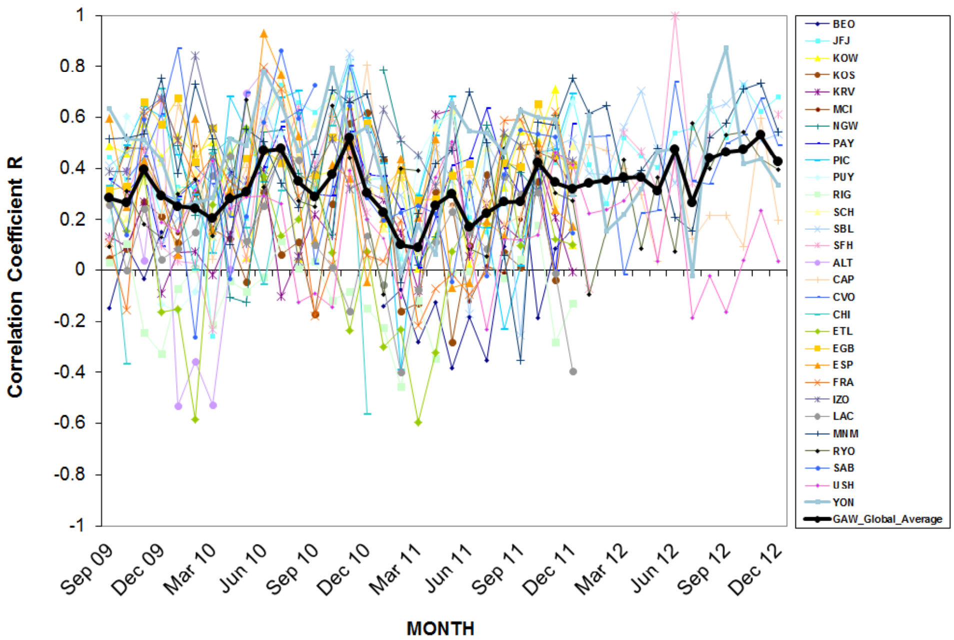

Figure 12: Correlation coefficient (R), derived from the evaluation of the MACC_osuite with GAW CO surface observations over the period September 2009 to December 2012 (black line: global average of 29 GAW stations. Multi-coloured lines: individual station results, see legend to the right).

Gelöscht:

Gelöscht: 2

Gelöscht: a2b

Gelöscht: 1

Gelöscht: _new

Gelöscht: Modified normalized mean bias (MNMB) in % (top left) and

Gelöscht: c

Gelöscht: _

Gelöscht: ¶

Gelöscht: (top right)

Gelöscht: ¶

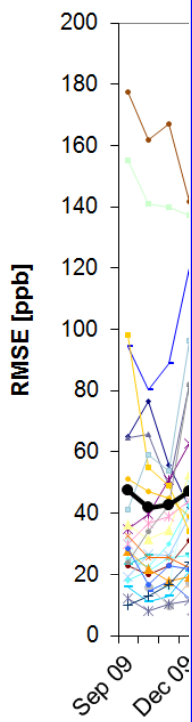

Gelöscht:

Figure 2b2c: Root mean square error (RMSE) in ppb derived from the evaluation of the MACC_osuite with GAW CO surface observations over the period September 2009 to December 2012 (black line: global average of 29 GAW stations multi-coloured lines: individual station results, see legend to the right).¶

Gelöscht: Seitenumb... [12]

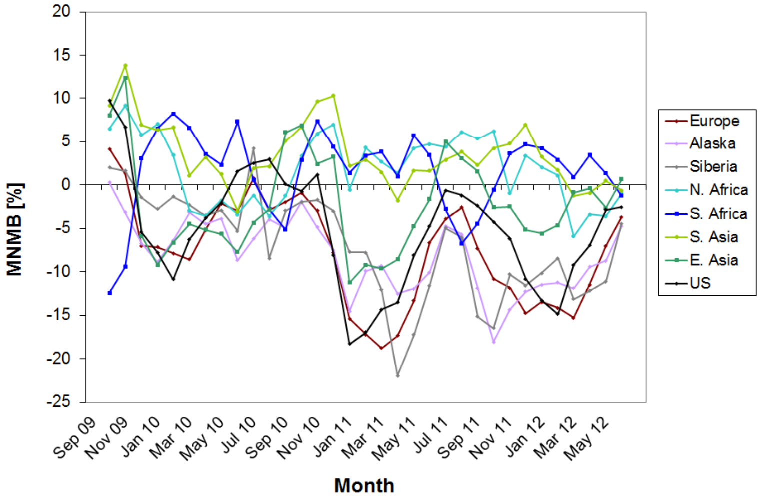

Figure 13: Monthly average of modified normalized mean biases (MNMBs) derived from the comparison of the MACC_osuite with MOPITT CO total columns for 8 different regions during the period 09/2009 to 06/2012 (see legend on the right).

Gelöscht: 4

Gelöscht: _new

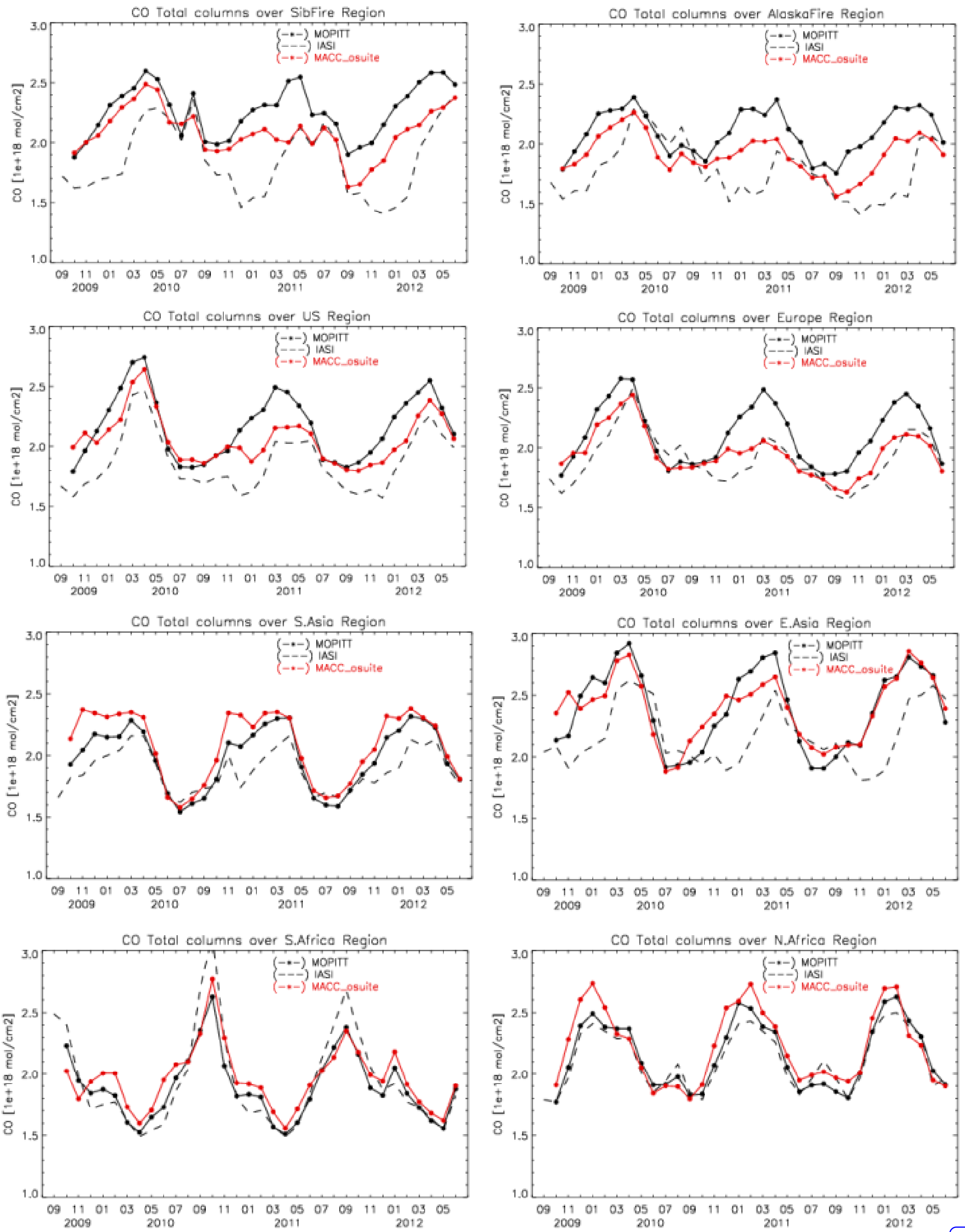

Figure 14: Time series plots of MOPITT CO total columns (black line) compared to IASI CO total columns (black dashed line) and the MACC_osuite CO total columns (red line) for 8 different regions (defined in Figure 1) during the period 09/2009 to 06/2012. Top: Siberia (left), Alaska (right), second row: United States (left), Europe (right), third row: South Asia (left), East Asia (right) bottom: South Africa (left), North Africa (right).

Gelöscht: 5

Gelöscht: _new

Gelöscht: Fires-

Gelöscht: Fires-

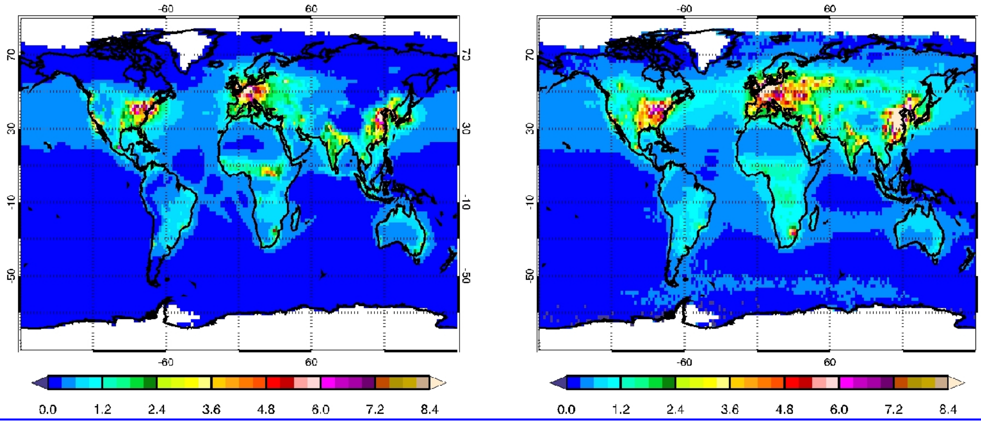

Figure 15: Long-term average of daily tropospheric NO_2 VCD [10^{15} molec cm^{-2}] from September 2009 to March 2012 for (left) MACC_osuite simulations and (right) SCIAMACHY satellite observations. Blue colours represent low values; red/brown colours represent high values.

Formatiert: Schriftart: Times New Roman, 12 pt, Nicht Kursiv, Schriftartfarbe: Schwarz

Formatiert: Schriftart: Times New Roman, 12 pt, Nicht Kursiv, Schriftartfarbe: Schwarz

Formatiert: Schriftart: Times New Roman, 12 pt, Nicht Kursiv, Schriftartfarbe: Schwarz

Formatiert: Schriftart: Times New Roman, 12 pt, Nicht Kursiv, Schriftartfarbe: Schwarz

Formatiert: Schriftart: (Standard) Times New Roman, 12 pt, Nicht Kursiv, Schriftartfarbe: Schwarz

Formatiert: Zchn Zchn3, Zeilenabstand: 1,5 Zeilen

Gelöscht: ¶

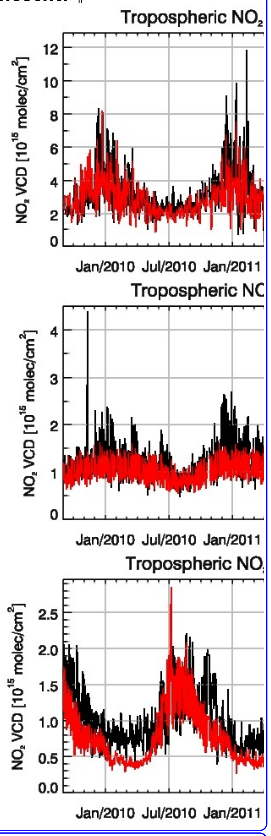

Formatiert: Schriftartfarbe: Schwarz

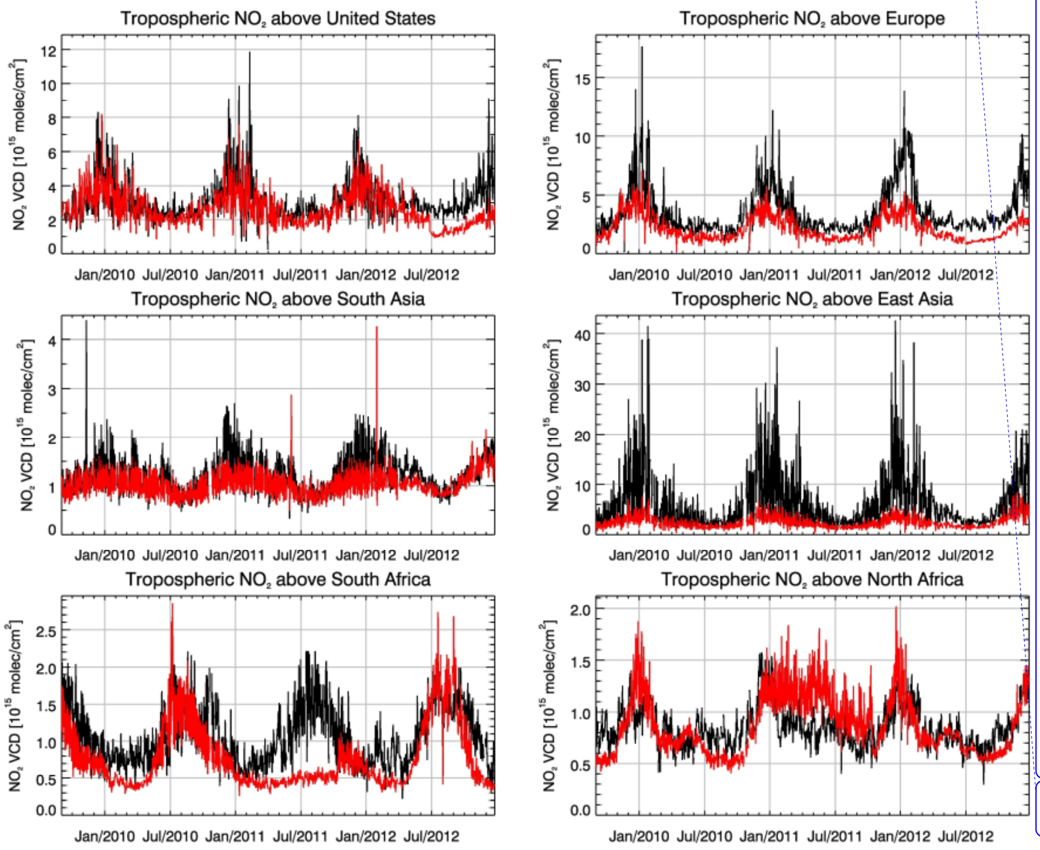

Figure 16: Time series of daily tropospheric NO2 VCD [10^{15} molec cm-2] averaged over different regions. Top: United States (left), Europe (right), second row: South Asia (left), East Asia (right), bottom: South Africa (left), North Africa (right). Black lines show satellite observations (SCIAMACHY up to 03/2012, GOME-2 from 04/2012 to 12/2012), red lines correspond to the MACC_osuite simulations.

Gelöscht: 6

Gelöscht: _new

Formatiert: Schriftartfarbe: Schwarz

Formatiert: Schriftartfarbe: Schwarz, Nicht Hochgestellt/ Tiefgestellt

Formatiert: Schriftartfarbe: Schwarz

Formatiert: Schriftart: Schriftartfarbe: Schwarz

Formatiert: Schriftart: Schriftartfarbe: Schwarz

Formatiert: Schriftart: Schriftartfarbe: Schwarz

Formatiert: Schriftartfarbe: Schwarz

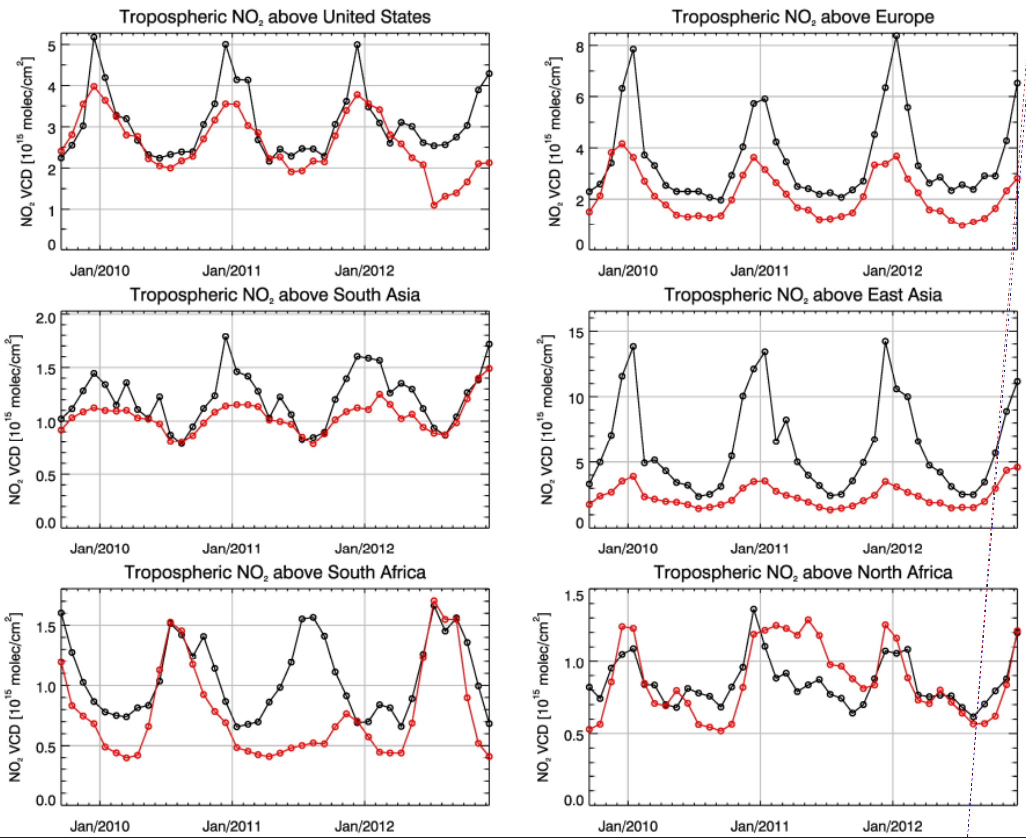

Figure 17: As in Fig. 16 but for monthly means of daily tropospheric NO_2 VCD [10^{15} molec cm^{-2}] averaged over different regions. Top: United States (left), Europe (right), second row: South Asia (left), East Asia (right), bottom: South Africa (left), North Africa (right).

Gelöscht: <sp>

Gelöscht: ¶
Seitenumbruch

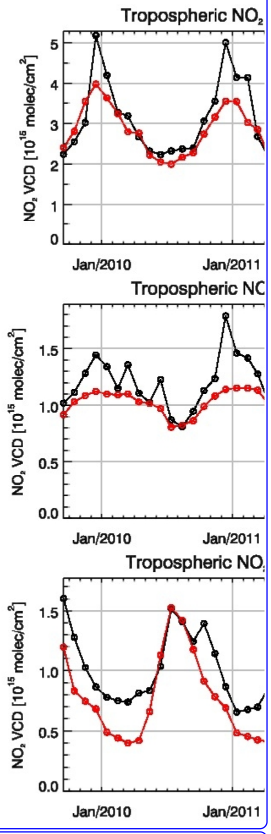

Gelöscht: 8

Gelöscht: new

Gelöscht: ure

Gelöscht: 6

Gelöscht: ¶
Seitenumbruch ... [13]

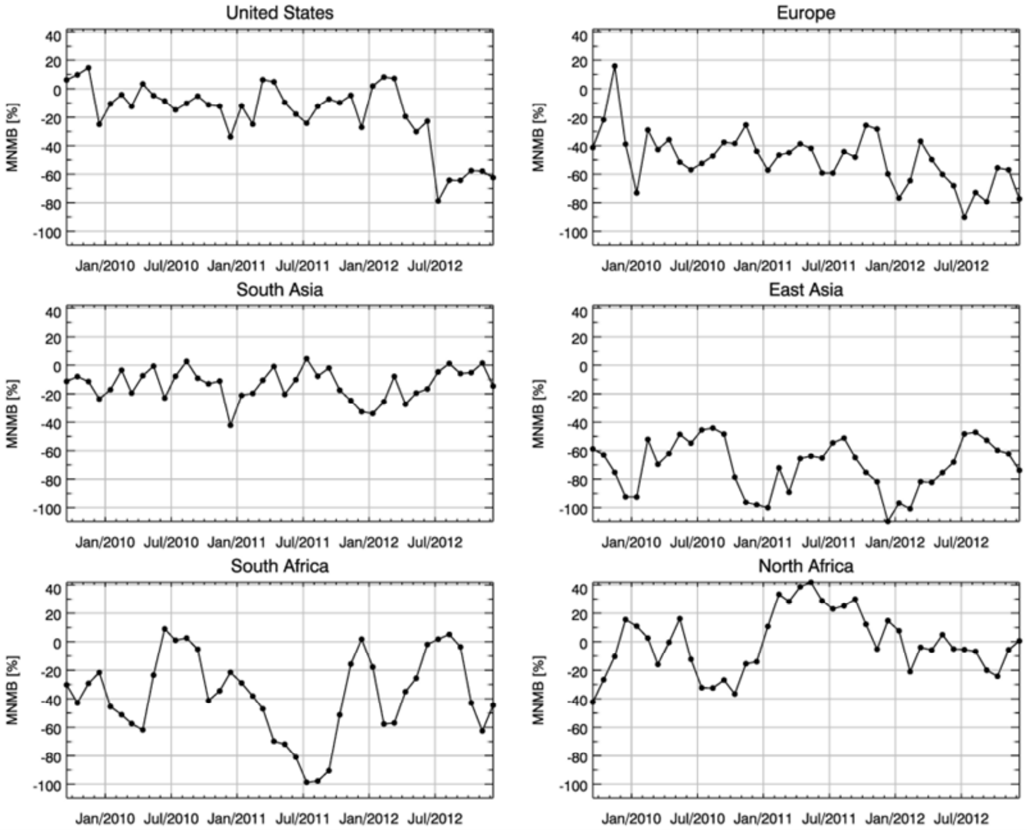

Figure 18: Modified normalized mean bias [%] for monthly means of daily tropospheric NO_2 VCD averaged over different regions (see Fig.1 for latitudinal and longitudinal boundaries) derived from the MACC_osuite simulations and satellite observations (SCIAMACHY up to 03/2012, GOME-2 from 04/2012 to 12/2012). Top: United States (left), Europe (right), second row: South Asia (left), East Asia (right), bottom: South Africa (left), North Africa (right).Values have been calculated separately for each month.

Gelöscht: 9
Gelöscht: -new
Gelöscht: of
Gelöscht: text

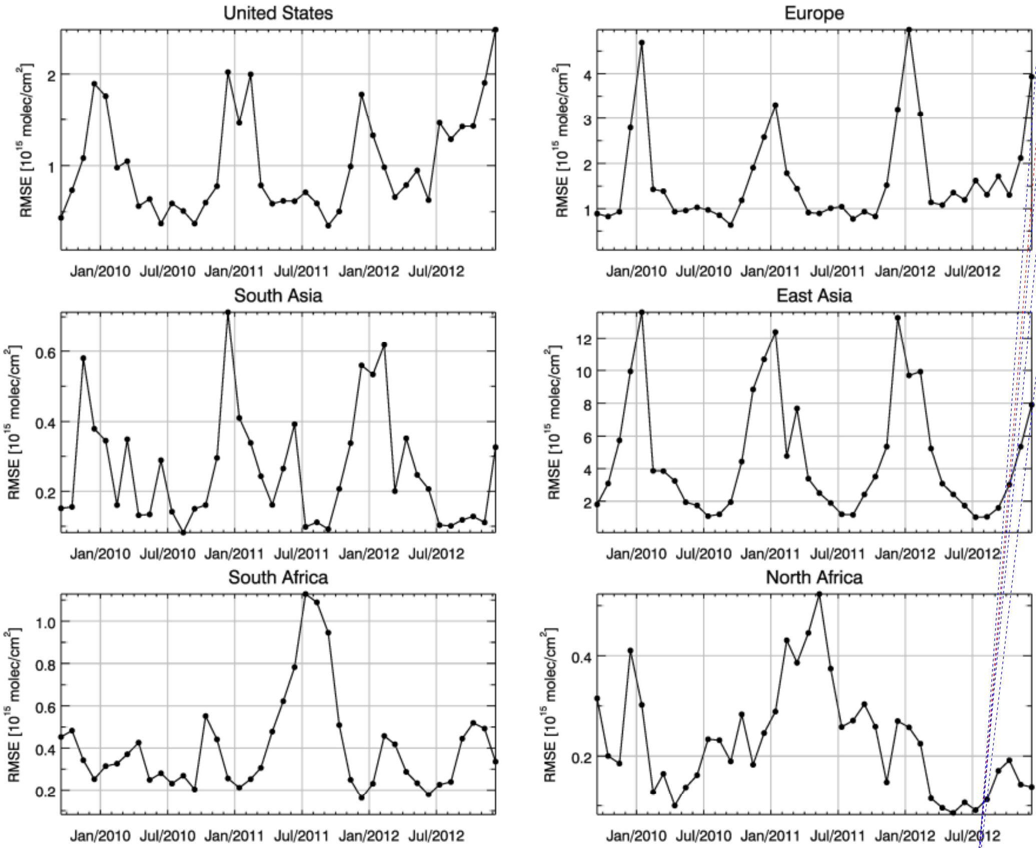

Figure 19: As in Fig. 18 but for the root mean square error [10^{15} molec cm^{-2}].

Formatiert: Schriftart: Nicht Kursiv, (Asiatisch) Chinesisch (VR China)

Gelöscht: _new

Formatiert: Schriftart: Nicht Kursiv, (Asiatisch) Chinesisch (VR China)

Formatiert: Abstand zwischen asiatischem und westlichem Text anpassen, Abstand zwischen asiatischem Text und Zahlen anpassen

Gelöscht: ¶
<sp>¶

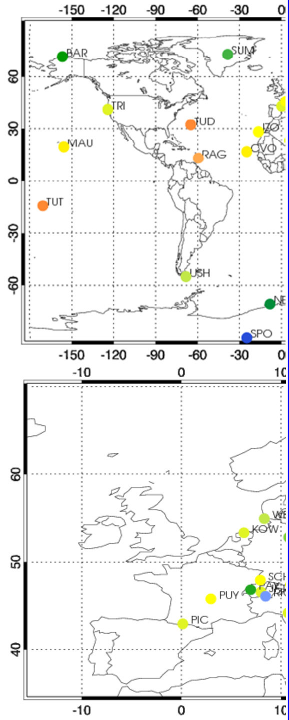

Figure 11: Modified normalized mean biases (MNMBs) [%] derived from the evaluation of the MACC_osuite with GAW O_3 surface observations during the period 09/2009 to 12/2012 globally (top), and for Europe (below). Blue colours represent large negative values; red/brown colours represent large positive values.¶ ... [14]

Formatiert: Schriftart: Nicht Kursiv, (Asiatisch) Chinesisch (VR China)

Formatiert: Schriftart: (Asiatisch) Chinesisch (VR China)

Formatiert: Englisch (USA)

Formatiert: Englisch (USA)

Formatiert: Englisch (USA)

Formatiert: Englisch (USA)

Formatiert: Englisch (USA)